UNIVERSITY OF CALIFORNIA, SAN DIEGO

# The Role of Amyloid Precursor Protein in Amyloid-Beta-Mediated Synaptic Dysfunction

A dissertation submitted in partial satisfaction of the requirements for the degree Doctor of Philosophy

in

Molecular Pathology

by

Brea June Midthune

Committee in charge:

Professor Edward Koo, Chair
Professor Roberto Malinow
Professor Subhojit Roy
Professor Guy Salvesen
Professor Christina Sigurdson

2012

The Dissertation of Brea June Midthune is approved, and it is acceptable in quality and form for publication on microfilm and electronically:

_____

_____

_____

_____

_____

Chair

University of California, San Diego

2012

# DEDICATION

To my family:
I would not be here today without your love and constant support.

# EPIGRAPH

The best scientist is open to experience and begins with romance - the idea that anything is possible.

Ray Bradbury

# TABLE OF CONTENTS

# LIST OF ABBREVIATIONS

AMPA: 2-amino-3-(5-methyl-3-oxo-1,2- oxazol-4-yl)propanoic acid

ACSF: artificial cerebral spinal fluid

AD: Alzheimer's Disease

aa: amino acids

Aβ: amyloid beta

APP: amyloid precursor protein

APLP1: amyloid precursor-like protein1

APLP2: amyloid precursor-like protein 2

AICD: APP intracellular domain

DISC: death-inducing signaling complex

DIV: days *in vitro*

EPSC: excitatory post synaptic current

fEPSP: field excitatory post synaptic potential

GABA: gamma-aminobutyric acid

GFP: green fluorescent protein

HFS: high frequency stimulus

ko: knock out

LTP: long-term potentiation

LTD: long-term depression

ms: millisecond

NFT: neurofibrillary tangle

NMDA: N-methyl-D-aspartate

pA: picoampere

PP: paired-pulse

TM: transmembrane

wt: wild-type

# LIST OF FIGURES

# ACKNOWLEDGEMENTS

First, I would like to acknowledge and thank my advisor, Dr. Edward Koo, for his support and invaluable guidance throughout my five years in the lab.

Also, I would like to thank the Koo lab members who have given me constant support, whether it be academically or personally. A special thank you goes to Sheue-Houy, for guiding me and believing in me, to Floyd for the sweet treats and special orders, and to Hoang, for the patience to help the technophobe in me.

Additionally, I would like to thank Dr. Roberto Malinow, for allowing me to utilize the Malinow lab equipment to perform my seemingly endless experiments and the Malinow lab for adopting me as one of their own. A special thank you goes to Sadegh Nabavi, for the constant stream of support, knowledge, and advice, and for the generous use of your rig.

And finally, I would like to extend my sincere gratitude to my thesis committee; I have enjoyed our meetings and I appreciate the time that you have put forth.

Chapter III, in part, has been published in Molecular and Cellular Neurodegeneration. 2011, Midthune, Brea; Tyan, Sheue-Houy; Walsh, Jessica J; Sarsoza, Floyd; Eggert, Simone; Hof, Patrick R.; Dickstein, Dara L.; Koo, Edward H. "Deletion of the amyloid precursor-like protein 2 (APLP2) does not affect hippocampal neuron morphology or function", Molecular and Cellular Neuroscience, 2012 Apr;49(4):448-55. The dissertation author was the primary investigator and author of this paper.

Chapter IV, in full, is a reprint of the material as it appears in Journal of Biological Chemistry, 2009. Eggert, Simone; Midthune, Brea; Cottrell, Barbara; Koo

Edward H. “Induced dimerization of the amyloid precursor protein leads to decreased amyloid-beta protein production”, Journal of Biological Chemistry, 2009 Oct 16;284(42):28943-52. The dissertation author was the second author of this paper and contributed to the experiments working with SPA4CT (C99), figures 8 and S3.

.

# CURRICULUM VITAE

## EDUCATIONAL BACKGROUND

| | |
|---|---|
| August 2006-2012 | Ph.D. in Molecular Pathology<br>University of California, San Diego<br>La Jolla, CA |
| September 1998-May 2002 | B.S. in Biological Sciences,<br>Minor in Spanish<br>Pacific Lutheran University<br>Tacoma, WA |

## RESEARCH EXPERIENCE

| | |
|---|---|
| September 2007 – Present | Ph.D. student in the lab of Dr. Edward Koo<br>Mechanisms of amyloid-beta induced synaptotoxicity in Alzheimer's disease |
| June 2007-August 2007 | Graduate Research Rotation in the lab of Dr. John Guatelli, UC San Diego<br>NEF's role in HIV-1 entry and infectivity |
| April 2007-June 2007 | Graduate Research Rotation in the lab of Dr. Edward Koo UC San Diego,<br>Amyloid precursor protein trafficking and mechanisms of cell death in Alzheimer's Disease |
| January 2007 – March 2007 | Graduate Research Rotation in the lab of Dr. Stuart Lipton, Burnham Institute for Medical Research, La Jolla<br>The role of neuronal death in HIV-1 related dementia |
| September 2006-December 2006 | Graduate Research Rotation in the lab of Dr. Bruce Torbett, Scripps Research Institute, La Jolla<br>HIV-1 protease resistance and molecular evolution |

| | |
|---|---|
| September 2004 – August 2006 | Research Technician in the lab of Dr. Jan Schnitzer, Sidney Kimmel Cancer Center, San Diego<br>Caveolae trafficking and signalling via the endothelium for targeted drug and gene therapy |

## Publications

**Midthune, B.,** Malinow R., Koo E.H. (2011) Elimination of APP caspase cleavage site D664 attenuates A-beta mediated synaptic depression. (In Preparation)

Walsh J.J., Tyan S.-H., **Midthune, B.**, Eggert, S., Hof, P.R., Koo, E.H., Dickstein, D.L. Comparison of neuronal morphology in the prefrontal cortex of APP knockout and APLP2 knockout mice. (In Preparation)

**Midthune, B.**, Tyan, S.-H., Walsh, J.J., Sarsoza, F., Eggert, E., Hof, P.R., Dickstein, D.L., Koo, E.H. (2012) Deletion of amyloid precursor-like protein 2 (APLP2) does not affect neuron morphology or funtion. Mol. Cell. Neurosci. (2012), doi:10.1016/j.mcn.2012.02.001

Eggert, S., **Midthune B.**, Cottrell BA., Koo EH., Induced dimerization of the amyloid precursor protein leads to decreased amyloid beta production. J. Biol. Chem. (2009) **284,** 28943-28952

## Abstracts/Poster Presentations

**Midthune, B.,** Malinow R., Koo E.H. (2011) Elimination of APP caspase cleavage site D664 attenuates A-beta mediated synaptic depression. Alzheimer's Association

**Midthune, B.**, Tyan, S.-H., Walsh, J.J., Sarsoza, F., Eggert, E., Hof, P.R., Dickstein, D.L., Koo, E.H. (2010) APLP2 contains distinct neuronal functions from its homologue, APP. Society for Neurosience workshop: Update on Alzheimer's Disease.

Walsh J.J., Tyan S.-H., **Midthune, B.**, Eggert, S., Hof, P.R., Koo, E.H., Dickstein, D.L. (2010) Comparison of neuronal morphology in the prefrontal cortex of APP knockout and APLP2 knockout mice. Society for Neuroscience.

Walsh J.J., Tyan S.-H., **Midthune, B.**, Shih, A., Eggert, S., Hof, P.R., Koo, E.H., Dickstein, D.L. (2010) Comparison of neuronal morphology in pyramidal neurons of the CA1, dentate gyrus, and prefrontal cortex in APP knockout and APLP2 knockout mice. Alzheimer's Association International Conference on Alzheimer's Disease.

**Midthune, B.**, Tyan, S.-H., Walsh, JJ., Eggert, S., Dickstein D.L., Hof P.R., Koo E.H. (2009) The morphological and functional significance of the APP homologue, APLP2. Society for Neuroscience Conference

Eggert, S., **Midthune B.**, Cottrell BA., Koo EH., Dimerization of APP and the APP gene family members APLP1 and APLP2 (2007) Society for Neuroscience Conference

**SCHOLARHIPS AND AWARDS**

| | |
|---|---|
| May 2011 – April 2012 | Neuroplasticity of Aging Training Grant, NIH |
| May 2010 – April 2011 | Neuroplasticity of Aging Training Grant, NIH |
| May 2009 – April 2010 | Neuroplasticity of Aging Training Grant, NIH |
| August 2009 | Alzheimer's Association Young Scholar Award |

| | |
|---|---|
| May 2008 – April 2009 | Neuroplasticity of Aging Training Grant, NIH |
| September 2007 – April 2008 | Neuroplasticity of Aging Training Grant, NIH |
| August 1998-May 2002 | President's Scholarship, Pacific Lutheran University |
| August 1998-May 2002 | Q-Club Scholarship, Pacific Lutheran University |

# ABSTRACT OF THE DISSERTATION

## The Role of Amyloid Precursor Protein in Amyloid-Beta-Mediated Synaptic Dysfunction

by

Brea June Midthune

Doctor of Philosophy in Molecular Pathology

University of California, San Diego, 2012

Professor Edward Koo, Chair

Amyloid precursor protein (APP) is a type one transmembrane protein and has two mammalian homologues, amyloid precursor-like protein 1 (APLP1) and amyloid

precursor-like protein 2 (APLP2). APP is the parent molecule to amyloid-β (Aβ), the amyloidogenic species found in the plaques of people with Alzheimer's disease (AD). Several lines of evidence suggest Aβ to lie at the center of AD pathology, with converging evidence to indicate that synapses are the site of the initial damage.

Recent studies have shown that APP may be necessary for the toxicity induced by Aβ, in part by cleavage of a caspase site on the intracellular domain of the APP protein and the subsequent release of the toxic molecule, C31. This caspase cleavage is shown to induce APP-mediated Aβ toxicity in cell culture models, however assays were based on contribution to cell death. Thus, the physiologic relevance of the cleavage event has never been tested and in particular, whether this pathway contributes to synaptic damage is unclear.

Here, we seek to test the role of caspase cleavage of APP in Aβ-induced synaptic damage and to test the specificity of this event by testing whether caspase cleavage of APLP2, the protein most homologous to APP, also contributes to these Aβ-driven synaptic changes. Additionally, because APP dimerization was shown to be necessary for the Aβ-induced caspase cleavage of APP and subsequent release of C31, we wanted to test the effects of dimerization on APP proteolysis and Aβ production.

# Chapter I: Introduction

## I.A. Alzheimer's disease

Alzheimer's disease (AD) is the most common form of dementia amongst the elderly population. Age is the greatest known risk factor and reports indicate that after 65 years of age, the risk of developing AD doubles every 5 years and it is estimated that nearly 50% of those over the age of 85 suffer from AD [1]. In 2010, it was estimated that 35.6 million people suffered from dementia worldwide and the economic impact has topped 600 billion dollars annually[1]. With the average lifespan lengthening due to higher standards of living and improved healthcare, the number of people with AD is expected to increase over 100% in developed countries and up to 300% in developing countries, such as India and China, by 2050 [1, 2]. Currently, there is no cure for AD and approved treatments are only marginally effective in delaying disease progression in select individuals, indicating a real need for additional research towards understanding and treating the debilitating disease [3].

AD was first described in 1907 by German neuropathologist and psychiatrist, Alois Alzheimer. AD is pathologically diagnosed by the presence of extracellular amyloid plaques and intracellular neurofibrillary tangles that are accompanied by progressive synaptic dysfunction and cognitive decline, often with increased difficulty with language and visual perception [3]. Since the initial characterization of the pathology of AD, scientists have sought to discover whether the intracellular neurofibrillary tangles (NFTs) or the extracellular plaques are the primary source of toxicity. NFTs are composed of

hyperphosphorylated tau, a microtubule binding protein that is important for maintaining microtubule stability[4]. The hyperphosphorylation serves to impair the normal function of tau, resulting in aberrant protein trafficking and is seen in traumatic brain injury, as well as many other neurodegenerative diseases [5,6,7].

Though it is probable that both the plaques and tangles contribute to the progression of AD, early on several lines of evidence converged to form a hypothesis that included the amyloid component of the plaques as the primary etiological factor (thus, NFTs are a secondary characteristic) and the term "The Amyloid Cascade Hypothesis" was coined in 1992 by Hardy and Higgins [8]. In this seminal paper, the authors stated that that "deposition of amyloid β protein, the main component of the plaques, is the causative agent of Alzheimer's pathology and that the neurofibrillary tangles, cell loss, vascular damage and dementia follow as a direct result of this deposition" and this was originally based from the fact that Alzheimer's pathology invariably developed in individuals carrying an extra copy of amyloid precursor protein (APP), the parent molecule to amyloid beta (Aβ), and that a number of familial genetic mutations in APP or the proteins known to cleave APP resulted in early-onset AD [8]. Each of the familial mutations favors the production of the longer, more aggregation prone species of Aβ that contains 42 amino acids (aa) (Aβ42), which is also the major isoform contained in the plaques. The most abundant form of Aβ contains 40 aa (Aβ40) [9,10]. Though total amounts of Aβ are not always found to be increased in patients with AD, the ratio of Aβ42 to Aβ40 is increased and this thought to be crucial for disease progression[10, 11].

## I.B. Aβ toxicity

Aβ is generated through sequential cleavages of its parent protein, APP, by β- and γ-secretases (Figure I.1)[12, 13]. Though it is clear that several factors contribute to the progression of the disease, the bulk of data suggest Aβ to be the primary etiological factor, which leads to synaptic dysfunction, cognitive impairment and the eventual loss of neurons [14]. Intracellular and extracellular protein aggregates are known to be drivers of many neurodegenerative disorders [15] and the initial interpretations of Aβ toxicity in AD implicated the extracellular fibrillar forms of Aβ to lead to the synapse dysfunction and neuronal cell death. This was refuted, however, as plaque load did not correlate well with the severity of disease [16]. Subsequent findings demonstrated that levels of soluble Aβ and synapse loss correlate to a much higher extent and this lead to the suggestion that the soluble species of Aβ imparts the major source of toxicity, driving the progression of AD [17, 18]. Subsequent studies have largely corroborated this theory, though difficulties in maintaining a consistent toxic concentration of Aβ has been a major issue and has made it difficult to interpret studies.

Importantly, APP is cleaved in such a way that a variety of lengths of Aβ exist, creating a heterogenous mixture with a variety of solubilities and aggregation properties[19, 20]. As mentioned previously, Aβ42 is thought to be the major source of toxicity, due the fact that it contains additional hydrophophic amino acids, adding to its propensity to aggregate[21, 22]. This is important, as recent studies have convincingly proven that the oligomerization state of Aβ is crucial for its toxic properties and this is

likely to be the major reason for the wide range of results in Aβ toxicity studies[14, 23, 24]. Recent reports show that while monomers remain relatively benign, low concentrations of dimers and trimers rapidly leads to synaptic dysfunction and synapse loss[24], suggesting that synapses may be the initial site of Aβ toxicity, though it should be noted that other oligomer states of Aβ have been reported to contain toxic properties, such as the so-called *56[25].

Thus, while many reports have shown that the application of soluble Aβ leads to a rapid reduction in spines, synaptic depression, impaired synaptic plasticity and cognitive decline there remains questions as to which species is the most relevant to AD[26]. While current evidence points to a disease that progresses via Aβ-driven synapse loss, the molecular mechanisms mediating the synaptic dysfunction and neuronal toxicity are still largely unknown.

## I.C. Caspases

Caspases are a family of cysteine-dependent aspartate directed proteases that propagate intra- and inter-cellular signaling and are traditionally associated to their role as executioners of apoptosis, a regulated form of cell death[27]. There are 14 known mammalian caspases, 11 of which are encoded in the human genome[28]. Apoptotic caspases are generally segregated into two major groups, initiators (caspase-2, -8, -9, -10) and effectors (caspase-3,-6,-7) and are initially synthesized in an inactive form called a zymogen[27]. Effector caspases become active upon proteolytic cleavage by initiator caspases, while initiator caspases are auto-activated upon dimerization [28, 29].

In mammalian cells, the apoptotic response is mediated through either of two main pathways, the intrinsic pathway or the extrinsic pathway, depending on the origin of the death stimuli (Figure I.2). Upon certain stimuli, the intrinsic pathway is activated and regulated by a family of apoptosis regulating proteins, the B-cell lymphoma 2 (bcl-2) family. This family consists of 25 genes, many of which function as pro- and anti-apoptotic proteins that interact with one another to drive a final outcome. Under apoptotic conditions, the pro-apoptotic bcl-2 proteins oligomerize and insert themselves into the mitochondrial membrane, releasing several key proteins into the cytoplasm. One key pro-apoptotic protein is cytochrome *c*, which binds to and activates apoptotic protease activating factor 1 (APAF1), in the cytoplasm. The binding of cytochrome *c* to APAF1 induces a conformational change that allows APAF1 to bind to ATP/dATP to form an apoptosome, which mediates the activation of initiator caspase-9 thereby triggering a cascade of caspase activation[30].

The extrinsic pathway is mediated by so-called death receptors that mediate and internalize external pro-apoptotic signals upon the binding of specific death ligands. The binding of the homotrimeric death ligand induces dimerization of the receptors and this recruits initiator caspase-8 and allows for the formation of a death inducing signaling complex (DISC). This promotes the activation of caspase-8, which then leads to the activation of downstream, effector caspases, ultimately resulting in amplification of the signal[27, 31].

While caspases are often associated with their role in the traditional apoptotic pathways that lead to cell death, many recent lines of evidence indicate that caspases and caspase activation are important for a variety of non-apoptotic functions. Caspases are

now known to be involved in immunity, cell differentiation and proliferation and synaptic plasticity[32]. This indicates a broad spectrum of diversity in function and highlights the fact that caspases are not proteins driving non-specific toxic processes, but are involved in specific and highly regulated signaling pathways.

## I.D. Caspases in neurodegeneration

Apoptotic mechanisms involving caspases are well documented to help refine neuronal circuitry in the developing nervous system and have also long been implicated in normal aging neurons, as well as several neurodegenerative disorders, such as amyotrophic lateral sclerosis (ALS), Huntington's Disease, and Parkinson's Disease[33]. The fact that caspases appear long before neuronal death occurs had lead to questions as to the precise role and time scale of caspase activation in neurodegenerative disorders[34].

Several papers implicate caspase involvement in AD as well. Western blots and immunohistochemical staining from several studies reveal a statistically significant increase in activated caspases in the brains of patients with AD when compared to age match control brains [35, 36], while synaptic fractionation reveals an increase of activated caspase-3 [37]. Additionally, neuronal death is well defined as hippocampal volume decreases with progression disease progression[38]. Recently, it was reported that caspase activation is apparent by three months of age in one mouse model of AD, a time at which synaptic dysfunction and cognition was found to initially decline, and that caspase activity is necessary for acute Aβ mediated impairment in long-term potentiation[38, 39].

Collectively, this provides evidence that caspases are localized to the synapse and may contribute to neuronal dysfunction and synapse loss early in disease progression.

Interestingly, Jo et al. published a role for caspase activation in long-term depression (LTD), a physiological type of synaptic plasticity important for learning and memory and showed that the degree and duration of caspase activity affects whether neurons display signs of synaptic plasticity versus apoptosis[40]. While this is interesting, it is still unknown whether caspase activation in AD results from a disturbance of the normal physiological process or if the event is independent.

## I.E. APP-mediated Aβ toxicity

Various studies demonstrated a role for APP in Aβ–mediated toxicity[35, 41]. Recently, our lab used APP knockout ($APP^{-/-}$) mice to test the hypothesis that APP-mediated Aβ toxicity is important for early events in AD, such as synaptic dysfunction and the retraction of spines. Using primary hippocampal cultures from these mice, we see no additional spine loss upon administration of Aβ, while we see a 40% reduction in spines after Aβ incubation from wild type neurons. Additionally, we found that brain slices from young $APP^{-/-}$ animals are resistant to the Aβ-induced reduction in LTP as seen in control animals[42]. These results from our lab indicate that APP is necessary to impart Aβ synaptotoxicity.

Interestingly, APP can be cleaved by caspases at site 664, the intracellular C-terminal region of the protein (Figure I.3). Gervais et al. originally identified an increase of activation of caspases caspase cleaved APP in the brains of people with AD, which

was later extended to show that it was preferentially increased in early stages of AD [36, 43]. How this cleavage event may be important for the progression AD is still unclear, yet several groups have reported that the introduction of either of the two intracellular protein products derived from this cleavage, termed J-casp and C31, impart toxicity on their own [35, 44]. Though intriguing and informative, these studies used transient overexpression of C31 in a variety stable cell lines with cellular death as the final outcome, thus whether caspase cleavage of APP and release of C31 is important for early synaptic dysfunction is still unclear.

## I.F. APP and Aβ: Binding partners?

Due to the sequence and structure, initial reports hypothesized APP to be a cell surface receptor. Reports that Notch, a similarly cleaved transmembrane protein signals via proteolytic processing strengthened this hypothesis [45]. However, efforts at finding a *de facto* ligand for APP have proven difficult, though several have been suggested [45]. Mounting evidence favors Aβ as a binding partner and it is shown to bind to its cognate region, APP597-624 [35 46]. Though APP had already been known to homo- and hetero-dimerize with APLP1 and APLP2, co-immunoprecipitation revealed that APP also binds to Aβ and that addition of Aβ increases this homo-dimerization event. This study went on to show that dimerization, in turn, increases cell death in N2a cells and interestingly, this event was modulated by the caspase cleavage of the intracellular portion of APP[46]. Interestingly, this suggests that the interaction of APP and Aβ promotes oligomerization of APP and caspase activation, a mechanism similar to the classical extrinsic apoptotic

pathway, whereby APP is acting as the death receptor and Aβ constitutes its death ligand (Figure I.4).

## I.G. APP dimerization and proteolysis

Biochemical and structural data has shown that APP is able to homo- and hetero-dimerize via the cognate E1, E2 and Aβ domains. While not a lot is known about the function of dimerization that occur*s in vivo, in vitro* studies suggest a function for homodimerization in cell-cell adhesion, cell signaling, and in caspase activation[47, 48].

APP's association with itself and other proteins is known to affect its cleavage by β- and γ–secretase. And as predicted, the dimerization event has been reported to alter the proteolytic cleavage of APP, though results have been conflicting. For example, mutation of a lysine residue by cysteine at the juxtamembrane region of APP (K624C mutant) resulted in constitutive APP dimerization via a disulfide bond, and this resulted in an increase of Aβ levels[49]. In the opposite approach, a decrease of toxic Aβ42 was reported upon the disruption of the GxxxG transmembrane dimerization motif of APP[50] and mutant G33I abolished both dimerization and Aβ production. Still, others studying the GxxxG have reported increased APP dimerization at the C-terminal domain leads to a decrease in Aβ[51]. The reason for the difference is unknown, but it is suggested that the mutations themselves may affect secretase cleavage, independent of the dimerization event.

## I.H. APP and its homologues

APP belongs to a family of proteolysis dependent type 1 transmembrane proteins, which includes the mammalian proteins amyloid precursor-like protein 1 (APLP1) and amyloid precursor-like protein 2 (APLP2) [14]. All three undergo extensive proteolytic processing, producing a number of secreted fragments (Figure I.5) [52]. APP and APLP2 are the most homologous, both with isoforms containing a KPI domain and a highly overlapping multi tissue expression pattern [53]. Though functions are not fully elucidated, these proteins are highly conserved and homologues are known to exist in rodents, C. elegans (APL) [54] and Drosophila (APPL) [55]. Rodent studies revealed that the deletion of just one gene in this family produces mice that are viable and fertile with relatively mild phenotypes.

Interestingly, two of three double knock-outs ($APP^{-/-}$;$APLP2^{-/-}$ and $APLP2^{-/-}$;$APLP1^{-/-}$) begat perinatal lethality [56, 57], suggesting these proteins retain vitally important functions masked by functional redundancy. Though this redundancy has lead to some difficulties in extracting and interpreting defined roles, further studies of APP indicate more discrete functions in numerous neuronal processes such as: cell adhesion, dendritic outgrowth, axonal transport, synapse formation and synapse modulation [53]. This diversity of roles is attributed to its numerous proteolytic products. For example, it is reported that the extracellular secreted product (sAPP) is important for neurite outgrowth while the holoprotein acts in cellular adhesion and axonal transport. Furthermore, the Aβ fragment of APP is important for synapse modulation and is also the neurotoxic species implicated in AD [58, 59]. Studies of APLP1 and APLP2 have been far less extensive due to

the fact that they do not contain the Aβ domain, though more studies need to be done in order to completely understand the relevance of this family of proteins as a whole. Our lab and others have shown that the loss of APP affects dendritic outgrowth, synapse formation and function [60, 61] and confers resistance to Aβ toxicity [41, 62] and whether this extends to its homologues is unknown.

# I.I. Figures

Figure I.1

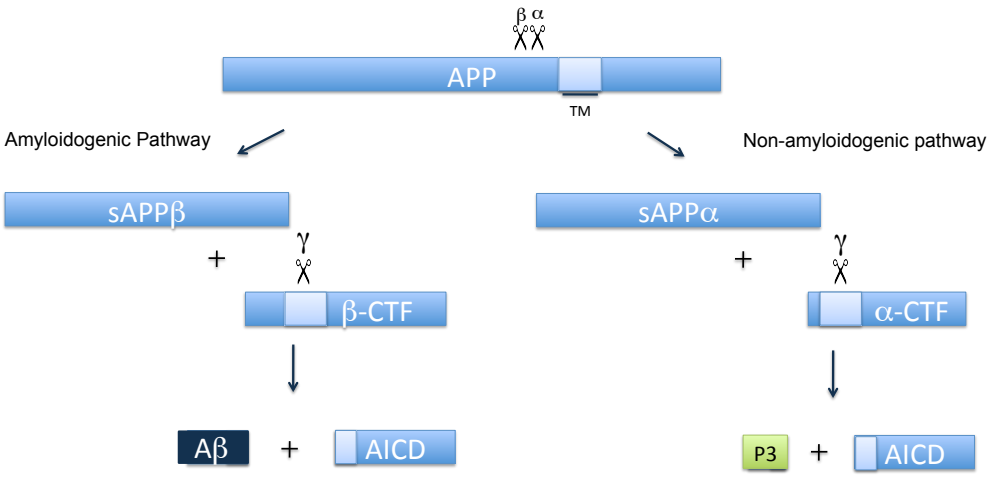


**Figure I-1:** A schematic diagram of APP and the generation of Aβ. APP is first cleaved by either α- or β-secretase, leading to either of two distinct pathways, the amyloidogenic pathway or the non-amyloidogenic pathway. Aβ is produced via the amyloidogenic pathway and is initiated upon β−secretase cleavage to yield sAPPβ and β-CTF. β-CTF is then cleaved by γ-secretase to release Aβ and APP intracellular domain (AICD). Alternatively, the non-amyloidogenic pathway commences with cleavage by α-secratase to generate sAPPα and α-CTF. α-CTF is then cleaved by γ-secretase to yield the products, P3 and AICD. TM indicates transmembrane domain.

Figure I.2

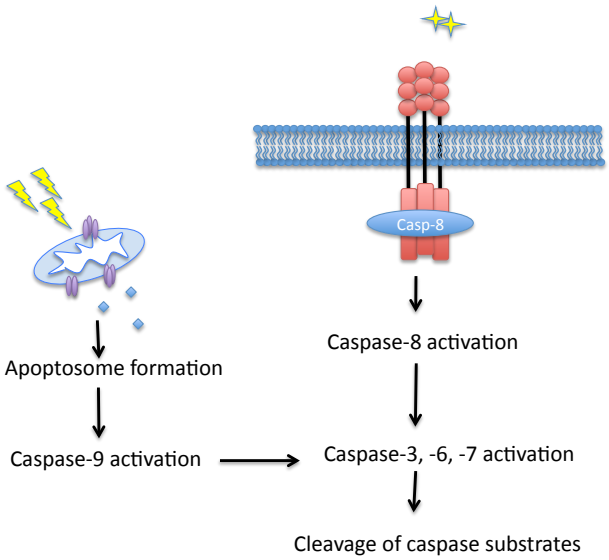


**Figure I.2:** Classical apoptotic pathways. The intrinsic pathway involves the oligomerization and insertion of proapoptotic proteins into the mitochondrial membrane upon certain stimuli. This leads to the release of key proteins into the cytoplasm that bind Apaf1 to form an apoptosome, allowing for the activation of caspase-9. The extrinsic pathway involves specific death ligands that bind to their specific death receptor, leading to the dimerization of the receptor. Caspase-8 is then recruited and activated upon dimerizaiton and formation of the death-inducing signaling complex (DISC). Both pathways are initiated via ininitiator caspases and propagated via the activation of effector caspases, allowing for the amplification of signal and cleavage of substrates.

Figure I.3

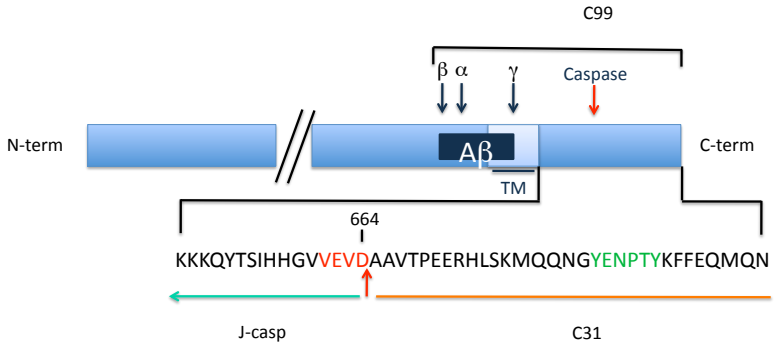


**Figure I.3:** Caspase cleavage of APP at site 664 (APP695 numbering). Caspase cleavage of APP at site 664 generates two intracellular cleavage products, J-casp and C31. TM indicates transmembrane domain. Red text signifies the caspase recognition motif. Adapted from Weidemann A. et al., 1999.

Figure I.4

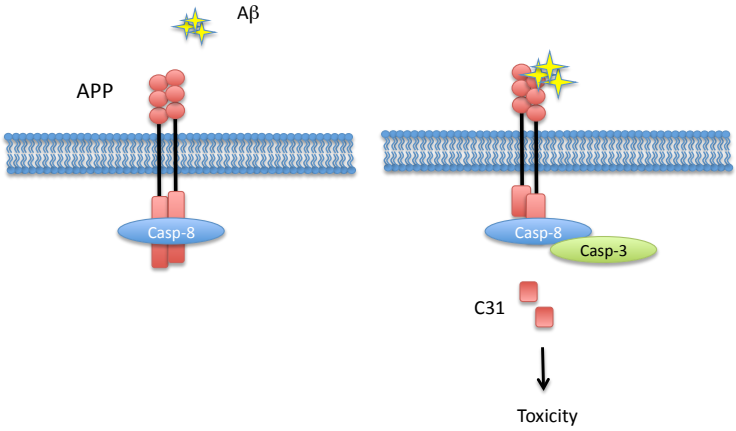


**Figure I.4:** APP as a death receptor. In this model, APP acts as a death receptor with Aβ as its death ligand. Upon binding, APP dimerizes or oligomerizes and recruits caspase-8 to form a death-inducing signaling complex (DISC). This leads to the activation of caspase-8 and downstream caspases, the subsequent cleavage of APP and release of C31.

Figure I.5

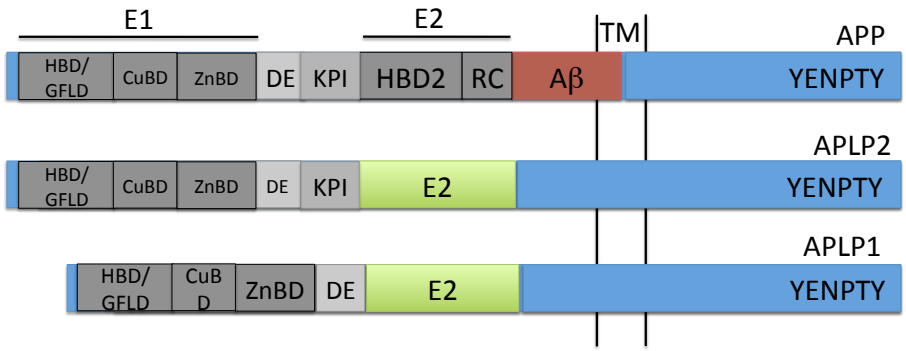


**Figure I.5:** APP and its homologues. All homologues contain the heparin-binding/growth-factor-like domains (HBD/GFLD), the copper- Zinc-binding domains (CuBD and ZnBD), the acidic domain (DE) and a YENPTY protein interaction sequence. Neither APLP2 nor APLP1 contain the aggregation prone Aβ domain. TM indicates the transmembrane domain.

References

1. Prince AWaM. Alzheimer's Disease International World Alzheimer's Report 2010, The Global Impact of Dementia. Alzheimer's Disease International. 2010 21 September 2010.

2. Association. As. 2012 Alzheimer's disease facts and figures. Alzheimer's and Dementia: The Journal of the Alzheimer's Association March 2012(8):131–68.

3. Tayeb HO, Yang HD, Price BH, Tarazi FI. Pharmacotherapies for Alzheimer's disease: beyond cholinesterase inhibitors. Pharmacol Ther. 2012 Apr;134(1):8-25.

4. Weingarten MD, Lockwood AH, Hwo SY, Kirschner MW. A protein factor essential for microtubule assembly. Proc Natl Acad Sci U S A. 1975 May;72(5):1858-62.

5. Bramblett GT, Goedert M, Jakes R, Merrick SE, Trojanowski JQ, Lee VM. Abnormal tau phosphorylation at Ser396 in Alzheimer's disease recapitulates development and contributes to reduced microtubule binding. Neuron. 1993 Jun;10(6):1089-99.

6. Lee VM, Trojanowski JQ. The disordered neuronal cytoskeleton in Alzheimer's disease. Curr Opin Neurobiol. 1992 Oct;2(5):653-6.

7. Gabbita SP, Scheff SW, Menard RM, Roberts K, Fugaccia I, Zemlan FP. Cleaved-tau: a biomarker of neuronal damage after traumatic brain injury. J Neurotrauma. 2005 Jan;22(1):83-94.

8. Hardy JA, Higgins GA. Alzheimer's disease: the amyloid cascade hypothesis. Science. 1992 Apr 10;256(5054):184-5.

9. Scheuner D, Eckman C, Jensen M, Song X, Citron M, Suzuki N, et al. Secreted amyloid beta-protein similar to that in the senile plaques of Alzheimer's disease is increased in vivo by the presenilin 1 and 2 and APP mutations linked to familial Alzheimer's disease. Nat Med. 1996 Aug;2(8):864-70.

10. Kuperstein I, Broersen K, Benilova I, Rozenski J, Jonckheere W, Debulpaep M, et al. Neurotoxicity of Alzheimer's disease Abeta peptides is induced by small changes in the Abeta42 to Abeta40 ratio. EMBO J. 2010 Oct 6;29(19):3408-20.

11. Selkoe DJ. Alzheimer's disease: genes, proteins, and therapy. Physiol Rev. 2001 Apr;81(2):741-66.

12. Kang J, Lemaire HG, Unterbeck A, Salbaum JM, Masters CL, Grzeschik KH, et al. The precursor of Alzheimer's disease amyloid A4 protein resembles a cell-surface receptor. Nature. 1987 Feb 19-25;325(6106):733-6.

13. Esch FS, Keim PS, Beattie EC, Blacher RW, Culwell AR, Oltersdorf T, et al. Cleavage of amyloid beta peptide during constitutive processing of its precursor. Science. 1990 Jun 1;248(4959):1122-4.

14. Hardy J, Selkoe DJ. The amyloid hypothesis of Alzheimer's disease: progress and problems on the road to therapeutics. Science. 2002 Jul 19;297(5580):353-6.

15. Benilova I, Karran E, De Strooper B. The toxic Abeta oligomer and Alzheimer's disease: an emperor in need of clothes. Nat Neurosci. 2012 Mar;15(3):349-57.

16. Terry RD, Masliah E, Salmon DP, Butters N, DeTeresa R, Hill R, et al. Physical basis of cognitive alterations in Alzheimer's disease: synapse loss is the major correlate of cognitive impairment. Ann Neurol. 1991 Oct;30(4):572-80.

17. Lue LF, Kuo YM, Roher AE, Brachova L, Shen Y, Sue L, et al. Soluble amyloid beta peptide concentration as a predictor of synaptic change in Alzheimer's disease. Am J Pathol. 1999 Sep;155(3):853-62.

18. McLean CA, Cherny RA, Fraser FW, Fuller SJ, Smith MJ, Beyreuther K, et al. Soluble pool of Abeta amyloid as a determinant of severity of neurodegeneration in Alzheimer's disease. Ann Neurol. 1999 Dec;46(6):860-6.

19. Iwatsubo T, Saido TC, Mann DM, Lee VM, Trojanowski JQ. Full-length amyloid-beta (1-42(43)) and amino-terminally modified and truncated amyloid-beta 42(43) deposit in diffuse plaques. Am J Pathol. 1996 Dec;149(6):1823-30.

20. Qi-Takahara Y, Morishima-Kawashima M, Tanimura Y, Dolios G, Hirotani N, Horikoshi Y, et al. Longer forms of amyloid beta protein: implications for the mechanism of intramembrane cleavage by gamma-secretase. J Neurosci. 2005 Jan 12;25(2):436-45.

21. Jarrett JT, Berger EP, Lansbury PT, Jr. The carboxy terminus of the beta amyloid protein is critical for the seeding of amyloid formation: implications for the pathogenesis of Alzheimer's disease. Biochemistry. 1993 May 11;32(18):4693-7.

22. Jarrett JT, Lansbury PT, Jr. Seeding "one-dimensional crystallization" of amyloid: a pathogenic mechanism in Alzheimer's disease and scrapie? Cell. 1993 Jun 18;73(6):1055-8.

23. Hartley DM, Walsh DM, Ye CP, Diehl T, Vasquez S, Vassilev PM, et al. Protofibrillar intermediates of amyloid beta-protein induce acute electrophysiological changes and progressive neurotoxicity in cortical neurons. J Neurosci. 1999 Oct 15;19(20):8876-84.

24. Townsend M, Shankar GM, Mehta T, Walsh DM, Selkoe DJ. Effects of secreted oligomers of amyloid beta-protein on hippocampal synaptic plasticity: a potent role for trimers. J Physiol. 2006 Apr 15;572(Pt 2):477-92.

25. Lesne S, Koh MT, Kotilinek L, Kayed R, Glabe CG, Yang A, et al. A specific amyloid-beta protein assembly in the brain impairs memory. Nature. 2006 Mar 16;440(7082):352-7.

26. Ma T, Klann E. Amyloid beta: linking synaptic plasticity failure to memory disruption in Alzheimer's disease. J Neurochem. 2012 Jan;120 Suppl 1:140-8.

27. Pop C, Salvesen GS. Human caspases: activation, specificity, and regulation. J Biol Chem. 2009 Aug 14;284(33):21777-81.

28. Shi Y. Mechanisms of caspase activation and inhibition during apoptosis. Mol Cell. 2002 Mar;9(3):459-70.

29. Riedl SJ, Shi Y. Molecular mechanisms of caspase regulation during apoptosis. Nat Rev Mol Cell Biol. 2004 Nov;5(11):897-907.

30. Martinou JC, Youle RJ. Mitochondria in apoptosis: Bcl-2 family members and mitochondrial dynamics. Dev Cell. 2011 Jul 19;21(1):92-101.

31. Scott FL, Stec B, Pop C, Dobaczewska MK, Lee JJ, Monosov E, et al. The Fas-FADD death domain complex structure unravels signalling by receptor clustering. Nature. 2009 Feb 19;457(7232):1019-22.

32. Yi CH, Yuan J. The Jekyll and Hyde functions of caspases. Dev Cell. 2009 Jan;16(1):21-34.

33. Yuan J, Yankner BA. Apoptosis in the nervous system. Nature. 2000 Oct 12;407(6805):802-9.

34. Friedlander RM. Apoptosis and caspases in neurodegenerative diseases. N Engl J Med. 2003 Apr 3;348(14):1365-75.

35. Lu DC, Rabizadeh S, Chandra S, Shayya RF, Ellerby LM, Ye X, et al. A second cytotoxic proteolytic peptide derived from amyloid beta-protein precursor. Nat Med. 2000 Apr;6(4):397-404.

36. Gervais FG, Xu D, Robertson GS, Vaillancourt JP, Zhu Y, Huang J, et al. Involvement of caspases in proteolytic cleavage of Alzheimer's amyloid-beta precursor protein and amyloidogenic A beta peptide formation. Cell. 1999 Apr 30;97(3):395-406.

37. Louneva N, Cohen JW, Han LY, Talbot K, Wilson RS, Bennett DA, et al. Caspase-3 is enriched in postsynaptic densities and increased in Alzheimer's disease. Am J Pathol. 2008 Nov;173(5):1488-95.

38. Jack CR, Jr., Petersen RC, Xu Y, O'Brien PC, Smith GE, Ivnik RJ, et al. Rates of hippocampal atrophy correlate with change in clinical status in aging and AD. Neurology. 2000 Aug 22;55(4):484-89.

39. D'Amelio M, Cavallucci V, Middei S, Marchetti C, Pacioni S, Ferri A, et al. Caspase-3 triggers early synaptic dysfunction in a mouse model of Alzheimer's disease. Nat Neurosci. 2011 Jan;14(1):69-76.

40. Li Z, Jo J, Jia JM, Lo SC, Whitcomb DJ, Jiao S, et al. Caspase-3 activation via mitochondria is required for long-term depression and AMPA receptor internalization. Cell. 2010 May 28;141(5):859-71.

41. Lorenzo A, Yuan M, Zhang Z, Paganetti PA, Sturchler-Pierrat C, Staufenbiel M, et al. Amyloid beta interacts with the amyloid precursor protein: a potential toxic mechanism in Alzheimer's disease. Nat Neurosci. 2000 May;3(5):460-4.

42. Tyan SH, Shih AY, Walsh JJ, Murayama H, Sarsoza F, Ku L, et al. Amyloid precursor protein (APP) regulates synaptic structure and function. Mol Cell Neurosci. 2012 Aug 3.

43. Banwait S, Galvan V, Zhang J, Gorostiza OF, Ataie M, Huang W, et al. C-terminal cleavage of the amyloid-beta protein precursor at Asp664: a switch associated with Alzheimer's disease. J Alzheimers Dis. 2008 Feb;13(1):1-16.

44. Park SA, Shaked GM, Bredesen DE, Koo EH. Mechanism of cytotoxicity mediated by the C31 fragment of the amyloid precursor protein. Biochem Biophys Res Commun. 2009 Oct 16;388(2):450-5.

45. Annaert W, De Strooper B. Presenilins: molecular switches between proteolysis and signal transduction. Trends Neurosci. 1999 Oct;22(10):439-43.

46. Shaked GM, Kummer MP, Lu DC, Galvan V, Bredesen DE, Koo EH. Abeta induces cell death by direct interaction with its cognate extracellular domain on APP (APP 597-624). FASEB J. 2006 Jun;20(8):1254-6.

47. Soba P, Eggert S, Wagner K, Zentgraf H, Siehl K, Kreger S, et al. Homo- and heterodimerization of APP family members promotes intercellular adhesion. EMBO J. 2005 Oct 19;24(20):3624-34.

48. Lu DC, Shaked GM, Masliah E, Bredesen DE, Koo EH. Amyloid beta protein toxicity mediated by the formation of amyloid-beta protein precursor complexes. Ann Neurol. 2003 Dec;54(6):781-9.

49. Scheuermann S, Hambsch B, Hesse L, Stumm J, Schmidt C, Beher D, et al. Homodimerization of amyloid precursor protein and its implication in the amyloidogenic pathway of Alzheimer's disease. J Biol Chem. 2001 Sep 7;276(36):33923-9.

50. Munter LM, Voigt P, Harmeier A, Kaden D, Gottschalk KE, Weise C, et al. GxxxG motifs within the amyloid precursor protein transmembrane sequence are critical for the etiology of Abeta42. EMBO J. 2007 Mar 21;26(6):1702-12.

51. Kienlen-Campard P, Tasiaux B, Van Hees J, Li M, Huysseune S, Sato T, et al. Amyloidogenic processing but not amyloid precursor protein (APP) intracellular C-terminal domain production requires a precisely oriented APP dimer assembled by transmembrane GXXXG motifs. J Biol Chem. 2008 Mar 21;283(12):7733-44.

52. Eggert S, Paliga K, Soba P, Evin G, Masters CL, Weidemann A, et al. The proteolytic processing of the amyloid precursor protein gene family members APLP-1 and APLP-2 involves alpha-, beta-, gamma-, and epsilon-like cleavages: modulation of APLP-1 processing by n-glycosylation. J Biol Chem. 2004 Apr 30;279(18):18146-56.

53. Jacobsen KT, Iverfeldt K. Amyloid precursor protein and its homologues: a family of proteolysis-dependent receptors. Cell Mol Life Sci. 2009 Jul;66(14):2299-318.

54. Hornsten A, Lieberthal J, Fadia S, Malins R, Ha L, Xu X, et al. APL-1, a Caenorhabditis elegans protein related to the human beta-amyloid precursor protein, is essential for viability. Proc Natl Acad Sci U S A. 2007 Feb 6;104(6):1971-6.

55. Luo L, Tully T, White K. Human amyloid precursor protein ameliorates behavioral deficit of flies deleted for Appl gene. Neuron. 1992 Oct;9(4):595-605.

56. von Koch CS, Zheng H, Chen H, Trumbauer M, Thinakaran G, van der Ploeg LH, et al. Generation of APLP2 KO mice and early postnatal lethality in APLP2/APP double KO mice. Neurobiol Aging. 1997 Nov-Dec;18(6):661-9.

57. Zheng H, Jiang M, Trumbauer ME, Sirinathsinghji DJ, Hopkins R, Smith DW, et al. beta-Amyloid precursor protein-deficient mice show reactive gliosis and decreased locomotor activity. Cell. 1995 May 19;81(4):525-31.

58. Hsieh H, Boehm J, Sato C, Iwatsubo T, Tomita T, Sisodia S, et al. AMPAR removal underlies Abeta-induced synaptic depression and dendritic spine loss. Neuron. 2006 Dec 7;52(5):831-43.

59. Kamenetz F, Tomita T, Hsieh H, Seabrook G, Borchelt D, Iwatsubo T, et al. APP processing and synaptic function. Neuron. 2003 Mar 27;37(6):925-37.

60. Fitzjohn SM, Morton RA, Kuenzi F, Davies CH, Seabrook GR, Collingridge GL. Similar levels of long-term potentiation in amyloid precursor protein -null and wild-type mice in the CA1 region of picrotoxin treated slices. Neurosci Lett. 2000 Jul 7;288(1):9-12.

61. Seabrook GR, Smith DW, Bowery BJ, Easter A, Reynolds T, Fitzjohn SM, et al. Mechanisms contributing to the deficits in hippocampal synaptic plasticity in mice lacking amyloid precursor protein. Neuropharmacology. 1999 Mar;38(3):349-59.

62. Sola Vigo F, Kedikian G, Heredia L, Heredia F, Anel AD, Rosa AL, et al. Amyloid-beta precursor protein mediates neuronal toxicity of amyloid beta through Go protein activation. Neurobiol Aging. 2009 Sep;30(9):1379-92.

# Chapter II: Absence of APP Intracellular Caspase Cleavage Site Attenuates Aβ-Mediated Synaptic Depression

## II.A. Abstract

Increasing evidence favors the synapse as the initial site of neuronal damage by amyloid-beta protein (Aβ) and such synaptic damage is thought to underlie the cognitive deficits seen in Alzheimer's disease (AD). While local caspase activation has been documented in synaptic preparations, recent studies have indicated a role for caspases in AD-related neuronal dysfunction and memory loss. However, the mechanisms linking caspase activation, Aβ and AD are not known.

Interestingly, previous studies have suggested that Aβ-induced cell death is attenuated in the absence of APP and this effect may be mediated by the intracellular caspase cleavage of APP, leading to the release of C31 peptide. However, virtually all cell-based studies assessed cell death and support for this mechanism in Aβ-induced synaptic dysfunction has not been rigorously tested.

Previously, it was shown that that expression of the APP C-terminal fragment (C99) resulted in a reduction of AMPAR- and NMDAR-mediated synaptic transmission, concomitant with a loss of dendritic spines, and this was shown to be due to Aβ production. Similarly, we demonstrate that caspase activity is necessary for this type of acute Aβ-induced synaptic depression and that this is mediated via caspase-3. Additionally, we show that substitution of the obligatory aspartate residue at site 664 abrogates caspase cleavage and that this attenuates Aβ-mediated synaptic depression. This suggests a link between Aβ, caspase activation, and synaptic

dysfunction in AD that is mediated through APP. Ongoing studies are focused on whether there are structural correlates (i.e. preservation of dendritic spines) that accompany these electrophysiological changes. However, it remains to be established how APP contributes to synaptic injury in the context of other proposed pathways of Aβ toxicity.

## II.B. Introduction

Alzheimer's disease (AD) is an age-related progressive neurodegenerative disorder that affects memory and cognition. AD is pathologically characterized by intracellular neurofibrillary tangles composed of hyper-phosphorylated tau, extracellular plaques rich in amyloid-beta (Aβ), and synapse loss, with significant neuronal death detected in late stages of the disease. The majority of studies implicate Aβ, a proteolytic product of amyloid precursor protein (APP), as the primary etiological factor and the synapse as the initial site of damage with synapse dysfunction and synapse loss preceding neuronal death. Though the specific pathways in which Aβ exerts this syanptotoxicity remain largely unknown, recent lines of evidence suggests a role for caspase activation in Aβ-mediated synaptic dysfunction[1].

Caspases are cysteine-dependent aspartate-directed proteases traditionally associated with apoptosis, a cellular process that directs programmed cell death. Caspases are initially produced as zymogens, but become active upon specific stimuli[2]. Consistent with the progressive neuron loss seen in late-stage AD, increased caspase activation is also detected in the brains of people with AD [3-6], with reports that the primary site of increased caspase activation is localized to the

synapse [7]. Caspase activation is reported to be upregulated early in AD progression [8, 9] and recently it was reported that increased caspase-3 activation is detectable in an animal model of AD that lacks cell death. Moreover, inhibition of caspase-3 activity ameliorated Aβ-induced synaptic depression and behavioral deficits at 3 months of age [10]. This indicates that caspases may have a role in synaptic dysfunction that precedes apoptotic cell death.

Interestingly, among the many proposed pathways that Aβ exerts its effects, studies have shown that caspase cleavage of APP is a necessary component for Aβ-mediated toxicity. Caspase cleavage of APP is known to occur in the brains of people with AD, and this cleavage event correlates with disease severity[11]. Additionally, there is a battery of work identifying the molecular mechanisms linking Aβ-mediated toxicity and the caspase cleavage of APP. The majority of these studies demonstrate that the toxicity is exerted via the release of the APP C-terminal product, C31[6, 12, 13]. These studies are quite convincing, yet most of the initial reports are cell-based studies that assessed cell death, hence whether or not this mechanism is relevant to synapse dysfunction is not clear. Since then, various studies utilizing a transgenicc mouse model have suggested a role for caspase cleavage of APP in early AD pathology and symptoms, but the results have varied[14-16]. Thus, while there is support for a role of APP in Aβ-mediated synaptic dysfunction, it has not been rigorously tested.

Here, we demonstrate that caspase activation is necessary for Aβ-mediated synaptic depression and this specifically involves caspase-3. We also report that elimination of APP caspase cleavage site D664 ameliorates Aβ-mediated synaptic

depression, suggesting that caspase cleavage of APP is a necessary event. Additionally, preliminary observations indicate that APP cleavage product, C31, imparts neuronal toxicity, however more studies need to be done. We are working on a system of reduced C31 expression to test whether sub-lethal levels of C31 are sufficient to induce the reduction in AMPAR- and NMDAR-mediated synaptic transmission.

## II.C. Materials and Methods

### Hippocampal Slice Culture

Hippocampal slice cultures were prepared from 6- to 8-day-old Sprague Dawley rats and maintained as described previously (Stoppini et al, 1991). Briefly, hippocampal slices were cut in ice cold low sodium cutting buffer at a thickness of 400 uM using a McIIwan Chopper and maintained on semipermable membrane inserts in six well plates and maintained at 35° C. Medium was changed every 2-3 days.

### Constructs and Virus Preparation

Sindbis virus (Invitrogen) containing APP b-CTF (CT100) IRES eGFP was used as described (Kamenetz et al, 2003). An aspartate to alanine substitution was introduced at APP site 664 (695 numbering) using site directed mutagenesis (Quikchange, Stratagene). Sindbis virus was prepared using an expression system (Invitrogen) and in accordance with manufacturer's directions. Briefly, RNA was prepared from cDNA viral constructs (mMessage mMachine SP6, Ambion) and delivered into BHK cells along with helper virus via electroporation and allowed to

incubate for 36 hours. Medium was collected and virus was spun at 35,000 RPM for 90 min at 4°.

**Aβ Immunoprecipitation and Western Blots**

BHK cells were infected with Sindbis virus and allowed to incubate overnight. Medium was extracted and mixed with antibody mAb Ab-9 (2 mg/ml), protease inhibitor (Sigma), mouse IgG agarose and sepharose at 4° overnight. Mixture was washed and loaded with 2X sample buffer with DTT and run on a 12% Bis/Tris gel. Samples were transferred onto nitrocellulose and Aβ was detected with 82E1. Cell lysates were made with standard RIPA buffer and 4X sample buffer with DTT and run a 12% Bis/Tris gel and transferred to nitrocellulose. Antibodies used: Ab-9 (Aβ 1-16) (T.Golde); 82E1 (Aβ N-term); CT-15 (APP 680-695); B436 (Aβ 1-16); a-664 (APP caspase cleavage site 664) (D. Bredesen); 6E10 (Aβ 1-16) (Covance).

**ELISA**

Aβ sandwich ELISAs were preformed as described previously (Kukar et al. 2005). Briefly, media was collected and diluted appropriately. mAb mm26.2.1.35 (anti-Aβ 35-42) (T. Golde) was used as the capture antibody and mAb 6E10 (Ab 1-16) (Covance) was used for detection.

**Electrophysiology**

The CA1 region of organotypic slices were locally and sparsely infected with Sindbis virus at day 6-8 and whole-cell patch recordings of CA1 neurons were performed at least 14 hours after infection. For whole-cell patch recordings, cultures were superfused with a warmed (28°–29°C) recording solution of the following composition: (mM) NaCl, 119; KCl, 2.5; $NaHCO_3$, 26; $NaH_2PO_4$, 1; $MgCl_2$, 4; D-

glucose, 11; $CaCl_2$, 4 with added 2 μM chloro adenosine and 50 μM picrotoxin. The recording solution was continuously bubbled with 95% $O_2$ / 5% $CO_2$ at a flow rate of approximately 2 ml/min. Internal solution was composed of: (mM) cesium methanesulfonate 15, CsCl 20, HEPES 10, $MgCl_2$ 2.5, $Na_2ATP$ 4, $Na_3GTP$ .4, sodium phosphocreatine 10, and EGTA .6, at pH 7.2. In most recordings, two independent stimulating electrodes were placed in Schaffer collateral-CA1 input and subiculum-CA1 input. Two adjacent neurons were patched in a whole-cell configuration and simultaneously recorded, one of which was infected as signified by GFP expression. AMPAR-mediated EPSC amplitude ($EPSC_{AMPA}$) were measured by averaging a 5 ms window about the peak of the EPSC amplitude at a holding potential of −60 mV, and NMDAR-mediated EPSC amplitude ($EPSC_{NMDA}$) was measured by averaging a 10 ms window at +40 mV 140-150 ms after stimulation. For caspase inhibitor experiments, slices were incubated in medium containing 100uM of Z-VAD-FMK (R&D Systems) overnight. Equal parts DMSO were used as a control. The paired Student's t-test was used for statistical analysis.

## II.D. Results

*Inhibition of caspases ameliorates Aβ-mediated synaptic depression*

To test the role of caspases in Aβ-induced synaptic changes, we utilized a model whereby one can directly test modifications in post-synaptic currents using whole-cell patch clamp recording from two cells simultaneously. This method allows for direct comparison of neuronal activity without the confounding effects of random genomic integration that can occur in transgenic models. In this experiment, we

sparsely infected the CA1 region of the hippocampus with Sindbis virus that overexpresses APP derivative, C99 and green fluorescent protein (GFP). C99 is sufficient to induce Aβ-mediated synaptic depression in hippocampal cultures[17] and was chosen over APP full length due to the fact that this increases the production of Aβ and decreases the production of sAPPα and sAPPβ, both of which contain neurotrophic properties that could interfere with analysis. After 14-20 hours of incubation, we performed simultaneous whole-cell recordings by stimulating at two sites and recording excitatory postsynaptic currents (EPSCs) from one neuron that overexpresses C99 and a neighboring cell that does not (Figure II.1). Once we verified that C99 did, in fact, cause synaptic dysfunction by reducing postsynaptic AMPA and NMDA (but not GABA) transmission as previously reported [17] (AMPA: infected neurons 63 ± 9% of uninfected neurons, n = 12, pathway = 20, $p \leq .01$; NMDA: infected neurons 77 ± 8% of uninfected neurons, n = 12, pathway = 20, $p \leq .05$; GABA: infected neurons 107 ± 18% of uninfected neurons, n = 13, pathway = 19; Figure II.2), we incubated slices with cell permeant pan-caspase inhibitor, z-VAD-fmk overnight and performed paired recordings. We found that z-VAD-fmk completely restored the Aβ-induced synaptic depression (100 uM, AMPA: infected neurons 93 ± 8% of uninfected neurons, n = 14, pathway = 18, $p \geq .05$; NMDA: infected neurons 105 ± 10% of uninfected neurons, n = 13, pathway = 15, $p \geq .05$; Figure II.3). To ensure that the effect was specific to caspase inhibition, we incubated slices with z-FA-fmk, a well-characterized control for fmk conjugated caspase inhibitors and found no attenuation of Aβ synaptotoxicity, suggesting the attenuation of toxicity with z-VAD-fmk application is specific to caspases (100 um, AMPA:

infected neurons 67 ± 9% of uninfected neurons, n = 12, pathway = 17, $p \leq .01$; NMDA: infected neurons 81 ± 10% of uninfected neurons, n = 8, pathway = 13, $p \leq .05$; Figure II.4). Previous studies have implicated caspase-3 as an important effector caspase in Aβ toxicity and synaptic plasticity[10, 18, 19], thus we next tested caspase-3 inhibitor, z-DEVD-fmk. Again, we found that incubation with this compound restored AMPA and NMDA transmission to normal levels (5 uM, AMPA: infected neurons 102 ± 11% of uninfected neurons, n = 8, pathway = 14, $p \geq .05$; NMDA: infected neurons 100 ± 15% of uninfected neurons, n = 8, pathway = 14, $p \geq .05$; Figure II.5). Caspase inhibitors are well known to be promiscuous, thus we verified the specificity of caspase-3 involvement via expression of C99 in caspase-3 knockout (ko) mice (Caspase-3 ko, AMPA: infected neurons 144 ± 21% of uninfected neurons, n = 7, pathway = 13, $p \geq .05$; NMDA: infected neurons 120 ± 24% of uninfected neurons, n = 7, 13, $p \geq .05$; Figure II.6).

*Elimination of APP caspase cleavage site D664 prevents synaptic depression induced by Aβ*

Initial work done in cell culture showed that APP is necessary for Aβ toxicity[6, 20] and recently this hypothesis has been extended to include Aβ-mediated synaptic depression[21]. Others and we previously reported that APP is cleaved by caspases and that this cleavage is upregulated in individuals with AD[5, 6]. This led us to ask whether the caspase cleavage of APP was also important for synaptic dysfunction. In this experiment, we overexpressed C99 with an aspartate to alanine mutation at site 664 (C99_D664A). This mutation abrogates cleavage by caspases,

leaving the C-terminal region in tact. To make sure that the mutation does not alter cleavage and reduce Aβ production, we collected media from BHK cells infected with C99 or C99_D664A and found similar levels of total Aβ via western blot, with comparable levels of C99 expression from total cell lysate. Additionally, there was no difference in Aβ42 when tested by ELISA. (Figure II.7). Then we performed paired recordings from neurons expressing C99_D664A vs. wt (uninfected) and found that the abrogation of caspase cleavage was sufficient to eliminate Aβ induced synaptic depression (AMPA: infected neurons 93 ± 8% of uninfected neurons, n = 17, pathway = 26, $p \geq .05$; NMDA: infected neurons 90 ± 9% of uninfected neurons, n = 17, pathway = 24, $p \geq .05$; Figure II.8).

*Overexpression of C31 leads to neuronal toxicity*

In the proposed model, Aβ elicits toxicity via its interaction with APP, which leads to the recruitment and activation of caspases. APP is ultimately cleaved by caspases, releasing the C-terminal fragment, C31. Interestingly, removal of the C31 fragment ameliorates Aβ toxicity in a cell culture system[12, 13], while overexpression of C31 is sufficient to induce cell death on its own[12, 13], suggesting that the release of C31 is necessary to induce cellular toxicity. Here, we seek to test whether C31 also contributes to the Aβ-induced synaptic depression. To do this, we utilized the same viral expression system and sparsely infected CA1 pyramidal cells so that they overexpressed C31-GFP. Preliminary observations indicate that the high levels of C31-GFP were toxic to the cell as judged by neuronal morphology. Visually, these neurons displayed abnormal dendritic morphology and most infected neurons no

longer displayed prominent apical dendrites (data not shown). Additionally, we were unable to record from these neurons, as they were unable to hold a seal, suggesting that membrane integrity was compromised. Because we are not interested in cell death, but are interested in testing the role of C31 in synaptic dysfunction, we did not utilize additional methods to determine specific cellular pathology. Instead, we are working to create a system to overexpress C31 at lower levels so that we will be able to utilize the paired, whole-cell patch clamping method to test the physiology of these neurons as compared to uninfected neurons.

## II.E Discussion

Caspase activation and neuronal death have been documented in AD for over two decades. However, recent evidence indicates that caspases may be important for cellular processes extending beyond apoptosis[19, 22]. The protracted presence of caspases localized to the synapse and increased caspase activity precluding neuronal death has led to the idea that caspases may be important for early synaptic dysfunction. Molecular mechanisms linking Aβ, the proposed primary source of toxicity in AD, to caspase activation are still under debate. Because previous reports indicate that APP may function as a molecular link between Aβ toxicity and cell death, we sought to test whether this was also relevant for synaptic dysfunction, a pathological stage that precedes cell death.

In this study, we utilized pharmacological intervention and genetic manipulation to show that Aβ-driven synaptic depression is mediated by caspases and that caspase-3 contributes to this molecular pathway. Next, we showed that caspase

cleavage of APP is necessary for acute Aβ-induced synaptic depression. To do this, we inhibited the ability of C99 to be cleaved through substitution of the obligatory aspartate residue necessary for caspase cleavage and found that the removal of this caspase cleavage site was enough to restore synaptic function. Importantly, we verified that the aspartate to alanine substitution did not affect C99 expression or production of Aβ, thus suggesting that the caspase cleavage of APP is necessary for Aβ-induced synaptic depression.

Our results confirm recent reports that caspase activity may be an early and important modulator of synaptic function in AD and extend these findings by demonstrating that caspase cleavage of APP is necessary for Aβ-induced synaptic dysfunction. Recent lines of experimental evidence demonstrated that caspase activity depresses basal glutamatergic synaptic transmission in a transgenic mouse model of AD as early as 3 months of age[10]. Our results support this notion and extend it by showing that caspase-3 activation is necessary to depress both AMPA and NMDA transmission in an alternative rodent model that subjects neurons to acute, high levels of Aβ without genetic manipulation. While supra-physiological expression levels inherently present obstacles for interpreting data, this suggests a process that can occur rapidly and does not require a protracted time course to exert its effects.

Interestingly, Jo et al. recently reported that caspase-3 activation is also necessary for long-term depression (LTD), a physiological form of synaptic plasticity important for learning and memory[18]. This study supports a mechanism whereby caspase activation is precise, localized and can occur over seconds and does not implicate impending neuronal death. While this study does not correlate Aβ with

caspase-driven synaptic dysfunction, the presented lines of evidence paint a picture that places caspases as a key player in learning and memory and may present a scenario where even a slight alteration of caspase activation results in severe consequences and disease pathology.

While our studies collectively emphasize the importance of caspase activity in physiological and pathological synaptic function, the underlying mechanisms remain elusive. Our APP-driven hypothesis is based on previous studies done in cell culture that convincingly demonstrated the necessity for APP and the APP caspase site in Aβ-elicited *cell death* [6, 12]. The presented study demonstrates that the caspase cleavage of APP is also involved in Aβ-driven *synaptic depression*, a pathological stage that precedes neuronal cell death and correlates with cognitive deficits. This evidence is supported by data indicating that the absence of APP ameliorates Aβ-induced synaptic depression [20] and by reports that the presence of caspase cleaved APP in human brains is detectable, and cleavage correlates with disease severity [5, 6, 11]. While we cannot rule out other proposed caspase substrates such as Akt1, Gsk3β, calcineurin, and tau, our results present evidence for a role of the caspase cleavage of APP and evidence suggests this toxicity is via the release of the C-terminal fragment.

While still preliminary, both the observance that apical dendrites appear retracted in C31-GFP expressing cells and the fact that these neurons cannot hold a seal, presumably due to compromised membrane integrity, are highly suggestive of a pathological role for C31. Because the overexpression of C31 does not depend on cleavage events, the levels of C31 in this experiment are expected to be greater than

what is generated via the overexpression of C99. Thus, in order to obtain less toxicity and mimic previous experiments, I am currently working on a system whereby C31 is expressed at lower levels.

While it is not yet clear whether the release of C31 leads to synaptic dysfunction, our observations support a role for C31 in neuronal toxicity. However, the mechanism of this toxicity is not known. Interestingly, a similar mechanism is suggested to be at the center of Huntington's Disease (HD). HD is a neurodegenerative disease affecting cognition and motor function and is caused by a polyglutamine expansion on the N-terminus of the protein, huntingtin (htt). Analogous to APP and Aβ in AD, one pathological hallmark of the disease is an accumulation of HTT fragments, suggesting aberrant proteolytic cleavage of the protein. While caspase cleavage of this protein had long been known[23, 24], in 2006 it was found that caspase cleavage of htt contributes to neuronal dysfunction and this is mediated via the nuclear translocation of the N-terminal cleavage product[25]. Previous reports claim that the APP intracellular domain is translocated to the nucleus, though this has been difficult to confirm[26, 27] and whether this type of function might extend specifically to C31 has not been tested. Alternatively, it has been reported that inactivation of caspases attenuates the toxicity of C31, indicating that caspase activity may also be downstream of C31[13]. This suggests that C31 may function to propagate or amplify local caspase activation to exert toxicity. Whether C31 acts as an adaptor molecule or affects caspase cleavage via an alternate mechanism is not known. Thus, the question as to how C31 exerts its effects remains to be defined.

While our study is in accordance with recent papers revealing a role for caspase-3 as a modulator of synaptic plasticity in both physiological and pathological circumstances, Lu et al. claimed that caspase-3 was not a mediator of caspase cleavage of APP and that other caspases, namely caspase-8 and caspase-6, were more important for the caspase cleavage of APP[13]. While I cannot comment on the importance of other caspases since they were not tested in this study, one possible explanation is the difference in assessed outcomes. While somewhat difficult to interpret, various stages of caspase activation and pathology have been documented in other neurodegenerative diseases [28] and while we were assessing synaptic depression, Lu et al., assessed cell death. Additionally, effector caspases need one of two initiator caspases, caspase-8 or caspase-9, for initial activation, thus it is expected that one of these two are important in the Aβ-mediated synaptic depression upstream of caspase-3 activation.

In summary, we show that caspase cleavage of APP is necessary to induce acute Aβ-mediated synaptic depression. Preliminary evidence points towards the release of C31 as the mediator of toxicity, though more studies need to be done in order to verify these primary observations. While this presents an intriguing mechanism for Aβ-induced synaptic dysfunction and a new role for APP, its therapeutic relevance is not clear. As presented in this paper, caspases perform many roles and are responsible for highly regulated signaling events. The use of inhibitors has been tried therapeutically for several neurodegenerative diseases with varying degrees of adverse side effects and efficacy [29-31]. While recent advancements suggest a possibility for caspase inhibitors of greater specificity and less toxicity[32], the fact

that caspase-3 is involved in normal neuronal function will make such efforts very difficult. Thus, it is critical to understand the up- and down-stream events of Aβ production and caspase activation.

# II.F. Figures

Figure II.1

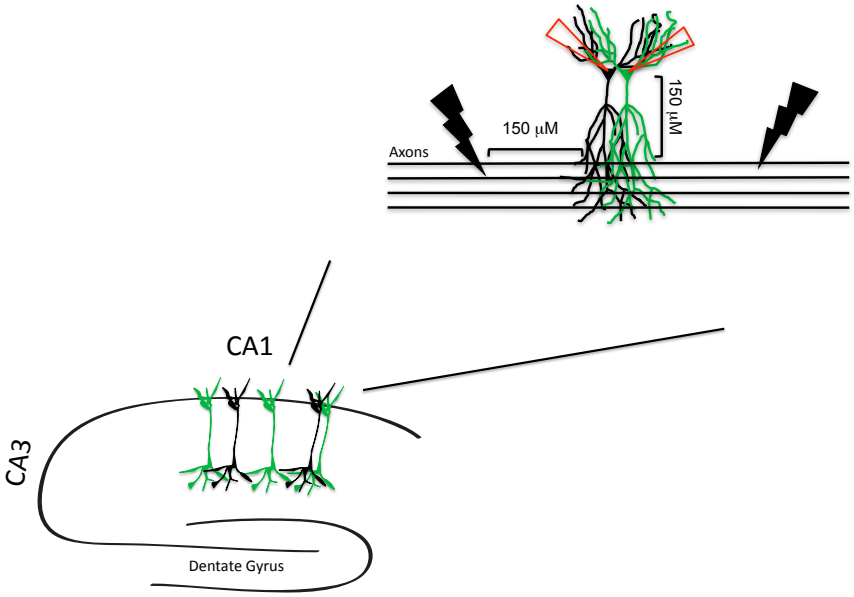


**Figure II.1:** A schematic diagram of the paired, whole-cell recording experimental method. Lower diagram: CA1 pyramidal neurons are sparsely infected with Sindbis virus expressing APP or APP β-CTF (C99) IRES eGFP. Upper diagram: EPSCs are intracellularly recorded simultaneously from paired neurons when evoked with bipolar electrodes situated at the Schaffer collateral-CA1 input and subiculum-CA1 input, allowing for direct comparison of NMDAR- and AMPAR-mediated currents. In this case, paired neurons are defined by two neurons, one infected and identified by GFP expression and one uninfected, with cell bodies that are side-by-side or one cell body apart.

Figure II.2

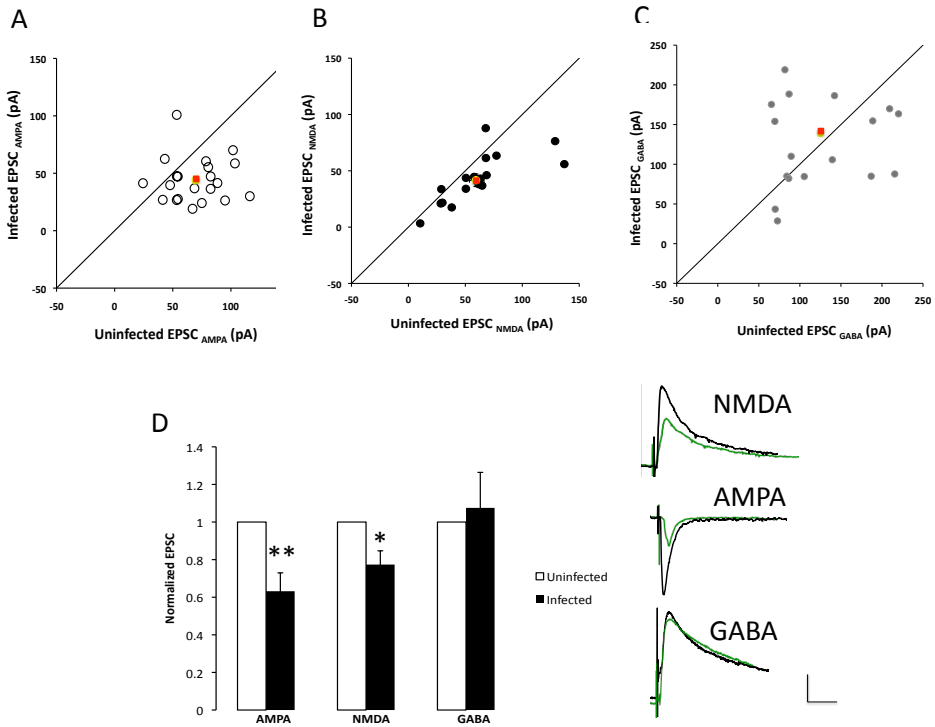


**Figure II.2**: Expression of C99 depresses AMPAR- and NMDAR- but not GABAR- mediated synaptic transmission. A) Pairwise comparison of the effects of post-synaptic CA1 pyramidal neurons expressing C99 versus nearby uninfected neurons on basal AMPA-EPSC amplitude (n = 12, pathway = 20). Red marker indicates mean amplitudes. B) Pairwise analysis of the effects of post-synaptic CA1 pyramidal neurons expressing C99 versus nearby uninfected cells on NMDA-EPSC amplitude (n = 12, pathway = 20). Red marker indicates mean amplitudes. C) Pairwise analysis of the effects of post-synaptic CA1 pyramidal neurons expressing C99 versus nearby uninfected cells on GABA-EPSC amplitude (n = 13, pathway = 19). Red marker indicates mean amplitudes. D) Left: AMPA, NMDA and GABA currents normalized to the paired, uninfected neuron. Right: Representative traces overlaid. Scale bar: 30 pA, 30 ms. ** p<.01, * p<.05

Figure II.3

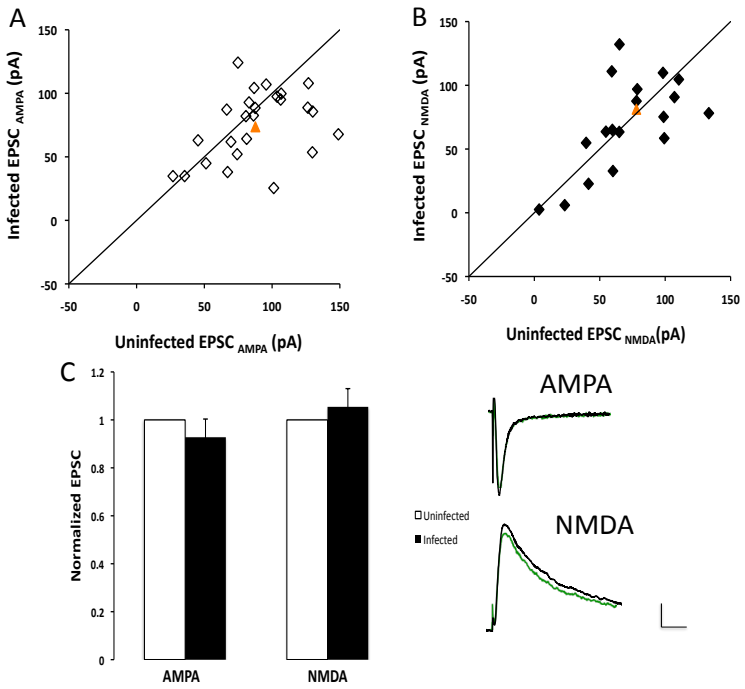


**Figure II.3**: Pan-caspase inhibitor z-VAD-fmk prevents Aβ-induced depression of AMPAR- and NMDAR-mediated synaptic transmission. A) Pairwise comparison of AMPAR-mediated current from post-synaptic CA1 pyramidal neurons expressing C99 versus nearby uninfected neurons after overnight incubation with caspase inhibitor z-VAD-fmk (n = 14, pathway = 18). Orange triangle indicates mean amplitudes. B) Pairwise analysis NMDAR-mediated current from post-synaptic CA1 pyramidal neurons expressing C99 versus nearby uninfected neurons after overnight incubation with z-VAD-fmk (n = 13, pathway = 15). Orange triangle indicates mean amplitudes. C) Left: AMPA and NMDA currents normalized to the paired uninfected neuron. Right: Representative traces overlaid. Scale bar for traces: 30 pA, 30 ms.

Figure III.4

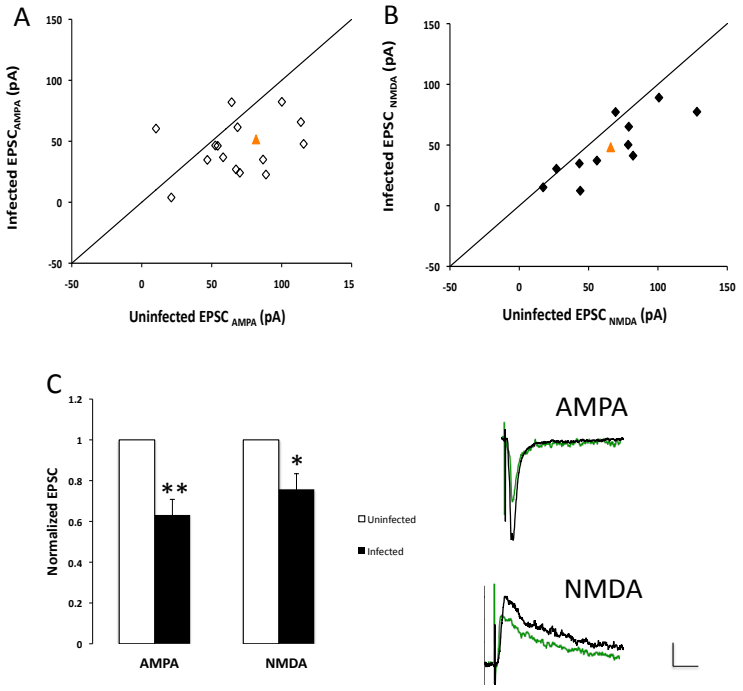


**Figure II.4**: Caspase control z-FA-fmk does not affect AMPA-EPSC amplitude or NMDA-EPSC amplitude in neurons expressing C99. A) Pairwise comparison of AMPAR-mediated post-synaptic CA1 pyramidal currents in neurons expressing C99 versus nearby uninfected neurons that were incubated overnight with caspase inhibitor control z-FA-fmk (n = 12, pathway = 17). B) Pairwise analysis of NMDAR-mediated post-synaptic CA1 pyramidal neurons expressing C99 versus nearby uninfected neurons incubated overnight with caspase inhibitor control, z-FA-fmk (n = 9, pathway = 13). Orange triangle indicates mean amplitudes. C) Left: AMPA and NMDA currents normalized to the paired uninfected neuron. Right: Representative traces overlaid. Scale bar for traces: 30 pA, 30 ms. *p<.05, ** p<.01

Figure II.5

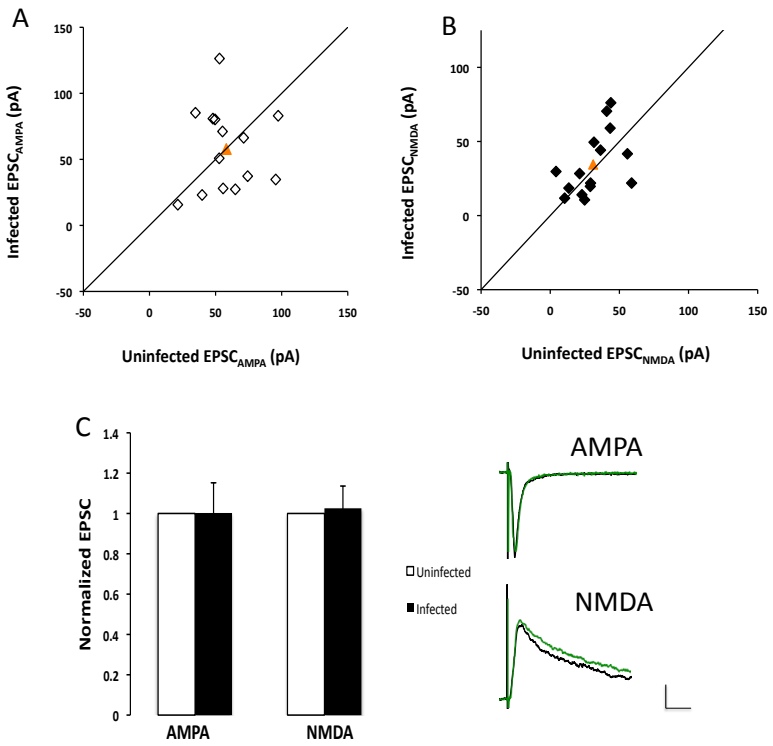


**Figure II.5**: Caspase-3 inhibitor z-DEVD-fmk prevents APP-induced depression of AMPAR- and NMDAR-mediated EPSCs. A) Pairwise comparison of AMPAR-mediated currents from post-synaptic CA1 pyramidal neurons expressing C99 versus a nearby uninfected neuron after overnight incubation with caspase inhibitor z-DEVD-fmk (n = 9, pathway = 14). B) Pairwise analysis of NMDAR-mediated currents of post-synaptic CA1 pyramidal neurons expressing C99 versus nearby uninfected neurons after overnight incubation with caspase inhibitor z-DEVD-fmk (n = 9, pathway = 14). Orange triangle indicates mean amplitudes. C) Left: AMPA and NMDA currents normalized to the paired uninfected neuron. Right: Representative traces overlaid. Scale bar for traces: 30 pA, 30 ms.

Figure II.6

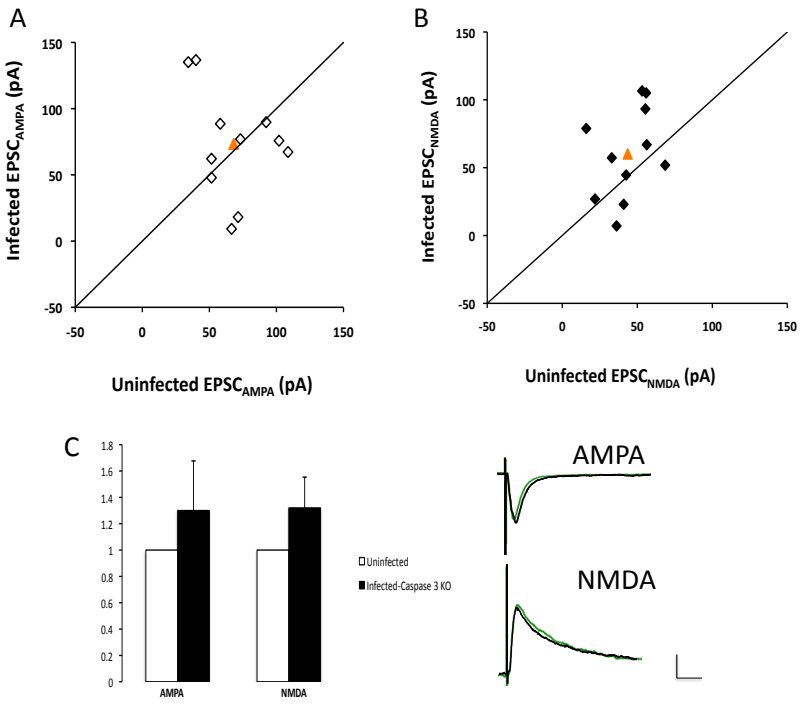


**Figure II.6**: Absence of caspase-3 ameliorates APP-induced synaptic depression. A) In caspase-3 ko animals, a pairwise comparison of the effects of post-synaptic CA1 pyramidal neurons expressing C99 versus nearby uninfected neurons (n = 7, pathway = 13) on basal AMPA-EPSC amplitude. B) In caspase-3 ko mice, a pairwise analysis of the effects of post-synaptic CA1 pyramidal neurons expressing C99 versus nearby uninfected cells on NMDA-EPSC amplitude from all experiments (n = 7, pathway = 13) . Orange triangle indicates mean amplitudes. C) Left: AMPA and NMDA currents normalized to the paired uninfected neuron. Scale bar for traces: 30 pA, 30 ms.

Figure II.7

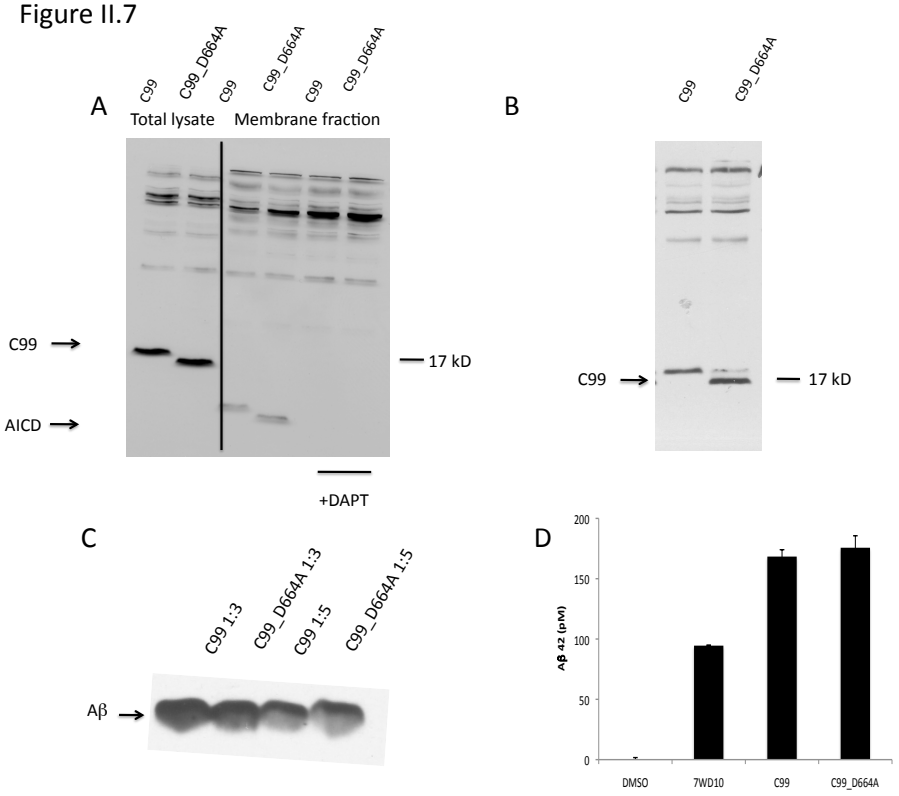


**Figure II.7**: Comparable expression of wild type and D664A mutant constructs and Aβ generation. BHK cells were infected with sindbis virus expressing CT99 or C99_D664A IRES eGFP. A) Western blotting of total protein revealed similar levels of expression of β-CTF while the membrane fraction showed equal amounts of AICD. B) To verify the protein shift is not due to a truncation of the protein, mAb 6E10, which recognizes the N-terminus of β-CTF, was used for detection. C) Aβ was immunoprecipitated from media infected with various dilutions of virus revealing similar levels of total Aβ. D) Aβ 42 was quantified by ELISA as described in methods. Cell line 7Wd10 (wild type APP overexpression CHO cell line) was used as a control (n = 2).

Figure II.8

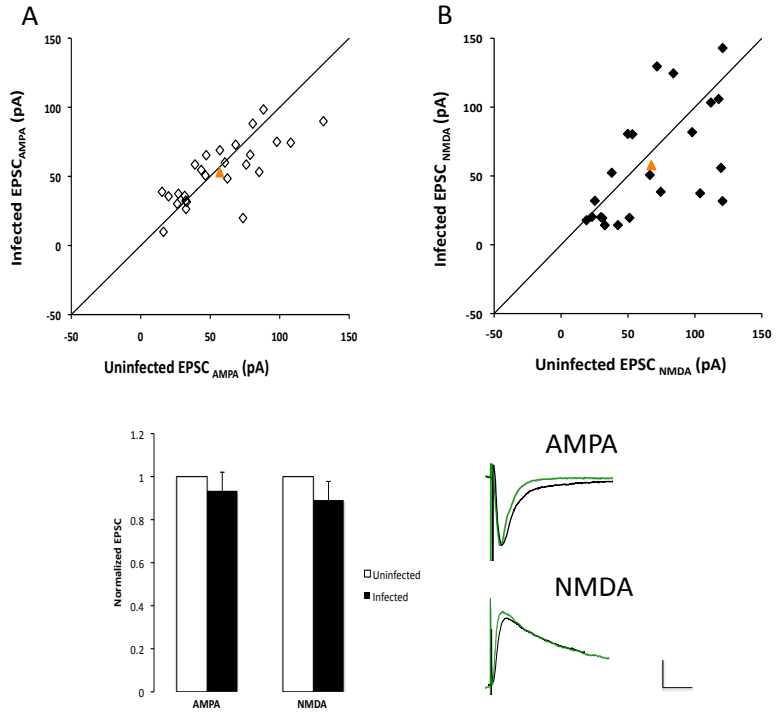


**Figure II.8**: Absence of APP caspase cleavage site attenuates APP-induced depression of AMPAR- and NMDAR-mediated synaptic transmission. A) Pairwise comparison of the effects of post-synaptic CA1 pyramidal neurons expressing C99-D664A versus nearby uninfected neurons on basal AMPA-EPSC amplitude (n = 17, pathway = 26). B) Pairwise analysis of the effects post-synaptic CA1 pyramidal neurons expressing C99_D664A versus nearby uninfected neurons on basal NMDA-EPSC amplitude (n = 17, pathway = 24). Orange triangle indicates mean amplitudes. C) Left: AMPA and NMDA currents normalized to the paired uninfected neuron. Right: Representative traces overlaid. Scale bar for traces: 30 pA, 30 ms.

References

1. Selkoe DJ. Toward a comprehensive theory for Alzheimer's disease. Hypothesis: Alzheimer's disease is caused by the cerebral accumulation and cytotoxicity of amyloid beta-protein. Ann N Y Acad Sci. 2000;924:17-25.

2. Pop C, Salvesen GS. Human caspases: activation, specificity, and regulation. J Biol Chem. 2009 Aug 14;284(33):21777-81.

3. Su JH, Anderson AJ, Cummings BJ, Cotman CW. Immunohistochemical evidence for apoptosis in Alzheimer's disease. Neuroreport. 1994 Dec 20;5(18):2529-33.

4. Yang F, Sun X, Beech W, Teter B, Wu S, Sigel J, et al. Antibody to caspase-cleaved actin detects apoptosis in differentiated neuroblastoma and plaque-associated neurons and microglia in Alzheimer's disease. Am J Pathol. 1998 Feb;152(2):379-89.

5. Gervais FG, Xu D, Robertson GS, Vaillancourt JP, Zhu Y, Huang J, et al. Involvement of caspases in proteolytic cleavage of Alzheimer's amyloid-beta precursor protein and amyloidogenic A beta peptide formation. Cell. 1999 Apr 30;97(3):395-406.

6. Lu DC, Rabizadeh S, Chandra S, Shayya RF, Ellerby LM, Ye X, et al. A second cytotoxic proteolytic peptide derived from amyloid beta-protein precursor. Nat Med. 2000 Apr;6(4):397-404.

7. Louneva N, Cohen JW, Han LY, Talbot K, Wilson RS, Bennett DA, et al. Caspase-3 is enriched in postsynaptic densities and increased in Alzheimer's disease. Am J Pathol. 2008 Nov;173(5):1488-95.

8. Gastard MC, Troncoso JC, Koliatsos VE. Caspase activation in the limbic cortex of subjects with early Alzheimer's disease. Ann Neurol. 2003 Sep;54(3):393-8.

9. Cribbs DH, Poon WW, Rissman RA, Blurton-Jones M. Caspase-mediated degeneration in Alzheimer's disease. Am J Pathol. 2004 Aug;165(2):353-5.

10. D'Amelio M, Cavallucci V, Middei S, Marchetti C, Pacioni S, Ferri A, et al. Caspase-3 triggers early synaptic dysfunction in a mouse model of Alzheimer's disease. Nat Neurosci. 2011 Jan;14(1):69-76.

11. Banwait S, Galvan V, Zhang J, Gorostiza OF, Ataie M, Huang W, et al. C-terminal cleavage of the amyloid-beta protein precursor at Asp664: a switch associated with Alzheimer's disease. J Alzheimers Dis. 2008 Feb;13(1):1-16.

12. Shaked GM, Kummer MP, Lu DC, Galvan V, Bredesen DE, Koo EH. Abeta induces cell death by direct interaction with its cognate extracellular domain on APP (APP 597-624). FASEB J. 2006 Jun;20(8):1254-6.

13. Lu DC, Shaked GM, Masliah E, Bredesen DE, Koo EH. Amyloid beta protein toxicity mediated by the formation of amyloid-beta protein precursor complexes. Ann Neurol. 2003 Dec;54(6):781-9.

14. Galvan V, Chen S, Lu D, Logvinova A, Goldsmith P, Koo EH, et al. Caspase cleavage of members of the amyloid precursor family of proteins. J Neurochem. 2002 Jul;82(2):283-94.

15. Galvan V, Zhang J, Gorostiza OF, Banwait S, Huang W, Ataie M, et al. Long-term prevention of Alzheimer's disease-like behavioral deficits in PDAPP mice carrying a mutation in Asp664. Behav Brain Res. 2008 Aug 22;191(2):246-55.

16. Saganich MJ, Schroeder BE, Galvan V, Bredesen DE, Koo EH, Heinemann SF. Deficits in synaptic transmission and learning in amyloid precursor protein (APP) transgenic mice require C-terminal cleavage of APP. J Neurosci. 2006 Dec 27;26(52):13428-36.

17. Kamenetz F, Tomita T, Hsieh H, Seabrook G, Borchelt D, Iwatsubo T, et al. APP processing and synaptic function. Neuron. 2003 Mar 27;37(6):925-37.

18. Jo J, Whitcomb DJ, Olsen KM, Kerrigan TL, Lo SC, Bru-Mercier G, et al. Abeta(1-42) inhibition of LTP is mediated by a signaling pathway involving caspase-3, Akt1 and GSK-3beta. Nat Neurosci. 2011 May;14(5):545-7.

19. Li Z, Jo J, Jia JM, Lo SC, Whitcomb DJ, Jiao S, et al. Caspase-3 activation via mitochondria is required for long-term depression and AMPA receptor internalization. Cell. 2010 May 28;141(5):859-71.

20. Tyan S-H, B. Midthune, S. Eggert, D. L. Dickstein and E. H. Koo. Role of Amyloid Precursor proteins and Abeta-induced synaptic dysfunction. Abstract, International Conference on Alzheimer's Disease, Honolulu, HI. 2010;Abstract # 1962.

21. Tyan SH, Shih AY, Walsh JJ, Murayama H, Sarsoza F, Ku L, et al. Amyloid precursor protein (APP) regulates synaptic structure and function. Mol Cell Neurosci. 2012 Aug 3.

22. Yi CH, Yuan J. The Jekyll and Hyde functions of caspases. Dev Cell. 2009 Jan;16(1):21-34.

23. Goldberg YP, Nicholson DW, Rasper DM, Kalchman MA, Koide HB, Graham RK, et al. Cleavage of huntingtin by apopain, a proapoptotic cysteine protease, is modulated by the polyglutamine tract. Nat Genet. 1996 Aug;13(4):442-9.

24. Martindale D, Hackam A, Wieczorek A, Ellerby L, Wellington C, McCutcheon K, et al. Length of huntingtin and its polyglutamine tract influences localization and frequency of intracellular aggregates. Nat Genet. 1998 Feb;18(2):150-4.

25. Graham RK, Deng Y, Slow EJ, Haigh B, Bissada N, Lu G, et al. Cleavage at the caspase-6 site is required for neuronal dysfunction and degeneration due to mutant huntingtin. Cell. 2006 Jun 16;125(6):1179-91.

26. Slomnicki LP, Lesniak W. A putative role of the Amyloid Precursor Protein Intracellular Domain (AICD) in transcription. Acta Neurobiol Exp (Wars). 2008;68(2):219-28.

27. Cao X, Sudhof TC. A transcriptionally [correction of transcriptively] active complex of APP with Fe65 and histone acetyltransferase Tip60. Science. 2001 Jul 6;293(5527):115-20.

28. Pasinelli P, Houseweart MK, Brown RH, Jr., Cleveland DW. Caspase-1 and -3 are sequentially activated in motor neuron death in Cu,Zn superoxide dismutase-mediated familial amyotrophic lateral sclerosis. Proc Natl Acad Sci U S A. 2000 Dec 5;97(25):13901-6.

29. Van Noorden CJ. The history of Z-VAD-FMK, a tool for understanding the significance of caspase inhibition. Acta Histochem. 2001 Jul;103(3):241-51.

30. Rohn TT. The role of caspases in Alzheimer's disease; potential novel therapeutic opportunities. Apoptosis. 2010 Nov;15(11):1403-9.

31. Yang L, Sugama S, Mischak RP, Kiaei M, Bizat N, Brouillet E, et al. A novel systemically active caspase inhibitor attenuates the toxicities of MPTP, malonate, and 3NP in vivo. Neurobiol Dis. 2004 Nov;17(2):250-9.

32. Rohn TT, Kokoulina P, Eaton CR, Poon WW. Caspase activation in transgenic mice with Alzheimer-like pathology: results from a pilot study utilizing the caspase inhibitor, Q-VD-OPh. Int J Clin Exp Med. 2009;2(4):300-8.

# Chapter III: Loss of APLP2 Does Not Affect Neuronal Structure and Function in CA1 Pyramidal Neurons, Nor Does It Affect Aβ-Induced Synaptic Dysfunction

## III.A. Abstract

APP plays a fundamental role in AD pathogenesis through the generation of the amyloid-β peptide. APP is part of a larger gene family with two mammalian homologues, APLP1 and APLP2. While APLP2 contains high sequence homology, a nearly identical expression pattern and is highly functionally redundant to APP, it does not contain the toxic Aβ region.

As previous studies from our lab and others have indicated, APP plays an important role in Aβ toxicity, independent of its role in Aβ production. We wanted to test the specificity of APP in this event and one way to test this is by asking whether homologue APLP2 also contributes to Aβ-mediated synaptic dysfunction. To do this, we took advantage of a line of mice with APLP2 genetically deleted ($APLP2^{-/-}$). Because deletion of APP leads to functional and structural abnormalities, we first characterized basal neuronal structure and function of CA1 pyramidal neurons in the $APLP2^{-/-}$ mice using a combined approach involving *in vitro* and *in vivo* techniques in young and aged animals.

Surprisingly, we found that unlike APP, APLP2 appears not to be essential for maintenance of dendritic structure, spine density, or synaptic function. Next, we tested a role for APLP2 in Aβ synaptotoxicity and found that lack of APLP2 does not affect Aβ-induced impairment in long-term potentiation. Taken together, these two outcomes

suggest there is a divergence in function between APP and APLP2 in neuronal structure and function and that the reported APP-mediated Aβ synaptotoxicity appears to be an effect specific to APP.

## III.B. Introduction

Alzheimer's disease (AD) is a neurodegenerative disorder of the central nervous system and the most common form of dementia in the elderly population. In addition to the presence of extracellular senile plaques and intraneuronal neurofibrillary tangles, there is significant neuronal and synaptic loss in the neocortex. Although AD aetiology remains unclear, neuronal and synaptic degeneration are thought to underlie the cause for cognitive decline, which is recognized to arise, at least in part, from the neurotoxic effects of amyloid-β peptides (Aβ) derived from the proteolytic cleavage of amyloid precursor protein (APP) [1].

APP belongs to a family of proteolysis-dependent type-1 glycoproteins that includes the mammalian proteins amyloid precursor-like protein 1 (APLP1) and amyloid precursor-like protein 2 (APLP2) [2]. These transmembrane proteins exhibit high sequence homology and undergo similar processing by multiple secretases, resulting in a number of secreted fragments [3], though neither APLP1 nor APLP2 contains the Aβ sequence [4]. APP and its proteolytic products were shown to be important for several aspects of neuronal development and possible functions include cell adhesion, neurite outgrowth and synaptic structure and function[5].

It is known that APLP2 and APP contain the highest degree of sequence homology within this family of genes and that they are expressed ubiquitously and in an overlapping spatial and temporal pattern [6]. Rodent studies revealed that knocking out just one gene in this family produces mice that are viable and fertile with relatively mild phenotypes[7-9]. Interestingly, two of three double knock outs ($APP^{-/-}$;$APLP2^{-/-}$ and $APLP2^{-/-}$;$APLP1^{-/-}$) begat perinatal lethality[7, 8] while the double deletion of APP and APLP1 culminated in a relatively mild phenotype[8], suggesting that APLP2 contains a vital role.

Our lab has recently reported that the deletion of APP abrogates Aβ-induced synaptic loss and these $APP^{-/-}$ mice no longer displayed Aβ-induced impairment in long-term potentiation (LTP), the molecular correlate to memory. Previous studies have shown that APP may be necessary for the toxicity induced by Aβ, in part by cleavage of a caspase site on the intracellular domain of the APP protein, as assessed via cell death [10-13]. Additionally, in the previous chapter, we reported that caspase cleavage of APP was also important for Aβ-induced glutamatergic synaptic depression. Together, these results suggest that APP is necessary for Aβ-mediated synaptic dysfunction.

While there is convincing evidence that indicates APP as a mediator of Aβ-induced synaptic dysfunction, many of the studies used the same $APP^{-/-}$ model and whether this is a general, nonspecific effect of this mouse line is uncertain. Because APP and APLP2 contain the highest degree of homology, we wanted to test the specificity of APP by asking whether APLP2 might also contribute to Aβ-mediated synaptic dysfunction by utilizing $APLP2^{-/-}$ mice. Because we and others found that the deletion of APP leads to impaired neuronal outgrowth and a decrease in spine density[14-16], a basic characterization of the neuronal morphology and function of the $APLP2^{-/-}$ mice needed to be done prior to testing the relevance of APLP2 in Aβ-mediated synaptic dysfunction. We

figured this may also identify potential roles for APLP2 in neuronal development and provide information as to the specific and shared roles of APP and APLP2.

We report that unlike our recent results demonstrating multiple defects in neuronal structure and function in APP deficient mice[16], loss of APLP2 resulted in no detectable neuronal abnormalities. Additionally, we report no difference in the degree of LTP impairment in APLP2$^{-/-}$ animals as compared to wild-type (wt) animals after Aβ treatment, suggesting that APLP2 is not necessary for Aβ-mediated synaptic dysfunction and that this reported effect is specific to the loss of APP.

## III.C. Materials and Methods

### Animals

APLP2$^{-/-}$ mice were kindly provided by Dr. Hui Zheng at Baylor College of Medicine and generated as described in von Koch et al. (1997) [7]. The transgenic line was maintained by crossing with C57BL/J6 breeders (Jackson Laboratories). APLP2$^{-/-}$ and wt (APLP2$^{+/+}$) mice were generated from heterozygous pairings. All animal procedures were approved by the Institutional Animal Care and Use Committee at University of California, San Diego and in accordance with the National Institutes of Health guidelines.

### Primary hippocampal culture

Hippocampal cultures were prepared and transfected as described elsewhere [17]. Hippocampi were excised from APLP2$^{-/-}$ mice and control littermates on postnatal days 0-1 (P0-P1), trypsinized and plated at a density of 300 cells/mm$^2$ on poly-L-lysine

(Sigma, St. Louis, MO, USA) coated coverslips. Cultures were maintained at 37°C and 5% $CO_2$ in neurobasal medium supplemented with 2% B-27, 2 mM L-glutamine and 25 μg/ml sodium pyruvate and the medium was changed every 3-4 days (unless noted, reagents from Invitrogen, Carlsbad, CA, USA). At 14-18 days *in vitro* (DIV) neurons were transfected with enhanced green fluorescent protein (eGFP) using a low efficiency calcium phosphate precipitation protocol. Briefly, medium from the neuronal cultures was replaced with new neurobasal medium plus 2% B27 incubated at 37°C, 5% $CO_2$ for 30 minutes. A DNA, $H_2O$ and $CaCl_2$ mixture was added to 2X Hepes Buffered Solution (HBS), pH 7.07, incubated for 20 minutes at room temperature (RT), added drop-wise to hippocampal cultures and incubated at 37ºC, 5% $CO_2$ for approximately 3.5 hours, or until cultures displayed ample precipitate. Cultures were then carefully washed twice with 37ºC 2X HBS, replacing only 50% of media per wash. Solution was then completely replaced with the pre-transfection conditioned neurobasal medium and fixed 1 day post-transfection.

**Image acquisition and spine quantification in primary hippocampal cultures**

Photomicrographs were obtained using an Olympus DSU IX-81 inverted microscope fitted with a spinning disk confocal attachment and a 60x/1.2 N.A. water immersion objective. Labeled transfected neurons were chosen randomly for imaging from neuronal cultures from three coverslips. For all dendritic spine analyses, the region of the apical dendrites after the first branch point was selected (secondary dendrite). Dendritic spine density was scored from three randomly chosen areas per neuron. Z-sections were taken at 0.3-μm intervals and were stacked with maximum projection. All

analyses were conducted blind to genotype. Data were expressed as means ± SEM from independent replicates. Primary hippocampal cultures were fixed on coverslips by adding a pre-warmed mixture of 4% sucrose/4% paraformaldehyde (Sigma, St. Louis, MO, USA) in phosphate-buffered saline (PBS) for 15 minutes at 37 °C. This was replaced with fresh 4% sucrose/4% paraformaldehyde in PBS for 15 minutes at RT. Cultures were then rinsed (3X with PBS) and permeabilized with 0.3% Triton X-100 for 10 minutes at RT and rinsed again. Neurons were blocked for 1 hour with 5% goat serum at 37 °C, rinsed with PBS Coverslips were mounted with Prolong gold antifade reagent (Molecular Probes, Eugene, OR, USA).

**Intracellular dye injections**

Mice were anesthetized with chloral hydrate (0.1 ml of a 15% solution, i.p.), and transcardially perfused with ice-cold 1% paraformaldehyde in 0.1 M PBS (pH 7.4) for one minute. This was followed by perfusion of 4% paraformaldehyde in 0.1 M PBS with 0.125% glutaraldehyde for 12 minutes. The brains were removed from the skull and postfixed overnight at 4°C in 4% paraformaldehyde in PBS with 0.125% glutaraldehyde and then transferred to PBS and sectioned on a Vibratome (Leica VT1000S, Bannockburn, IL, USA) into 200 µm sections and stored at 4°C in PBS. For intracellular injections, sections were incubated in 4',6-diamidino-2-phenylindole (DAPI; Sigma) for 5 minutes to reveal the cytoarchitectural features of the pyramidal layer of CA1 of the hippocampus. The sections were then mounted on nitrocellulose paper and immersed in ice-cold 0.1 M PBS. Pyramidal neurons in the CA1 were injected with an intracellular iontophoretic injection of 5% Lucifer Yellow (Molecular Probes, Eugene, OR, USA) in

distilled water under a DC current of 3-8 nA for 5-10 minutes, or until dye had completely filled distal processes and no further loading was observed [18-22]. Five to 10 neurons were injected per slice and placed far enough apart to avoid overlapping of their dendritic trees. Brain sections containing loaded neurons were then mounted on gelatin-coated glass slides and cover slipped in PermaFluor mounting medium (Immunotech).

**Neuronal and dendritic reconstruction**

In order for a loaded neuron to be included in the analysis, it had to satisfy the following criteria: (1) lie within the pyramidal layer of the CA1 as defined by cytoarchitectural characteristics; (2) demonstrate complete filling of dendritic tree, as evidenced by well-defined endings; (3) demonstrate intact primary and secondary branches; (4) demonstrate intact tertiary branches, with the exception of branches that extended beyond 50 μm in radial distance from the cell soma [18-21, 23]. Neurons meeting these criteria were reconstructed in 3-dimension (3D) with a 63x/1.4 N.A., Plan-Apochromat oil immersion objective on a Zeiss Axiophot 2 microscope equipped with a motorized stage, video camera system, and Neurolucida morphometry software (MBF Bioscience, Williston, VT, USA). Using NeuroExplorer software (MBF Bioscience) total dendritic length, number of intersections and the amount of dendritic material per radial distance from the soma, in 30-μm increments [24] were analyzed in order to assess morphological cellular diversity and potential differences among animal groups.

**Confocal microscopy and *in vivo* spine acquisition**

Using an approach that precludes sampling bias of spines, dendritic segments were selected with a systematic- random design [20, 22]. Dendritic segments, 20-25 μm in length, were imaged on the a Zeiss LSM 510 confocal microscope (Zeiss, Thornwood, NY, USA) using a 100X/1.4 N.A. Plan-Apochromat objective with a digital zoom of 3.5 and an Ar/Kr laser at an excitation wavelength of 488 nm. All confocal stacks were acquired at 512x512 pixel resolution with a z-step of 0.1 μm, a pinhole setting of 1 Airy unit and optimal settings for gain and offset. All confocal stacks included approximately 1 μm above and below the identified dendritic segment. On average 3 z-stacks were imaged per neuron. In order for a dendritic segment to be optically imaged it had to satisfy the following criteria: (1) the entire segment had to fall within a depth of 50 μm; (2) dendritic segments had to be either parallel or at acute angles to the coronal surface of the section; and (3) segments did not overlap other segments that would obscure visualization of spines [22, 25]. Confocal stacks were then deconvolved using an iterative blind deconvolution algorithm (AutoDeblur version 8.0.2; MediaCybernetics, Bethesda, MD, USA). This step is necessary since in the raw image, the image spread in the Z plane would limit the precise interpretation of 3D spine morphology.

**Spine analysis**

After deconvolution, confocal stacks were analyzed with NeuronStudio [26-28] (http://www.mssm.edu/cnic) to examine global and local morphometric characteristics of dendrites and spines such as dendritic spine densities, dendritic spine shape (stubby, thin and mushroom), and dendritic spine volume. This software allows for automated

digitization and reconstructions of 3D neuronal morphology from multiple confocal stacks on a spatial scale and averts the subjective errors encountered during manual tracing using a Rayburst-based spine analysis [27-30]. At least 5 neurons per mouse and at least 3 apical and 3 basal dendritic segments per neuron were analyzed with each segment manually inspected and appropriate corrections made using the NeuronStudio interface.

**Acute Slice Preparation**

Animals were anesthetized with isoflurane, decapitated, and brains were rapidly removed and placed into oxygenated ice-cold sucrose cutting buffer (mM: 83 NaCl, 2.5 $NaHCO_3$, 3.3 $MgSO_4$, 0.5 $CaCl_2$, 2.5 KCl, 80 sucrose and 22 glucose). A vibrating blade microtome (Leica) was used to prepare 400 μm-thick whole brain slices which were immediately placed into a recovery chamber containing oxygenated artificial cerebral spinal fluid (ACSF) (mM: 118 NaCl, 1.2 $NaH_2PO_4$, 3.7 KCl, 2.6 $NaHCO_3$, and 11 glucose) which was incubated at 37ºC for 45 minutes and then left at RT for an additional 45 minutes. Before analysis, the slice was carefully transferred to a submerged recording chamber and perfused with aCSF at 2 ml/minute and maintained at 29°C.

**Extracellular Field Recording**

Extracellularly recorded field excitatory postsynaptic potentials (fEPSPs) were recorded from in the striatum radiatum of the CA1 region of the hippocampus of mice at 1- 2 months and 10- 12 months of age. fEPSPs were evoked using a bipolar electrode (FHC, Bowdoin, ME, USA) positioned in the Schaffer collateral/commissural pathway. Stimuli were generated with a GRASS S88 stimulator coupled to an Iso-flex stimulation

isolation unit (AMPI, Jerusalem, Israel) and recorded using glass recording pipette filled with oxygenated ACSF solution (tip resistance, 1.5–2.5 MΩ) coupled to an Axopatch 1D amplifier (Molecular Devices, Sunnyvale, CA, USA). Data were analyzed using Igor (WaveMetrics Incorporated, Tigard, OR, USA). Basal synaptic transmission was assessed by comparing the input and output relationship of the fEPSPs recorded. The input–output relationship (I/O) was calculated by dividing the peak amplitude of the fEPSP by the peak amplitude of the fiber volley. Pre-synaptic release was examined using paired pulse facilitation. A second pulse was elicited 50 ms after the initial stimulation and ratio was calculated by dividing the peak amplitude of the second pulse by the peak amplitude of the first pulse. Long-term potentiation (LTP) was induced by four high frequency stimulations (HFS) delivered 5 minutes apart, each at 100 Hz for 1 s after a 20-minute baseline period. Baseline was set at 20-30% the maximum field response and stimulation was maintained at a frequency of .033 Hz. fEPSPs were monitored for 60 minutes after the final tetanus [31]. Each five consecutive data points were then pooled and averaged. For final analyses, each of these pooled data points was averaged across experiments for the final 30 minutes of each experiment and compared across samples.

**Statistical analysis**

Scores for analyses for each APLP2$^{-/-}$ animal and their wt counterparts were obtained by taking the average of the data from all neurons for each animal. An independent samples *t* test was performed on spine density, spine percentage, spine volume, dendritic length, and electrophysiology experiments. Sholl analysis data were

compared by repeated measures ANOVA with genotype ($APLP2^{-/-}$ vs. $APLP2^{+/+}$) as the between-group factor and distance from the soma as the repeated-measures factor. The α level was set at 0.05 for all analyses in the study, and all data were represented as mean ± SEM.

## III.D. Results

*APLP2 and spine density in primary hippocampal neurons*

Initial studies of $APLP2^{-/-}$ mice reported that these animals were viable and fertile, with no gross phenotype [7]. However, this report was limited and no subsequent studies have analyzed finer neurological measurements, traits that have been attributed to APP. Recently, our lab found that primary hippocampal neurons from $APP^{-/-}$ mice showed marked reduction in dendritic spines (~35%) when compared with their wt counterparts [32]. This result is striking when compared to the subtle phenotypes previously reported in the $APP^{-/-}$ animals and this prompted us to examine whether the deletion of APLP2 would affect spine density similarly. For this experiment, primary neuronal cultures were established from the hippocampus of $APLP2^{-/-}$ and wt littermates and the dendritic spines were quantified after neurons were transfected with eGFP at 15-18 DIV. Unlike APP deficient neurons, primary hippocampal neurons cultured from $APLP2^{-/-}$ mice contained the same number of spines as compared to neurons cultured from the hippocampi of wt littermates (Fig. III.1; $APLP2^{+/}$: 7.1 ± 0.13 spines/10 μm; $APLP2^{-/-}$: 6.76 ± 0.1 spines/10 μm, $p > 0.05$).

*APLP2 and spine density in vivo*

Although the accruing data attest to the notion that APP may be important for synapse formation/maintenance *in vivo*, there is still very little data on whether this is a shared function of APLP2. The results from cultured neurons indicated that loss of APLP2 did not affect the number of dendritic spines in an *in vitro* setting. Several of the neuronal abnormalities displayed by the $APP^{-/-}$ mice appear to be age-dependent with the majority of deficits evident by 8-12 months of age but not at 1-4 months of age [9, 14, 33, 34], including synaptic density. Accordingly, we investigated whether the loss of APLP2 affects spine and dendritic morphology in CA1 neurons *in vivo* in aged mice, defined here as 10-12 month old animals. Digitally reconstructed dendritic segments from $APLP2^{-/-}$ and wt mice are depicted in Figure III.2 A. Consistent with our data from primary cultures, we found that the absence of APLP2 did not affect spine density in aged mice ($APLP2^{+/+}$ = 2.33 ± 0.14 spines/μm; $APLP2^{-/-}$ = 2.15 ± 0.09 spines/μm, $p > .05$) (Fig. III.2 B). Next, spines were automatically and systematically measured and categorized into three subtypes: stubby, thin, or mushroom. Each spine subtype contains distinct properties and the proportion of spine subtypes is thought to reflect biological differences or changes in sensory input [35]. Here, we found that the percentage of spine subtypes were comparable across genotypes (Stubby: $APLP2^{+/+}$ = 35.5 ± 1.4%; $APLP2^{-/-}$ = 37.2 ± 1.2%; Thin: $APLP2^{+/+}$ = 48.2 ± 1.7%; $APLP2^{-/-}$ = 47.8 ± 1.5%; Mushroom: $APLP2^{+/+}$ = 16.3 ± .8%; $APLP2^{-/-}$ = 15.0 ± 1.4%, $p > .05$ for all comparisons)
(Fig. III.3 C). Furthermore, we measured and compared spine volume and found that loss of APLP2 did not affect total mean spine volume, nor does it affect mean spine volume per spine subtype (Stubby: $APLP2^{+/+}$ = 0.05 ± 0.002 $\mu m^3$; $APLP2^{-/-}$ = 0.05 ± 0.002 $\mu m^3$;

Thin: $APLP2^{+/+}$ = 0.037 ± 0.001 μm$^3$; $APLP2^{-/-}$ = 0.037 ± 0.001 μm$^3$,; Mushroom: $APLP2^{+/+}$ = 0.145 ± 0.007 μm$^3$; $APLP2^{-/-}$ = 0.142 ± 0.009 μm$^3$, $p > .05$ for all comparisons) (Fig. III.3 D).

*Dendritic length and arborization of $APLP2^{-/-}$ mice*

Previous reports showed that the CA1 pyramidal neurons from $APP^{-/-}$ mice displayed a reduced maximum projection length and a reduction in total dendritic length at 8-12 months of age [15] but our own recent studies demonstrated that this decrease in total dendrite length and reduced dendritic arborization was age dependent as these alterations were absent in 4-month-old mice [32]. Primary hippocampal cultures from $APLP2^{-/-}$ mice revealed no obvious change in dendrite formation or arborization, however, whether this is true *in vivo* and in aged animals is not known. To study this, the dendritic tree of CA1 pyramidal neurons were imaged and digitally reconstructed. Representative examples of CA1 dendritic arbor reconstructions and dendrograms are depicted in Figure III.3 A-B. As for the spine density measurements above, total dendritic length was not altered in the $APLP2^{-/-}$ mice when compared to controls ($APLP2^{+/+}$ = 1780 ± 118 μm; $APLP2^{-/-}$ = 1878 ± 131 μm, $p > .05$) (Fig. III.3 C). Additionally, detailed analyses of the various morphometric parameters (i.e., length and complexity) of individual apical dendrites in $APLP2^{-/-}$ mice and wt controls showed no significant differences in dendrite length or number of intersections per radial region from the soma ($p > .05$ for all measurements) (Fig. III.3D-E).

*Deletion of APLP2 and synaptic function*

Static measurements of neuronal structure may not accurately reflect actual synaptic function. Further, it has been reported that changes in synaptic function might also be age dependent in APP deficient mice [14, 15, 32, 34], thus we tested synaptic basal synaptic transmission and synaptic plasticity in both young and aged APLP2 deficient animals. First, extracellularly recorded field excitatory post synaptic potentials (fEPSPs) were used to assess the strength of basal synaptic transmission at the Schaffer collateral to CA1 synapse in acute hippocampal slices in young (1-2 months) and aged (10-12 months) mice as compared to their wt littermates. The input/output ratios were calculated and we found that the ratio was comparable between genotypes and across both age groups (Young: $APLP2^{+/+}$ = 4.35 ± 0.20; $APLP2^{-/-}$ = 4.27 ± 0.21, $p > .05$; Aged: $APLP2^{+/+}$ = 4.23 ± 0.28; $APLP2^{-/-}$ = 4.43 ± 0.3, $p > .05$) (Fig. III.4A). Simultaneously, we evaluated paired-pulse facilitation (PPF) by measuring the amplitudes of pairs of fEPSPs evoked 50 ms apart. We expressed this as a ratio ($fEPSP_2/fEPSP_1$), and compared the ratio across genotypes and age groups and found that PPF remains unaffected by the absence of APLP2 (Young: $APLP2^{+/+}$ = 1.59 ± 0.09; $APLP2^{-/-}$ = 1.57 ± 0.03, $p > .05$; Aged: $APLP2^{+/+}$ = 1.46 ± 0.05; $APLP2^{-/-}$ = 1.37 ± 0.03, $p > .05$) (Fig. III.4B). Finally, we tested for impairments in synaptic plasticity by measuring long-term potentiation (LTP) the cellular process thought to underlie learning and memory [36]. To induce LTP, four 1-s tetanic stimuli were given at 100 Hz, 5 minutes apart and fEPSPs were monitored for 60 minutes. We report that the percent increase in fEPSPs post-tetanus was indistinguishable between genotypes at each age group (Young: $APLP2^{+/+}$ = 191 ± 7%; $APLP2^{-/-}$ = 195 ± 7% $p > .05$; Aged: $APLP2^{+/+}$ = 197 ± 13%; $APLP2^{-/-}$ = 180 ± 17%, $p > .05$) (Fig. III.5).

*APLP2 and Aβ-induced LTP impairment*

In order to determine whether APLP2 contributes to Aβ related synaptic dysfunction, we utilized a previously published protocol that is shown to induce LTP impairment[31]. For this experiment, we incubated acute brain slices from young animals in 1 nM of Aβ for 20 minutes, once a 20 minute baseline was established. After the 20 minute incubation period, we induced LTP and monitored fEPSPs for 60 minutes. While we saw the expected LTP impairment in wt mice, we saw similar impairment with the $APLP2^{-/-}$ mice, indicating that the presence of APLP2 is not necessary for Aβ synaptotoxicity (Young: $APLP2^{+/+}$ = 110 ± 7%; $APLP2^{-/-}$ = 107 ± 6% $p > .05$) (Fig. III.6).

## III.E. Discussion

APLP2 contains a high degree of sequence and structural homology to APP but does not contain the Aβ region. This, coupled with an almost identical spatial and temporal pattern of expression presents a unique opportunity to explore whether the non-Aβ metabolites play a role in AD pathogenesis. Although initial reports on $APLP2^{-/-}$ mice indicated no overt phenotype [7], these studies are few and until recently, none had investigated in detail neuronal morphology, synaptic function, or spine formation, the physiological roles that have been attributed to APP. Here, we showed that APLP2 did not appear to be essential for spine numbers in primary hippocampal cultures. Our results further indicated that APLP2 did not seem to determine or maintain spine density, type,

or volume in CA1 pyramidal neurons *in vivo* in animals of 10-12 months of age. APLP2 by itself was also not required for proper dendrite elongation and organization in aged mice as assessed by total dendrite length, dendritic length per radial distance from the soma and number of intersections of dendrites per radial distance from the soma. Finally, we demonstrated that APLP2$^{-/-}$ mice did not exhibit any impairment in neuronal function as measured by basal synaptic transmission, paired-pulse ratio, and long-term potentiation at the CA1-CA3 synapses in young or old animals. Additionally, deletion of APLP2 does not affect Aβ-induced impairment of LTP, indicating that unlike APP, APLP2 appears not to play a role in Aβ synaptotoxicity.

Although the initial report showed no overt upregulation of APP or APLP1 in APLP2$^{-/-}$ mice [7], animal model studies leave little debate for the existence of functional redundancy. Although we cannot exclude a physiological role of APLP2 in synapse formation and function *in vivo*, the fact that endogenous APLP2 cannot functionally compensate for loss of APP suggests that APP contains neuronal functions that are either distinct from APLP2 or dominant to APLP2. A similar situation is at play in the two members of the presenilin gene family *PSEN1* (PS1) and *PSEN2* (PS2). Loss of PS1 is embryonically lethal [37, 38], yet loss of PS2 leads to viable animals with only mild phenotype [39]. Nonetheless, both PS1 and PS2 perform overlapping functions as familial AD mutations in both genes invariably result in alterations in the ratio of Aβ peptides, favoring the generation of the longer Aβ42 isoforms [40].

Although a potentially useful tool, knockouts of APP or APLP1 coupled with APLP2 deficiency leads to perinatal lethality in 80% of pups [7, 8]. In pursuit of distinguishing the domain(s) responsible for this phenotype, it was recently reported that

a substitution of tyrosine at position 682 to glycine in the YENPTY motif in the APP cytoplasmic domain was sufficient to induce this postnatal lethality when crossed against the APLP2$^{-/-}$ background, indicating that the C-terminal domain is essential for APP function [41]. Supporting this notion, mice with knock-in of sAPPβ into the APLP2$^{-/-}$ background, thus without the transmembrane or cytoplasmic domains of APP, still exhibited lethality and neuromuscular defects [42]. However, knock-in of sAPPα into similar APLP2 null background rescued the postnatal lethality although surviving mice showed neuromuscular abnormalities and impaired learning and memory, indicating that these are hypomorphic with respect to APP function [43]. Taken together, these studies indicated that functional domains are present in both the N-terminal ectodomain and the C-terminal cytoplasmic. Whether similar functional domains are present in APLP2 is not known. However, because APLP2 does not have the Aβ sequence, thus lacking the 17 amino acids at the C-terminus of sAPPα, one would predict that APLP2 does not have a similar trophic region in the juxtamembrane region. Notably, it was also shown that LTP appeared normal in APLP2 deficient mice, results entirely consistent with what we observed. Given our results, we conclude that like the electrophysiological properties, the neuronal morphology of APLP2 deficient animals is also normal.

The majority of studies indicate that genetic ablation of APP leads to a loss of function as implicated by a reduction in spines, reduced dendritic complexity and impaired synaptic function [9, 15, 30]. However, a few studies reported contradicting results, such as increased synapse number, miniature EPSP frequency and AMPAR- and NMDAR-mediated synaptic transmission [44, 45]. The reasons for these discrepancies are unknown but in addition to different experimental approaches and mouse strains, the age

and brain region that were studied may explain some of these results. For example, our own studies recently demonstrated a decrease in spine density and reduced dendritic length and complexity in CA1 pyramidal cells at 12-14 months but not at 4 months of age [32]. This surprising age-dependent change in neuronal morphology was not described in previous studies that examined only older animals. Given these results, we hypothesized that APLP2 deficiency may also display an age dependent phenotype. However, our electrophysiological experiments did not show any defects in either young or aged animals, thereby demonstrating convincingly that there is no age dependent alteration in synaptic function in APLP2 deficient animals.

Regardless, we currently favor the hypothesis that the APP family members share similar functions through the conserved domains. In part, we reason that while little work has been done on the neurotrophism of APLP2, there is evidence that it has neurotrophic activities [46, 47] and the overexpression of APP, APLP2, or APLP1, was each shown to rescue the migration defect seen in neuronal precursor cells derived from triple knockout animals [48]. Similarly, it has been reported that sAPPβ and the cognate APLP2 region contain a similar function in axonal pruning [49], reemphasizing a broad spectrum of functional redundancy.

While this study also indicates that presence of APLP2 is not necessary for Aβ induced impairment of LTP, the reason for this is yet to be determined. It is possible that APP is a preferred substrate and APLP2 is not being appreciably cleaved by caspases. Caspases tend to prefer non-bulky substrates at the P1' position and while the recognition sequence for APP is VEVDA, the recognition sequence for APLP1 and APLP2 is VEVDP. Proline is rather bulky as compared to alanine, suggesting that APP would be a

preferred substrate [10]. Consistent with this notion, while it was found that although APLP2 can be cleaved by caspase-3 *in vitro*, it did so with less efficiency than APP. Thus, even if the C-terminal peptide is toxic in and of itself, it is likely that caspase cleavage of APLP2 does not occur enough to impart appreciable toxicity. Alternatively, it is suggested that APP mediates Aβ toxicity through the binding of Aβ at the cognate Aβ region. Since the Aβ domain is a region of divergence, it is also possible that Aβ does not bind to APLP2 to initiate the downstream effects.

In conclusion, we found that unlike APP, APLP2 is dispensable for normal growth and maintenance of dendritic growth and arborization, spine formation, and neuronal function in an age-independent manner. Additionally, APLP2 also appears to depart from APP in that its presence is not necessary for Aβ-related synaptic dysfunction. Although it is interesting to surmise the source of change in function between APP and APLP2, it is likely that functional redundancy blurs the physiologic functions of each of these proteins. Future experiments may need to be carried out using a temporally controlled expression system in order to limit compensatory effects and to help resolve the complex interplay amongst this family of genes.

Chapter III, in part, has been published in Molecular and Cellular Neurodegeneration. 2011, Midthune, Brea; Tyan, Sheue-Houy; Walsh, Jessica J; Sarsoza, Floyd; Eggert, Simone; Hof, Patrick R.; Dickstein, Dara L.; Koo, Edward H. "Deletion of the amyloid precursor-like protein 2 (APLP2) does not affect hippocampal neuron morphology or function", Molecular and Cellular Neuroscience, 2012 Apr;49(4):448-55. The dissertation author was the primary investigator and author of this paper.

# III.F. Figures

Figure III.1

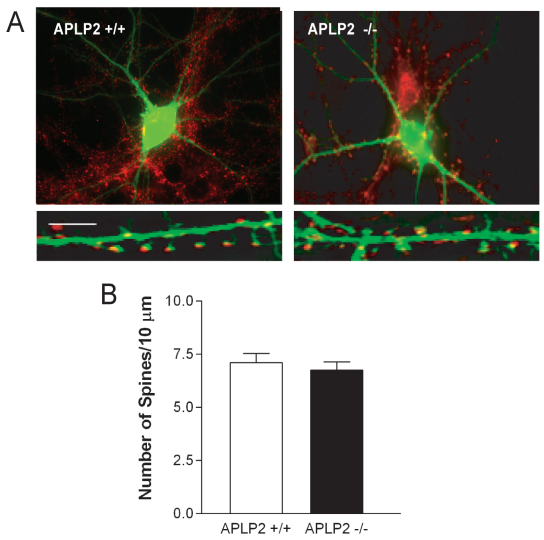


**Figure III.1.** Deletion of APLP2 does not affect spine density in primary culture. A) Representative images of cultured primary hippocampal neurons that were transfected with eGFP at DIV 15-18, fixed and imaged one day post transfection. Insets show the segments in the secondary dendrites that were quantified for spine numbers after magnification. B) Quantification of spine numbers from cultured neurons shown in (A). There were no differences in spine density between the two genotypes (wt: 41 neurons from n = 11 mice, APLP2$^{-/-}$: 56 neurons from n = 13 mice).

Figure III.2

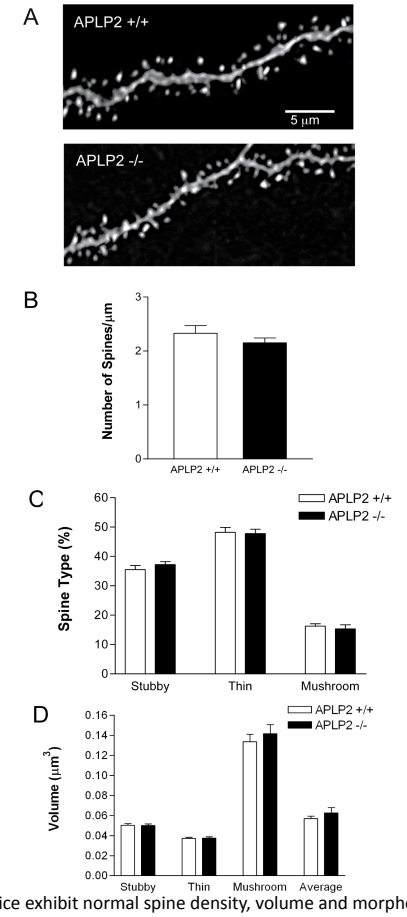


**Figure III.2.** Aged APLP2$^{-/-}$ mice exhibit normal spine density, volume and morphometry. A) Representative 3-dimensional reconstructions of CA1 pyramidal dendritic segments from 10-12 month old wt and APLP2$^{-/-}$ mice. Automated analysis of spine density displayed no changes in total spine density (B) or in percentage of spine type per dendritic segment (C) (n = 5 wt and 7 APLP2$^{-/-}$ mice, at least 5 neurons per mouse and at least 3 dendritic segments per neuron). D) Further morphometric analysis of spine volume revealed comparable mean spine volumes amongst spine types.

Figure III.3

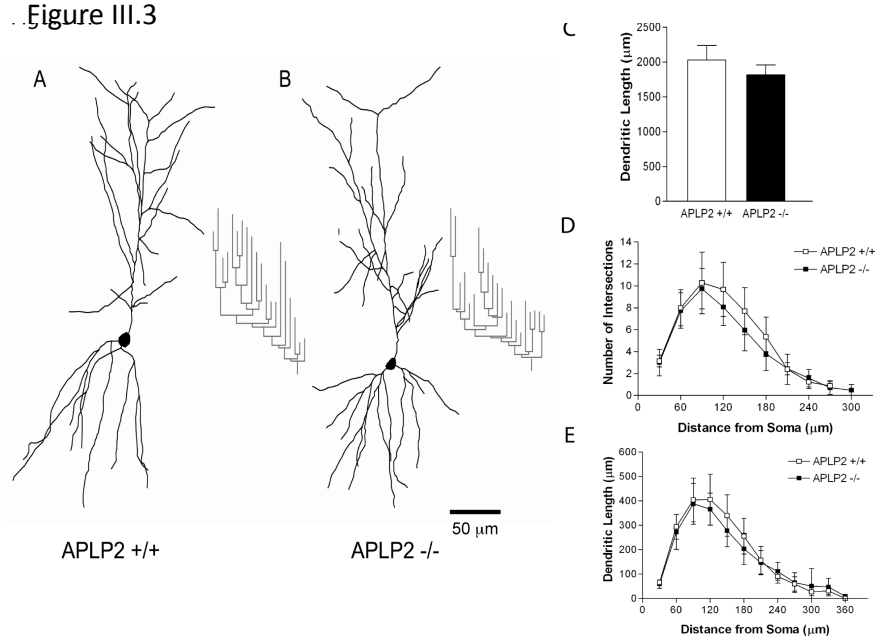


**Figure III.3.** Morphological alterations and dendritic length are not affected by the absence of APLP2 in aged animals *in vivo*. Representative examples of 3D reconstructions from pyramidal layer CA1 neurons in 10-month-old wt control (A) and APLP2$^{-/-}$ (B) mice. Reconstructed cells were obtained using NeuroExplorer (MBF) and rotated about the principal axis to depict apical and basal dendritic orientation. Total dendritic length (C), Sholl analyses (dendritic length per radial distance from soma (D)) and intersections per radial distance from the soma were compared from apical dendrites of CA1 pyramidal cells of APLP2$^{-/-}$ mice and their wt littermates at 10-12 months of age revealing no significant difference between genotype. Cells were traced using Neurolucida and quantified using NeuroExplorer software (n = 5 wt and 7 APLP2$^{-/-}$ mice). Values represent mean ± SEM.

Figure III.4

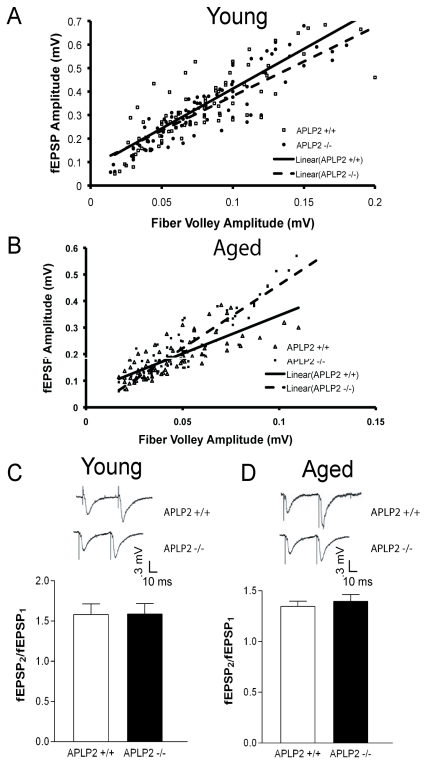


**Figure III.4.** Deletion of APLP2 does not alter basal synaptic transmission in young or aged mice. A) Scatter plots of the fEPSP amplitude versus fiber volley for 1-2 month old and 10-12 month old APLP2$^{-/-}$ and wt mice, fit by linear regression, demonstrated no significant difference in the input/output ratio between genotypes of young (A) or aged (B) animals (A; n = 14 wt, 15 APLP2$^{-/-}$ slices from 10 and 12 animals, respectively, B; n = 11 wt, 12 APLP2$^{-/-}$ slices from 6 and 7 animals respectively. Presynaptic release probability was examined by eliciting a second pulse 50 ms after the first pulse. No significant differences were found between genotypes at 1-2 months of age (C; n = 14 wt, 15 APLP2$^{-/-}$ slices from 10 and 12 animals, respectively) or 10-12 months of age (D; n = 11 wt, 12 APLP2$^{-/-}$ slices from 6 and 7 animals, respectively). Sample tracings located above the graph. Values represent mean ± SEM.

Figure III.5

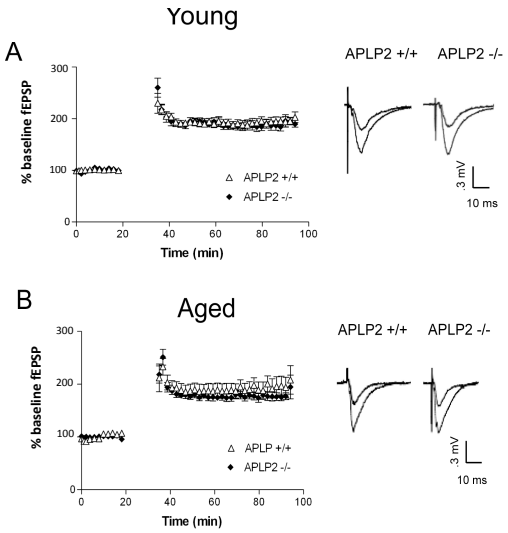


**Figure III.5.** APLP2$^{-/-}$ mice show normal LTP in young and aged mice. After a 20-minute baseline, LTP was induced by four 1-s tetanic stimuli delivered 5 minutes apart, each at 100 Hz. The percent increase in response after the tetanus was given was compared between the APLP2$^{-/-}$ mice and littermate animals at 1-2 months of age (A; n = 14 wt, 15 APLP2$^{-/-}$ slices from 10-12 animals/genotype) and at 10-12 months of age (B; n = 11 wt, 12 APLP2$^{-/-}$ slices from 6 - 7 animals/genotype). No significant difference was found across genotype or age group. Sample tracings to the right of each figure. Values represent mean ± SEM.

Figure III.6

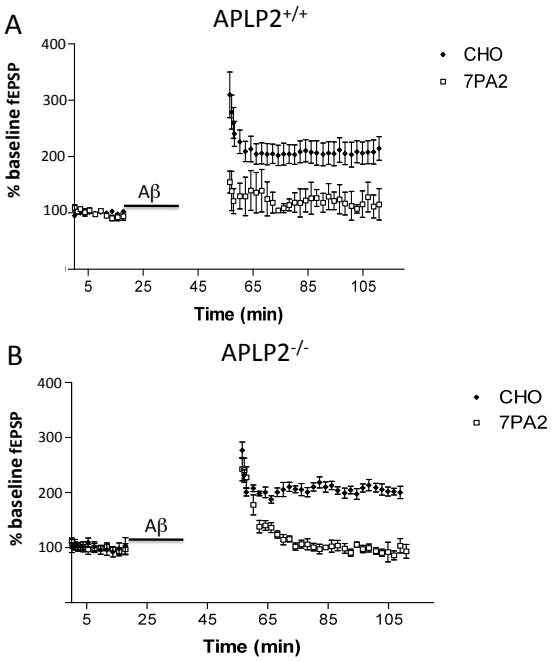


**Figure III.6**: Absence of APLP2 does not rescue LTP impairment after Aβ incubation. After a 20 min baseline, slices were washed for 20 minutes with oxygenated ACSF containing conditioned medium from 7PA2 cells, resulting in a concentration of 1 nM total Aβ. LTP was then induced by four tetani delivered 5 minutes apart, each at 100 Hz for 1 s. fEPSPs were monitored for 60 min after the final tetanus. A) Average time course of LTP in APLP2 +/+ mice after a 20 minute incubation in 1 nM total Aβ. As a control, slices from the same animal were incubated with equal parts conditioned medium from untransfected wt CHO cells. B) Average time course of LTP in APLP2 -/- mice after a 20 minute incubation in 1 nM total Aβ. Line indicates Aβ treatment time. No significant differences were seen between genotypes.

References

1. Hardy J, Selkoe DJ. The amyloid hypothesis of Alzheimer's disease: progress and problems on the road to therapeutics. Science. 2002 Jul 19;297(5580):353-6.

2. Coulson EJ, Paliga K, Beyreuther K, Masters CL. What the evolution of the amyloid protein precursor supergene family tells us about its function. Neurochem Int. 2000 Mar;36(3):175-84.

3. Eggert S, Paliga K, Soba P, Evin G, Masters CL, Weidemann A, et al. The proteolytic processing of the amyloid precursor protein gene family members APLP-1 and APLP-2 involves alpha-, beta-, gamma-, and epsilon-like cleavages: modulation of APLP-1 processing by n-glycosylation. J Biol Chem. 2004 Apr 30;279(18):18146-56.

4. Collin RW, van Strien D, Leunissen JA, Martens GJ. Identification and expression of the first nonmammalian amyloid-beta precursor-like protein APLP2 in the amphibian Xenopus laevis. Eur J Biochem. 2004 May;271(10):1906-12.

5. Jacobsen KT, Iverfeldt K. Amyloid precursor protein and its homologues: a family of proteolysis-dependent receptors. Cell Mol Life Sci. 2009 Jul;66(14):2299-318.

6. Wasco W, Gurubhagavatula S, Paradis MD, Romano DM, Sisodia SS, Hyman BT, et al. Isolation and characterization of APLP2 encoding a homologue of the Alzheimer's associated amyloid beta protein precursor. Nat Genet. 1993 Sep;5(1):95-100.

7. von Koch CS, Zheng H, Chen H, Trumbauer M, Thinakaran G, van der Ploeg LH, et al. Generation of APLP2 KO mice and early postnatal lethality in APLP2/APP double KO mice. Neurobiol Aging. 1997 Nov-Dec;18(6):661-9.

8. Heber S, Herms J, Gajic V, Hainfellner J, Aguzzi A, Rulicke T, et al. Mice with combined gene knock-outs reveal essential and partially redundant functions of amyloid precursor protein family members. J Neurosci. 2000 Nov 1;20(21):7951-63.

9. Zheng H, Jiang M, Trumbauer ME, Sirinathsinghji DJ, Hopkins R, Smith DW, et al. beta-Amyloid precursor protein-deficient mice show reactive gliosis and decreased locomotor activity. Cell. 1995 May 19;81(4):525-31.

10. Galvan V, Chen S, Lu D, Logvinova A, Goldsmith P, Koo EH, et al. Caspase cleavage of members of the amyloid precursor family of proteins. J Neurochem. 2002 Jul;82(2):283-94.

11. Lu DC, Rabizadeh S, Chandra S, Shayya RF, Ellerby LM, Ye X, et al. A second cytotoxic proteolytic peptide derived from amyloid beta-protein precursor. Nat Med. 2000 Apr;6(4):397-404.

12. Shaked GM, Kummer MP, Lu DC, Galvan V, Bredesen DE, Koo EH. Abeta induces cell death by direct interaction with its cognate extracellular domain on APP (APP 597-624). FASEB J. 2006 Jun;20(8):1254-6.

13. McPhie DL, Golde T, Eckman CB, Yager D, Brant JB, Neve RL. beta-Secretase cleavage of the amyloid precursor protein mediates neuronal apoptosis caused by familial Alzheimer's disease mutations. Brain Res Mol Brain Res. 2001 Dec 16;97(1):103-13.

14. Dawson GR, Seabrook GR, Zheng H, Smith DW, Graham S, O'Dowd G, et al. Age-related cognitive deficits, impaired long-term potentiation and reduction in synaptic marker density in mice lacking the beta-amyloid precursor protein. Neuroscience. 1999 Apr;90(1):1-13.

15. Seabrook GR, Smith DW, Bowery BJ, Easter A, Reynolds T, Fitzjohn SM, et al. Mechanisms contributing to the deficits in hippocampal synaptic plasticity in mice lacking amyloid precursor protein. Neuropharmacology. 1999 Mar;38(3):349-59.

16. Tyan SH, Shih AY, Walsh JJ, Murayama H, Sarsoza F, Ku L, et al. Amyloid precursor protein (APP) regulates synaptic structure and function. Mol Cell Neurosci. 2012 Aug 3.

17. Calabrese B, Shaked GM, Tabarean IV, Braga J, Koo EH, Halpain S. Rapid, concurrent alterations in pre- and postsynaptic structure induced by naturally-secreted amyloid-beta protein. Mol Cell Neurosci. 2007 Jun;35(2):183-93.

18. Duan H, Wearne SL, Morrison JH, Hof PR. Quantitative analysis of the dendritic morphology of corticocortical projection neurons in the macaque monkey association cortex. Neuroscience. 2002;114(2):349-59.

19. Duan H, Wearne SL, Rocher AB, Macedo A, Morrison JH, Hof PR. Age-related dendritic and spine changes in corticocortically projecting neurons in macaque monkeys. Cereb Cortex. 2003 Sep;13(9):950-61.

20. Hao J, Rapp PR, Leffler AE, Leffler SR, Janssen WG, Lou W, et al. Estrogen alters spine number and morphology in prefrontal cortex of aged female rhesus monkeys. J Neurosci. 2006 Mar 1;26(9):2571-8.

21. Radley JJ, Sisti HM, Hao J, Rocher AB, McCall T, Hof PR, et al. Chronic behavioral stress induces apical dendritic reorganization in pyramidal neurons of the medial prefrontal cortex. Neuroscience. 2004;125(1):1-6.

22. Radley JJ, Rocher AB, Miller M, Janssen WG, Liston C, Hof PR, et al. Repeated stress induces dendritic spine loss in the rat medial prefrontal cortex. Cereb Cortex. 2006 Mar;16(3):313-20.

23. Liston C, Miller MM, Goldwater DS, Radley JJ, Rocher AB, Hof PR, et al. Stress-induced alterations in prefrontal cortical dendritic morphology predict selective impairments in perceptual attentional set-shifting. J Neurosci. 2006 Jul 26;26(30):7870-4.

24. Sholl DA. Dendritic organization in the neurons of the visual and motor cortices of the cat. J Anat. 1953 Oct;87(4):387-406.

25. Radley JJ, Rocher AB, Rodriguez A, Ehlenberger DB, Dammann M, McEwen BS, et al. Repeated stress alters dendritic spine morphology in the rat medial prefrontal cortex. J Comp Neurol. 2008 Mar 1;507(1):1141-50.

26. Wearne SL, Rodriguez A, Ehlenberger DB, Rocher AB, Henderson SC, Hof PR. New techniques for imaging, digitization and analysis of three-dimensional neural morphology on multiple scales. Neuroscience. 2005;136(3):661-80.

27. Rodriguez A, Ehlenberger DB, Hof PR, Wearne SL. Rayburst sampling, an algorithm for automated three-dimensional shape analysis from laser scanning microscopy images. Nat Protoc. 2006;1(4):2152-61.

28. Rodriguez A, Ehlenberger DB, Dickstein DL, Hof PR, Wearne SL. Automated three-dimensional detection and shape classification of dendritic spines from fluorescence microscopy images. PLoS One. 2008;3(4):e1997.

29. Rodriguez A, Ehlenberger D, Kelliher K, Einstein M, Henderson SC, Morrison JH, et al. Automated reconstruction of three-dimensional neuronal morphology from laser scanning microscopy images. Methods. 2003 May;30(1):94-105.

30. Fitzjohn SM, Morton RA, Kuenzi F, Davies CH, Seabrook GR, Collingridge GL. Similar levels of long-term potentiation in amyloid precursor protein -null and wild-type mice in the CA1 region of picrotoxin treated slices. Neurosci Lett. 2000 Jul 7;288(1):9-12.

31. Townsend M, Shankar GM, Mehta T, Walsh DM, Selkoe DJ. Effects of secreted oligomers of amyloid beta-protein on hippocampal synaptic plasticity: a potent role for trimers. J Physiol. 2006 Apr 15;572(Pt 2):477-92.

32. Tyan S-H, B. Midthune, S. Eggert, D. L. Dickstein and E. H. Koo. Role of Amyloid Precursor proteins and Abeta-induced synaptic dysfunction. Abstract, International Conference on Alzheimer's Disease, Honolulu, HI. 2010;Abstract # 1962.

33. Phinney AL, Calhoun ME, Wolfer DP, Lipp HP, Zheng H, Jucker M. No hippocampal neuron or synaptic bouton loss in learning-impaired aged beta-amyloid precursor protein-null mice. Neuroscience. 1999;90(4):1207-16.

34. Senechal Y, Kelly PH, Dev KK. Amyloid precursor protein knockout mice show age-dependent deficits in passive avoidance learning. Behav Brain Res. 2008 Jan 10;186(1):126-32.

35. Alvarez VA, Sabatini BL. Anatomical and physiological plasticity of dendritic spines. Annu Rev Neurosci. 2007;30:79-97.

36. Kessels HW, Malinow R. Synaptic AMPA receptor plasticity and behavior. Neuron. 2009 Feb 12;61(3):340-50.

37. Shen J, Bronson RT, Chen DF, Xia W, Selkoe DJ, Tonegawa S. Skeletal and CNS defects in Presenilin-1-deficient mice. Cell. 1997 May 16;89(4):629-39.

38. Wong PC, Zheng H, Chen H, Becher MW, Sirinathsinghji DJ, Trumbauer ME, et al. Presenilin 1 is required for Notch1 and DII1 expression in the paraxial mesoderm. Nature. 1997 May 15;387(6630):288-92.

39. Herreman A, Hartmann D, Annaert W, Saftig P, Craessaerts K, Serneels L, et al. Presenilin 2 deficiency causes a mild pulmonary phenotype and no changes in amyloid precursor protein processing but enhances the embryonic lethal phenotype of presenilin 1 deficiency. Proc Natl Acad Sci U S A. 1999 Oct 12;96(21):11872-7.

40. Tanzi RE, Bertram L. Twenty years of the Alzheimer's disease amyloid hypothesis: a genetic perspective. Cell. 2005 Feb 25;120(4):545-55.

41. Barbagallo AP, Wang Z, Zheng H, D'Adamio L. A single tyrosine residue in the amyloid precursor protein intracellular domain is essential for developmental function. J Biol Chem. 2011 Mar 18;286(11):8717-21.

42. Li H, Wang B, Wang Z, Guo Q, Tabuchi K, Hammer RE, et al. Soluble amyloid precursor protein (APP) regulates transthyretin and Klotho gene expression without rescuing the essential function of APP. Proc Natl Acad Sci U S A. 2010 Oct 5;107(40):17362-7.

43. Weyer SW, Klevanski M, Delekate A, Voikar V, Aydin D, Hick M, et al. APP and APLP2 are essential at PNS and CNS synapses for transmission, spatial learning and LTP. EMBO J. 2011 Jun 1;30(11):2266-80.

44. Priller C, Bauer T, Mitteregger G, Krebs B, Kretzschmar HA, Herms J. Synapse formation and function is modulated by the amyloid precursor protein. J Neurosci. 2006 Jul 5;26(27):7212-21.

45. Bittner T, Fuhrmann M, Burgold S, Jung CK, Volbracht C, Steiner H, et al. Gamma-secretase inhibition reduces spine density in vivo via an amyloid precursor protein-dependent pathway. J Neurosci. 2009 Aug 19;29(33):10405-9.

46. Young-Pearse TL, Chen AC, Chang R, Marquez C, Selkoe DJ. Secreted APP regulates the function of full-length APP in neurite outgrowth through interaction with integrin beta1. Neural Dev. 2008;3:15.

47. Cappai R, Mok SS, Galatis D, Tucker DF, Henry A, Beyreuther K, et al. Recombinant human amyloid precursor-like protein 2 (APLP2) expressed in the yeast Pichia pastoris can stimulate neurite outgrowth. FEBS Lett. 1999 Jan 8;442(1):95-8.

48. Young-Pearse TL, Bai J, Chang R, Zheng JB, LoTurco JJ, Selkoe DJ. A critical function for beta-amyloid precursor protein in neuronal migration revealed by in utero RNA interference. J Neurosci. 2007 Dec 26;27(52):14459-69.

49. Nikolaev A, McLaughlin T, O'Leary DD, Tessier-Lavigne M. APP binds DR6 to trigger axon pruning and neuron death via distinct caspases. Nature. 2009 Feb 19;457(7232):981-9.

# Chapter IV: Induced Dimerization of the Amyloid Precursor Protein Leads to Decreased Amyloid-β Protein Production

Supplemental Material can be found at:
http://www.jbc.org/content/suppl/2009/07/13/M109.038646.DC1.html

THE JOURNAL OF BIOLOGICAL CHEMISTRY VOL. 284, NO. 42, pp. 28943–28952, October 16, 2009


## Induced Dimerization of the Amyloid Precursor Protein Leads to Decreased Amyloid-β Protein Production*[S]

Received for publication, June 28, 2009, and in revised form, July 12, 2009 Published, JBC Papers in Press, July 13, 2009, DOI 10.1074/jbc.M109.038646

**Simone Eggert, Brea Midthune, Barbara Cottrell, and Edward H. Koo**[1]

*From the Department of Neurosciences, University of California, San Diego, La Jolla, California 92093*

**The amyloid precursor protein (APP) plays a central role in Alzheimer disease (AD) pathogenesis because sequential cleavages by β- and γ-secretase lead to the generation of the amyloid-β (Aβ) peptide, a key constituent in the amyloid plaques present in brains of AD individuals. In several studies APP has recently been shown to form homodimers, and this event appears to influence Aβ generation. However, these studies have relied on APP mutations within the Aβ sequence itself that may affect APP processing by interfering with secretase cleavages independent of dimerization. Therefore, the impact of APP dimerization on Aβ production remains unclear. To address this question, we compared the approach of constitutive cysteine-induced APP dimerization with a regulatable dimerization system that does not require the introduction of mutations within the Aβ sequence. To this end we generated an APP chimeric molecule by fusing a domain of the FK506-binding protein (FKBP) to the C terminus of APP. The addition of the synthetic membrane-permeant drug AP20187 induces rapid dimerization of the APP-FKBP chimera. Using this system we were able to induce up to 70% APP dimers. Our results showed that controlled homodimerization of APP-FKBP leads to a 50% reduction in total Aβ levels in transfected N2a cells. Similar results were obtained with the direct precursor of β-secretase cleavage, C99/SPA4CT-FKBP. Furthermore, there was no modulation of different Aβ peptide species after APP dimerization in this system. Taken together, our results suggest that APP dimerization can directly affect γ-secretase processing and that dimerization is not required for Aβ production.**

The mechanism of β-amyloid protein (Aβ)[2] generation from the amyloid precursor protein is of major interest in Alzheimer disease research because Aβ is the major constituent of senile plaques, one of the neuropathological hallmarks of Alzheimer disease (1, 2). In the amyloidogenic pathway Aβ is released from the amyloid precursor protein (APP) (3) after sequential cleavages by β-secretase BACE1 (4–6) and by the γ-secretase complex (7, 8). BACE1 cleavage releases the large ectodomain of APP while generating the membrane-anchored C-terminal APP fragment (CTF) of 99 amino acids (C99). Cleavage of β-CTF by γ-secretase leads to the secretion of Aβ peptides of various lengths and the release of the APP intracellular domain (AICD) into the cytosol (9–11). The γ-secretase complex consists of at least four proteins: presenilin, nicastrin, Aph-I, and Pen-2 (12). Presenilin is thought to be the catalytic subunit of the enzyme complex (13), but how the intramembrane scission is carried out remains to be elucidated. Alternatively, APP can first be cleaved in the non-amyloidogenic pathway by α-secretase within the Aβ domain between Lys-16 and Leu-17 (14, 15). This cleavage releases the APP ectodomain (APPsα) while generating the membrane-bound C-terminal fragment (α-CTF) of 83 amino acids (C83). The latter can be further processed by the γ-secretase complex, resulting in the secretion of the small 3-kDa fragment p3 and the release of AICD.

APP, a type I transmembrane protein (16) of unclear function, may act as a cell surface receptor (3). APP and its two homologues, APLP1 and APLP2, can dimerize in a homotypic or heterotypic manner and, in so doing, promote intercellular adhesion (17). *In vivo* interaction of APP, APLP1, and APLP2 was demonstrated by cross-linking studies from brain homogenates (18). To date at least four domains have been reported to promote APP dimerization; that is, the E1 domain containing the N-terminal growth factor-like domain and copper binding domain (17), the E2 domain containing the carbohydrate domain in the APP ectodomain (19), the APP juxtamembrane region (20), and the transmembrane domain (21, 22). In the latter domain the dimerization appears to be mediated by the G*XXX*G motif near the luminal face of the transmembrane region (21, 23). In addition to promoting cell adhesion, APP dimerization has been proposed to increase susceptibility to cell death (20, 24).

Interestingly, by introducing cysteine mutations into the APP juxtamembrane region, it was shown that stable dimers through formation of these disulfide linkages result in significantly enhanced Aβ production (25). This finding is consistent with the observation that stable Aβ dimers are found intracellularly in neurons and *in vivo* in brain (26). Taken together, these results have led to the idea that APP dimerization can positively regulate Aβ production. However, other laboratories have not been able to confirm some of these observations using slightly different approaches (23, 27).

* This work was supported, in whole or in part, by National Institutes of Health Grant AG 12376 (to E. H. K.). This work was also supported in part by a Deutsche Forschungsgemeinschaft postdoctoral fellowship (to S. E.).

[S] The on-line version of this article (available at http://www.jbc.org) contains supplemental Figs. 1–4.

[1] To whom correspondence should be addressed: Dept. of Neurosciences, University of California, San Diego, LBR, 9500 Gilman Drive, La Jolla, CA 92093. Tel.: 858-822-1024; Fax: 858-822-1021; E-mail: edkoo@ucsd.edu.

[2] The abbreviations used are: Aβ, amyloid-β peptide; APP, amyloid precursor protein; CTF, C-terminal (CT) fragment; MALDI-TOF, matrix-assisted laser desorption/ionization time of flight mass spectrometry; FKBP, FK506-binding protein; ELISA, enzyme-linked immunosorbent assay; DAPT, *N*-(*N*-(3,5-difluorophenylacetyl)-L-alanyl)-*S*-phenylglycine *t*-butyl ester; HA, hemagglutinin; AICD, APP intracellular domain; HA, hemagglutinin; wt, wild type; Bis-Tris, 2-[bis(2-hydroxyethyl)amino]-2-(hydroxymethyl)propane-1,3-diol; Tricine, *N*-[2-hydroxy-1,1-bis(hydroxymethyl)ethyl]glycine.

To further address the question of how dimerization of APP affects cleavage by α-, β-, and γ-secretase, we chose to test this with a controlled dimerization system. Accordingly, we engineered a chimeric APP molecule by fusing a portion of the FK506-binding protein (FKBP) to the C terminus of APP such that the addition of the synthetic membrane-permeant bifunctional compound, AP20187, will induce dimerization of the APP-FKBP chimera in a controlled manner by binding to the FKBP domains. Using this system, efficient dimerization of APP up to 70% can be achieved in a time and concentration-dependent fashion. Our studies showed that controlled homodimerization of APP-FKBP leads to decreased total Aβ levels in transfected N2a cells. Homodimerization of the β-CTF/C99 fragment, the direct precursor of γ-secretase cleavage, showed comparable results. In addition, induced dimerization of APP did not lead to a modulation of different Aβ peptides as it was reported for G*XXX*G mutants within the transmembrane domain of APP (21).

## EXPERIMENTAL PROCEDURES

*DNA Constructs*—FKBP-tagged APP695 constructs were generated in a three-fragment ligation step. First, the 1054-bp EcoRI and XhoI 5′ fragment was released from APP695 pUAST (17). Second, an APP fragment from the 3′ end was generated by PCR from APP695 pUAST without a stop codon and appending an XbaI restriction site using the primer 5′-CGAGTTCCTACAACAGCAGCC-3′ and an antisense primer, 5′-GCGGTGTCTAGAGTTCTGCATCTGCTC-3′, and digested with XhoI and XbaI. These two fragments were ligated into the vector pC4F1 (with one FKBP domain) or pC4F2 (with two FKBP domains) (Ariad Pharmaceuticals, Cambridge, MA) using the restriction sites EcoRI and XbaI. To generate FKBP-tagged SPA4CT constructs, a silent mutation was first introduced into SPA4CT DA pCEP4 (28) at position Glu-22 (Aβ numbering) to remove the internal EcoRI site by site-directed mutagenesis (QuikChange, Stratagene, La Jolla, CA). A PCR fragment of the entire SPA4CT DA open reading frame was subsequently generated, again without the stop codon and with an Xba1 site added to the 3′ end and an EcoRI site added to the 5′end, and ligated into vector pC4F1 (with one FKBP domain) and vector pC4F2 (with two FKBP domains). A control FKBP-tagged AICD construct starting at Val-50 (Aβ numbering) was generated with a methionine residue added as a start codon and ligated into pC4F1 (or pC4F2).

To generate an APP695 CT HA construct without the FKBP fusion, the 3′-untranslated region of APP was amplified from APP695 wt NT HA pcDNA3.1 neo (17) with sense primer 5′-GTTTATAACTCGAGACCCCCGCCACAGC-3′, containing an XhoI site, and antisense primer, 5′-CCCGCG-GCTCTAGATCTTAAAGCATATGTAAAG-3′, containing an XbaI site. The PCR product was digested with XhoI and XbaI restriction enzymes and subcloned into the same sites in the pcDNA3.1+ neo vector. Sense primer 5′-GTGGCCGAG-GAGGAGATTCAGGA-3′, starting at position 1481 in the APP695 open reading frame and antisense primer, 5′-GCT-GACCTCGAGTTATGCGTAGTCTGGTACGTCGTACG-GATAGTTCTGCATCTGCTC-3′, containing the 3′ end of the APP695 open reading frame without a stop codon, the HA tag, and an XhoI restriction site, were used to amplify APP695 wt NT HA. The PCR product was digested with SacI and XhoI restriction enzymes. The EcoRI and SacI fragment from APP695 pUAST and the preceding SacI-XhoI 1736-bp PCR fragment were ligated into the EcoR1 and XhoI sites in the pcDNA3.1+ neo vector containing the 3′-untranslated region of APP. Subsequently, the L17C, K28C, K28S, and K28A mutations were introduced into the APP695 CT HA pcDNA3.1+ neo plasmid by site-directed mutagenesis (QuikChange).

*Antibodies, Cell Lines, Transfections, and Cell Culture*—Mouse Neuroblastoma N2a cells were maintained in Dulbecco's modified Eagle's medium supplemented with 10% fetal bovine serum and 1% penicillin/streptomycin. N2a cells were plated in 6-well plates and transfected with Lipofectamine 2000 according to the manufacturer's instructions. The dimerizing ligand, AP20187 (Ariad Pharmaceuticals), was added 7 h after transfection and continued from 1 to 17 h. Monoclonal antibodies included HA.11 to detect the HA epitope tag (Covance), 82E1 against the free N terminus of Aβ (IBL, Minneapolis MN), B436 recognizing the N-terminal region of Aβ (29), and 6E10 (Signet), WO2 (30), and Ab9 (31) against the amino acids 1–16 of human Aβ. The polyclonal sAPPβ antibody recognizes the ISEVKM sequence at the C terminus of wild type human sAPPβ (Immuno-Biological Laboratories, Inc., Minneapolis, MN). Antibody 6E10 was also used for detection of sAPPα, and β-secretase cleavage site-specific antibody 82E1 was also used for detection of the APPβ C-terminal fragment. The β-tubulin antibody E7-a1 was obtained from Developmental Studies Hybridoma Bank.

*SDS Electrophoresis and Immunoblotting*—Cells were lysed for 15 min at 4 °C in lysis buffer (50 mM Tris/HCl, pH 7.5, 150 mM NaCl, 5 mM EDTA, and 1% Nonidet P40) supplemented with protease inhibitors (Complete™ protease inhibitor mixture, Roche Applied Science). The supernatants were collected, and the protein concentration determined with a Micro BCA assay (Pierce). Equal amounts of protein samples were separated on 8 or 12% Bis-Tris SDS-PAGE or 12.5 or 15% Tris/glycine SDS-PAGE and then transferred to nitrocellulose membranes. To separate Aβ38, Aβ39, Aβ40, and Aβ42 species, media samples were immunoprecipitated with antibody B436 as above and separated on 10% Tris/Tricine gels containing 8 M urea (32). Synthetic Aβ peptide standards (AnaSpec) were separated in parallel with the experimental samples. After electrophoresis and transfer to nitrocellulose, the membranes were incubated with 82E1 monoclonal antibody which recognizes all full-length Aβ peptides starting at position 1.

*Blue Native Gel Electrophoresis*—Blue native gel electrophoresis was performed according to a protocol modified from Schägger *et al.* (33). In brief, cells in one 10-cm cell culture dish were washed once and collected in phosphate-buffered saline at 4 °C. The cell pellets were resuspended in 1 ml of homogenization buffer (250 mM sucrose in 20 mM HEPES, pH 7.4, with protease inhibitors) and then sheared by passing through a 27 × gauge needle 10 times. Postnuclear supernatant was collected after a low speed spin at 1000 × *g* for 15 min at 4 °C. The membranes were pelleted after centrifugation at 100,000 × *g*

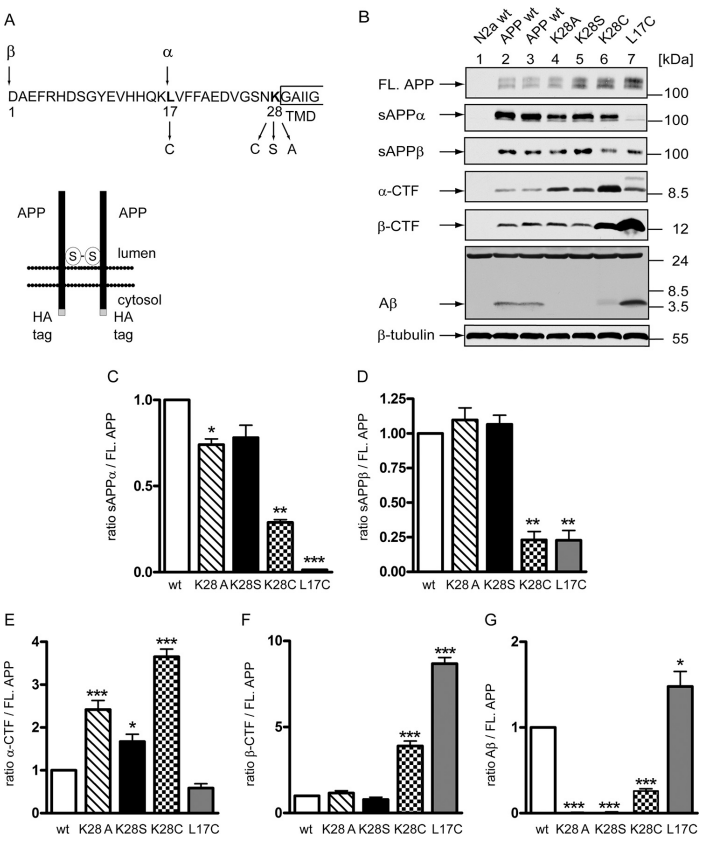


FIGURE 1. **Contrasting effects on A$\beta$ levels with L17C and mutations at K28.** *A*, schematic representation of the position of the APP mutants used and of the cysteine disulfide-bridge-induced dimerization (21, 25) of APP. *B*, N2a cells were transiently transfected with the construct APP695 CT HA and the four respective mutants: L17C, K28C, K28S, K28A. Cell lysates were analyzed via Western blotting of full-length (*FL*) APP and various different APP cleavage products. Full-length APP and α-CTFs were immunoblotted with an HA antibody, $\beta$-CTFs were detected with $\beta$-cleavage site-specific antibody 82E1. Detection of the same protein samples with a $\beta$-tubulin antibody served as a loading control. Conditioned media were immunoprecipitated with Aβ antibody B436 followed by Western blotting with Aβ antibody 82E1. Immunoblotting of sAPP$\alpha$ and sAPP$\beta$ in the media were detected by 6E10 and sAPP$\beta$ specific antibodies, respectively. Quantification of blots shown in *panel B*: *C*, sAPP$\alpha$; *D*, sAPP$\beta$; *E*, α-CTF; *F*, $\beta$-CTF; *G*, Aβ. Results are from an average of three independent experiments ±S.D. normalized to the APP wt control, one-way analysis of variance followed by Tukey's post hoc analyses (*, $p < 0.05$; **, $p < 0.01$; ***, $p < 0.001$).

for 1 h at 4 °C and washed once with 200 $\mu$l of homogenization buffer, and the centrifugation was repeated once. The pellets containing the membranes were resuspended in 200 $\mu$l of homogenization buffer. 100 $\mu$g of protein were solubilized with Blue Native sample buffer (1.5 M amino caproic acid, 0.05 M Bis-Tris, 10% *n*-dodedecyl-$\beta$-D-maltoside, and protease inhibitor at pH 7.5). The samples were incubated on ice for 30 min and then centrifuged for 10 min at 14,000 rpm at 4 °C in a microcentrifuge. Blue Native loading buffer (5.0% Serva Coomassie Brilliant Blue G250 and 1.0 M aminocaproic acid) was added to the supernatant. The samples were separated on 4–15% Tris-HCl gels (Criterion, Bio-Rad) overnight at 4 °C with Coomassie Blue containing cathode buffer (10× cathode buffer, pH 7.0, 0.5 M Tricine, 0.15 M Bis-Tris, 0.2% Coomassie Blue) and anode buffer (pH 7.0, 0.5 M Bis-Tris). The gel was transferred to a polyvinylidene difluoride membrane. The following molecular weight standards were used: thyroglobulin (669 kDa), apoferritin (443 kDa), catalase (240 kDa), aldolase (158 kDa), and bovine serum albumin (66 kDa), all from Sigma.

*Immunoprecipitation of Aβ*—N2a cells in six-well plates were transiently transfected with Lipofectamine 2000 according to the manufacturer's instructions. Overnight conditioned media were collected and incubated overnight at 4 °C with antibody B436 and anti-mouse IgG-agarose beads (American Qualex, San Clemente, CA). After 3 washes with buffer A (10 mM Tris-HCl, pH 7.5, 150 mM NaCl, 2 mM EDTA, 0.2% Nonidet P-40) and 1 wash with 10 mM Tris-HCl, pH 7.5, the beads were resuspended in 2× Laemmli sample buffer plus dithiothreitol and separated by 12% Bis-Tris SDS-PAGE.

*ELISA*—A$\beta$40 and A$\beta$42 species were quantified with sandwich ELISAs essentially as described (34). In brief, 100 $\mu$l of diluted media were analyzed on Immulon 4 HBX plates (Thermo Scientific, Waltham, MA) that were coated before with 25 $\mu$g/ml concentrations of the capture antibody in phosphate-buffered saline. For A$\beta$40, Ab9 was the capture antibody, and horseradish peroxidase-conjugated 13.1.1 (epitope Aβ-(35–40)) was the reporter antibody. For A$\beta$42, antibody 2.1.3 (epitope, Aβ-(35–42)) was the capture antibody, whereas horseradish peroxidase-conjugated Ab9 was the reporter antibody. The signal was developed with TMB (3,3′,5,5′-tetramethylbenzidine) solution and measured in an ELISA plate reader. All measurements were performed in triplicate.

*Mass Spectrometry Analysis*—Matrix-assisted laser desorption/ionization time of flight (MALDI-TOF) mass spectrometry of Aβ peptides was performed on a 4800 MALDI-TOF-TOF (Applied Biosystems/MDS-Sciex, Foster City, CA). Aβ peptides were immunoprecipitated from conditioned medium with antibody B436 coupled to Seize™ beads (Pierce). The

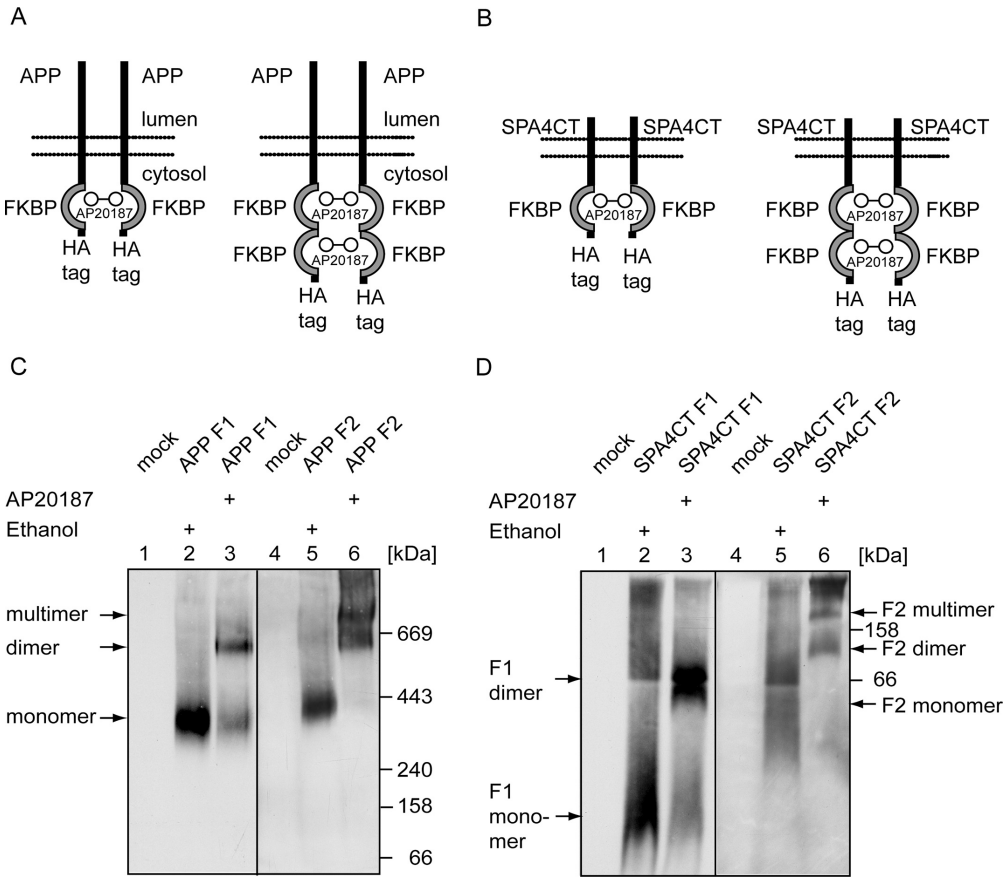


FIGURE 2. **Induced dimerization of C-terminal FKBP-tagged APP695 and SPA4CT analyzed by Blue Native gel electrophoresis.** *A*, schematic representation of APP695 F1 and APP695 F2 constructs consisting of an APP695-FKBP fusion protein with a C-terminal HA tag. APP695 F1 contains one 12-kDa FKBP tag, and APP695 F2 contains two FKBP tags fused in a tandem repeat. AP20187 is an analogue of rapamycin, which binds to FKBP, thereby inducing dimerization of APP-FKBP fusion proteins. *B*, schematic representation of the constructs SPA4CT F1 and SPA4CT F2, containing one FKBP or two FKBP tags, respectively. *C* and *D*, dimerization was induced with AP20187 (100 nM) overnight in N2a cells transiently transfected with APP695 F1/APP695 F2 (*C*) or with SPA4CT F1/SPA4CT F2 (*D*). Note, formation of dimers and multimers in the APP chimeric proteins seen by Blue Native PAGE followed by Western blotting with anti-HA antibody.

immunoprecipitates were eluted from the beads with 25% 0.1% trifluoroacetic acid, 75% acetonitrile, and the resulting samples were mixed 1:1 with α-cyano-4-hydroxycinnamic acid matrix in methanol:acetonitrile:water (36:56:8) (Agilent, Santa Clara, CA) and spotted on the MALDI target grid. Mass spectra were acquired from $m/z$ 3,500–5,000 Da in reflector positive mode at 10,000 shots/spectrum using single shot protection and delayed extraction times of 420 ns. The mass spectra are plotted as $m/z$ *versus* relative intensity.

## RESULTS

*Cysteine Induced Dimerization of APP*—Studies from Multhaup and co-workers (25) have shown that artificial dimerization of APP by introducing cysteine residues within the Aβ domain increased Aβ production. K28C mutation (using Aβ numbering) showed 6–7-fold augmentation in Aβ secretion (25), whereas the L17C mutation (21) showed unchanged Aβ40 levels but increased Aβ42 release, suggesting that dimers of APP facilitate Aβ generation. However, a recent study reported that a K28S mutation showed a marked (90%) reduction in Aβ production (35), possibly due to impairment in γ-secretase cleavage. As a result, we wish to first revisit these cysteine mutants as well as determine the effects of base substitutions at the lysine residue at position 28 (by Aβ numbering or position 624 by APP695 numbering). Accordingly, we examined APP

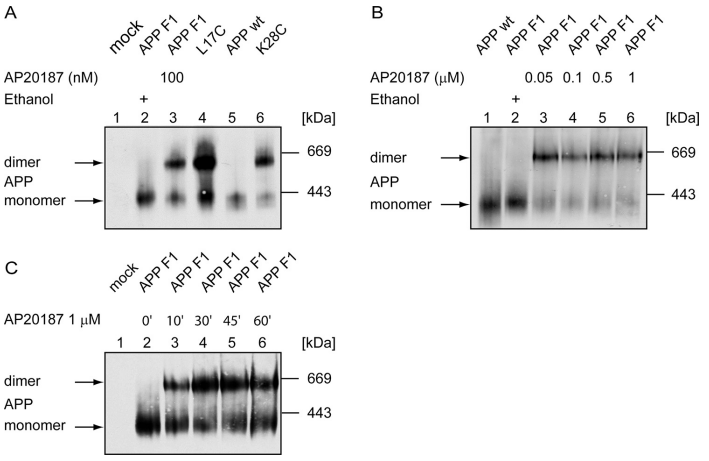


FIGURE 3. **APP dimers in various APP constructs analyzed by Blue Native gel electrophoresis.** *A*, N2a cells were transiently transfected with APP695 F1, APP695 CT HA wt, APP695 CT HA L17C, and APP695 CT HA K28C. Dimerization of APP695 F1 was induced with 100 nM AP20187 overnight, and controls were ethanol-treated cells as well as APP cysteine mutants. *B*, N2a cells were transiently transfected with the APP695 F1 construct and then treated overnight with various concentrations of AP20187 (0.05, 0.1, 0.5, and 1 μM). *C*, time course of induced dimerization of APP. APP dimerization was induced in N2a cells transiently transfected with APP695 F1 after treatment with 1 μM AP20187 from 0 to 60 min. In *A–C*, samples were analyzed via Blue Native PAGE followed by Western blotting with an anti-HA antibody.

processing and Aβ production in four different mutations: L17C, K28C, K28S, and K28A (Fig. 1*A*). All three mutations at Aβ28 (K28A, K28C, and K28S) resulted in a significant reduction in Aβ secretion. For K28A and K28S, the Aβ levels were essentially undetectable. The magnitude of reduction in Aβ production in the K28C mutation was slightly variable, depending on the Aβ antibody used for immunoprecipitations (supplemental Fig. 1). In parallel, there was a strong reduction in sAPPα secretion in the L17C mutant, indicating that impairment of α-secretase cleavage might have led to increased β-secretase cleavage, as seen in the concomitant rise in the level of β-CTF. Although there was a mild reduction in sAPPα and sAPPβ secretion in the K28C mutant, neither the K28A nor the K28S mutant showed any significant alterations in sAPPβ secretion. In addition, there was a substantial change in α-secretase processing for mutants K28S and K28A. Nevertheless, our findings are consistent with those reported by Ren *et al.* (35) that substitutions of the basic lysine residue at position 28 by other hydrophilic (Cys or Ser) or hydrophobic (Ala) amino acids led to marked reduction in Aβ production, presumably by affecting γ-secretase cleavage. However, in view of the K28C results it appears that dimerized APP does not consistently augment Aβ generation, especially if the K28C substitution led to other perturbations in APP processing.

*Blue Native Gel Analysis of Induced and Constitutive Dimerization of APP695 and C99*—In light of the above results, another approach to dimerize APP is needed to determine the impact of APP dimerization on Aβ production, especially one that minimizes secondary effects due to amino acid substitutions within the Aβ sequence. We used a regulated homodimerization system based on the human FKBP12 and a small bifunctional ligand, AP20187 (36). We engineered a chimeric APP construct containing the full-length human APP cDNA fused to one or two FKBP domains and a HA epitope tag at the C terminus (Fig. 2*A*). AP20187, an analogue of rapamycin, is a membrane-permeable compound that induces rapid dimerization of the FKBP or, in this case, APP695-FKBP. Either one FKBP domain (APP F1) or two FKBP domains (APP F2) were fused to the C terminus of APP to enable APP dimerization. To analyze the impact of APP dimerization on γ-secretase processing directly, we also fused one or two FKBP domains to a C99 or β-CTF construct, SPA4CT, as above, and these are termed SPA4CT F1 and F2, respectively (Fig. 2*B*). SPA4CT mimics the C99 β C-terminal fragment generated after BACE1 cleavage and is a direct substrate of γ-secretase cleavage (28).

To examine dimerization of these APP-FKBP chimeric constructs, APP695 F1 and APP695 F2 were transiently transfected into mouse N2a cells and treated overnight with AP20187. Blue Native PAGE showed that the majority of APP molecules were in the dimer form (about 70%), whereas the untreated control sample showed very little APP dimers (Fig. 2*C*). For comparison, both APP cysteine mutants (APP L17C and K28C) showed comparable levels of APP dimer formation using Blue Native PAGE (Fig. 3*A*). Dimerization of APP F2 was more efficient than APP F1 due to the additional FKBP domain with almost no APP monomer present (Fig. 2*C*). In addition, APP multimers, likely tetramers, were also detected. Of note, in the Blue Native gel system, the APP monomer migrated with a mobility of ~300 kDa (Fig. 2*C*), whereas the APP dimer had a molecular mass of twice the monomer size (~600 kDa). The apparent molecular mass of APP monomers and dimers in this gel system is in accordance with a recent publication by Sato *et al.* (37) and likely does not reflect their true molecular masses. This is consistent with the observation that migration of the two APP cysteine mutants was essentially the same as the APP-FKBP chimeric proteins using Blue Native PAGE (Fig. 3*A*). Furthermore, in non-reducing and SDS-denaturing gels, the cysteine mutants migrated at the predicted molecular masses and showed comparable ratios of monomers and dimers as seen in the Blue Native gels (supplemental Fig. 1).

In the SPA4CT F1 construct the addition of AP20187 also led to about 70% dimerization, similar to what was observed for APP F1 (Fig. 2*D*). Similarly, dimerization of SPA4CT F2 showed strong formation of dimers and higher order mul-

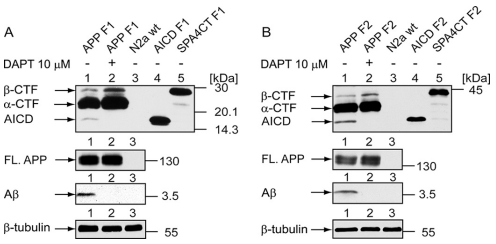


FIGURE 4. **APP695 F1 and APP695 F2 constructs are processed normally by γ-secretase.** N2a cells were transiently transfected with APP695 F1 (*A*) or APP695 F2 (*B*) and treated with 10 μM concentrations of the γ-secretase inhibitor DAPT for 8 h (*lane 2*). AICD, which co-migrated with a control AICD F1 (or AICD F2) construct, can be detected from both APP full-length (*FL*) constructs, and generation of this fragment can be blocked by DAPT. Similarly, Aβ is released into the medium in a DAPT-dependent manner from both APP F1 and APP F2 constructs. Full-length APP and CTFs in the cell lysates were immunoblotted with an anti-HA antibody, and β-tubulin was detected with antibody E7. Aβ was immunoprecipitated from conditioned medium with Aβ antibody B436 and immunoblotted with β-site-specific 82E1 antibody.

timers with almost complete absence of the monomeric species (Fig. 2*D*).

To determine the dose response of APP-FKBP chimeric protein to AP20187, APP F1-transfected cells were incubated overnight with different concentrations of AP20187 (50 nM, 100 nM, 500 nM, and 1 μM). After Blue Native gel electrophoresis, essentially the same level of dimerization (~70%) was seen in all four concentrations of AP20187 after overnight treatment (Fig. 3*B*). To determine the time course of dimerization, APP F1-transfected cells were incubated with either 500 nM or 1 μM AP20187 and analyzed from 10 to 60 min after treatment. Both concentrations led to rapid dimerization such that abundant dimers were present after only 10 min of treatment in accordance with previously published studies using this system (Fig. 3*C* for 1 μM, data not shown for 500 nM). Therefore, dimerization of the APP-FKBP chimera with AP20187 was rapid and efficient. The level of induced dimerization was also comparable with the APP cysteine mutants but has the advantage of not altering any Aβ amino acid residues.

*APP695 F1 and APP695 F2 Are Functional γ-Secretase Substrates*—To confirm that the addition of the FKBP sequences to the C terminus of APP did not perturb Aβ generation, APP695 F1 and APP695 F2 were transiently transfected into N2a cells, and the cells were analyzed for APP processing (Fig. 4). Abundant APP CTFs and AICD were detected in cells transfected with either construct. The latter species were confirmed by mobility to AICD F1 or AICD F2 control constructs, and production of this fragment was abolished after treatment with the γ-secretase inhibitor DAPT. The stability of AICD is likely due to the presence of the FKBP tag because a number of reports have shown stabilization of AICD after fusion with various protein tags (9, 38–40). Furthermore, high levels of Aβ were released from cells transfected with the APP F1 and APP F2 constructs, indicating no overt perturbation of γ-secretase cleavage. DAPT treatment inhibited Aβ production as well as AICD production from cells transfected with APP F1 and APP F2 (Fig. 4).

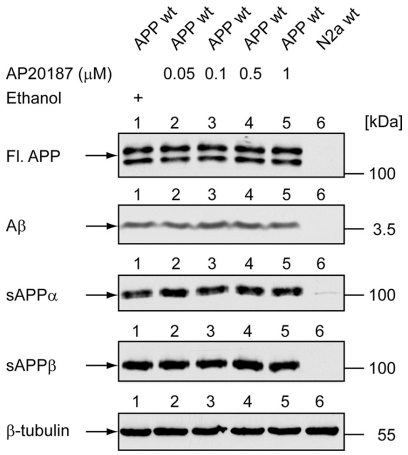


FIGURE 5. **AP20187 does not affect APP695 wt processing.** N2a cells stably expressing wild type full-length (*FL*) APP695 (without FKBP tag) were treated with increasing concentrations of AP20187 overnight. Cell lysates were analyzed via immunoblotting with antibody 6E10 for APP and antibody E7 for β-tubulin. Aβ was immunoprecipitated with antibody B436 and immunoblotted with antibody 82E1. sAPPα and sAPPβ in the media were detected by immunoblotting with 6E10 and sAPPβ-specific antibodies, respectively.

*Dimerization of APP695 F1 Leads to Decreased Aβ Production*—We next assessed the effects of induced dimerization on APP proteolytic processing. However, we first wish to ascertain that AP20187 does not by itself alter APP processing or Aβ generation. Accordingly, N2a cells stably transfected with wild type full-length APP695 (without the FKBP tag) were treated with increasing doses of AP20187. Indeed, at concentrations up to 1 μM, we did not detect any appreciable changes in full-length APP or in the levels of secreted sAPPα, sAPPβ, Aβ, indicating that this compound does not perturb APP metabolism (Fig. 5). Next, N2a cells were transiently transfected with the APP F1 construct and then treated overnight with 50 or 100 nM AP20187. After this treatment, steady state levels of full-length APP were consistently higher than control cells not treated with AP20187 (Fig. 6*A*). Levels of Aβ were essentially unchanged, but when corrected for the increased APP levels, there was a significant 50% reduction in Aβ secretion. Interestingly, AICD and β-CTF levels were slightly increased, whereas α-CTFs, sAPPα, and sAPPβ levels showed a mild reduction or no change. Similar results were obtained with the APP F2 construct (supplemental Fig. 2). In addition, similar changes were seen in intracellular Aβ levels after AP20187 treatment, suggesting that APP-FKBP-induced dimerization did not result in a selective retention of Aβ in intracellular compartments (supplemental Fig. 4).

Because it has been suggested that dimerization of APP modulates the production of shorter Aβ species (21), we proceeded to determine whether dimerization of APP695 induced by AP20187 resulted in the generation of different Aβ species. Therefore, media of N2a cells transfected with the APP695 F1 construct and treated with 50 and 100 nM AP20187 were analyzed on Tricine-urea gels to separate the

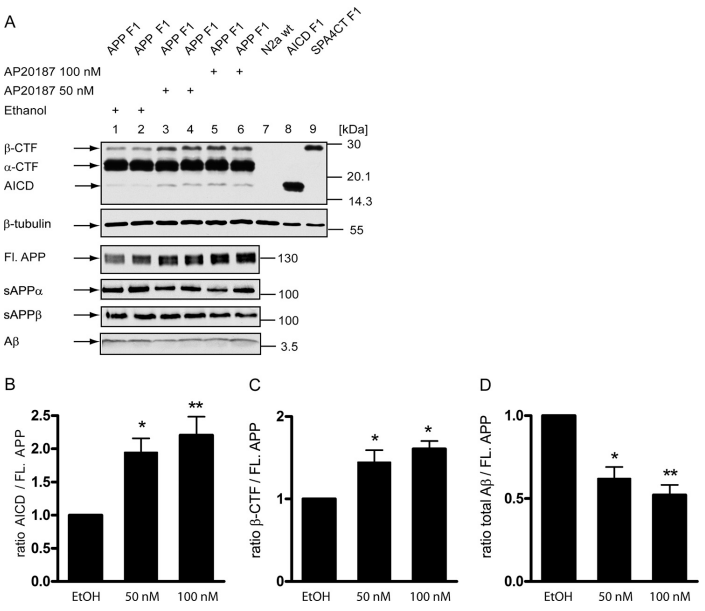


FIGURE 6. **Processing of APP695 F1 after induced dimerization.** N2a cells were transiently transfected with APP695 F1, and dimerization was induced with 50 and 100 nM AP20187 overnight. *A*, cell lysates from N2a cells transiently transfected with APP695 F1 and treated overnight with AP20187 (50 or 100 nM) were analyzed by immunoblotting for full-length (*FL*) APP, CTFs, and AICD with anti-HA antibody. Conditioned media were immunoblotted by antibody 6E10 for sAPPα and an sAPPβ-specific antibody for sAPPβ. Immunoprecipitation of total Aβ in the media was carried with Aβ antibody B436 and immunoblotting followed with antibody 82E1. Quantification of AICD (*B*), β-CTF (*C*), and Aβ (*D*) from blots from three independent experiments is shown in *panel A* ±S.D. (one-way analysis of variance followed by Tukey's post hoc analyses. *, $p < 0.05$; **, $p < 0.01$; ***, $p < 0.001$).

various Aβ species (Fig. 7*A*). By this approach the profile of Aβ-(38–42) peptides from the APP695 F1 construct (and the APP695 F2 construct, data not shown) was essentially unchanged, with Aβ40 being the predominant species as expected. Quantification of the different Aβ species from three independent experiments showed no significant change in their ratios. Finally, Aβ from cells transiently transfected with APP F1 or APP F2 were analyzed by MALDI-TOF after treatment with 500 nM AP20187 (Fig. 7, *B* and *C*). The results showed that there were no substantial changes in Aβ species from either APP F1 or APP F2 cells with or without AP20187 treatment. Taken together, our results showed that induced dimerization of APP reduced Aβ levels without modulation of individual Aβ species.

*Dimerization of C99 Leads to Decreased Aβ Production*—The above results suggested that dimerization of APP lowers Aβ generation, possibly at the level of γ-secretase cleavage. To confirm this interpretation, we next analyzed the processing of SPA4CT, the β-CTF fragment generated after BACE1 cleavage. Accordingly, we assessed Aβ and AICD levels in cells transfected with the C99/SPA4CT F1 or C99/SPA4CT F2 constructs, both of which can be efficiently dimerized (see Fig. 2*D*). Treatment with AP20187 led to an increase in C99/β-CTF fragment and AICD levels (Fig. 8*A*, supplemental Fig. 3), similar to the observations with full-length APP (see Fig. 6, supplemental Fig. 2). When normalized to steady state levels of β-CTF, levels of secreted total Aβ were markedly diminished (70–80%) in cells treated with 100 nM AP20187. The medium was also analyzed by ELISA to quantify the relative levels of Aβ40 and Aβ42 production (Fig. 8, *D* and *E*). Indeed, both species were reduced by ~70%, with slightly more reduction seen for the Aβ40 peptides. In sum, studies with both full-length APP and N-terminal-truncated APP (SPA4CT) constructs showed similar levels of reduction in Aβ secretion after induction of dimerization.

## DISCUSSION

It has been reported that APP contains a number of domains that mediate homo- and heterodimerization, the latter interacting with APLP1 and APLP2, and in support of the functionality of these domains, small amounts of APP are recovered as dimers *in vitro* and *in vivo* (17, 18, 21, 25). To date, a number of diverse physiological roles have been attributed to this dimerization event. In addition, based primarily on artificial cysteine mutations designed to induce disulfide bond formation, it has been suggested that APP dimerization accelerates Aβ production (25). However, subsequent studies have not consistently confirmed these initial observations (23, 27). In this study we chose to use a different approach to induce APP dimerization to explore the relationship between dimerization and Aβ generation without having to introduce cysteine mutations by creating APP-FKBP chimeric proteins. The addition of the bivalent compound AP20187 led to rapid and efficient formation of APP dimers in transfected cells. Fusion of one FKBP domain resulted in ~70% dimer formation, whereas fusion of two FKBP domains resulted in dimers and multimers, with almost a complete absence of APP monomers. However, when APP dimers or multimers were formed, there was a consistent decrease in Aβ secretion that ranged from 50 to 80% depending on whether one or two FKBP domains were inserted. Therefore, we conclude that APP dimerization does not directly promote Aβ generation and in fact negatively impacts Aβ production.

Previous studies analyzing the putative role of APP dimerization all used cysteine substitutions within the Aβ domain to create artificial disulfide bonds between adjacent APP molecules. This approach leads to efficient and constitutive dimerization of APP. However, inconsistent results have been

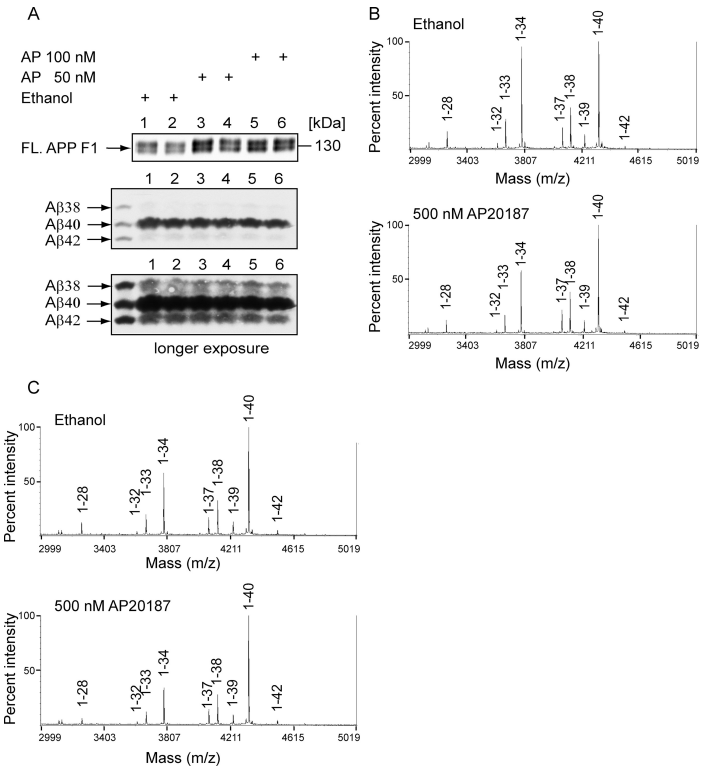


FIGURE 7. **No modulation of different Aβ species after induction of APP dimerization.** *A*, N2a cells transfected with APP695 F1 were treated overnight with 50 or 100 nM AP20187. Full-length (*FL*) APP in cell lysates was detected with an anti-HA antibody. The conditioned media were immunoprecipitated with Aβ antibody B436 and separated on a 10% Tricine-urea gel. No significant changes in the relative levels of the major Aβ species were observed. Synthetic $A\beta_{38}$, $A\beta_{40}$, and $A\beta_{42}$ peptides were run as control size markers. *B* and *C*, MALDI analysis of Aβ peptides secreted from APP695 F1 (*B*)- or APP695 F2 (*C*)-transfected N2a cells after treatment with 500 nM AP20187 as compared with ethanol treated controls.

reported regarding the effects on Aβ generation. Given the interests in the mechanisms of Aβ production, we decided to test the role of APP dimerization on APP processing by engineering APP-FKBP chimeric constructs that can be efficiently dimerized with the bivalent compound, AP20187. The advantage of this approach is that no mutations are introduced into the APP sequence, as the latter mutations may perturb processing by α-, β-, or γ-secretase by interfering with one of the enzymatic activities. For both of the published cysteine mutants (L17C and K28C), this is a critical point because, for example, the mutation L17C in APP is directly located at the α-secretase cleavage site and has the potential of interfering with α-secretase activity (21). Indeed, this is precisely the outcome we observed, as there was a significant reduction in α-secretase cleavage and a corresponding increase in β-secretase cleavage as measured by the levels of sAPPα and sAPPβ, respectively (Fig. 1). In fact, this alteration alone may explain the increase in Aβ release without potentially having to take into account any effects of actual APP dimerization. A second advantage of the FKBP-AP20187 system is the time- and concentration-dependent regulation of dimerization as compared with the constitutive dimerization of APP induced by cysteine mutations (Fig. 3). In our studies, although a tag of 122 amino acids was appended to the C terminus of APP, there were no overt perturbations in APP processing that we could observe. Both mass spectrometry and Tricine-urea gel electrophoresis showed the normal predicted profile of Aβ peptides without any alterations before or after dimerization from both APP F1 and APP F2 constructs. These findings are consistent with the apparent normal processing of APP GFP fusions used by a number of laboratories (38, 41–45). However, with this approach, our results unequivocally showed that forced dimerization of APP lowered rather than increased Aβ generation. Similar results were obtained with both full-length APP and C99 (SPA4CT) constructs, leading us to hypothesize that this reduction is due to an effect on γ-secretase cleavage and not on other aspects of APP processing, such as α- or β-secretase cleavage.

In our studies, although Aβ generation was significantly reduced, we did observe an increase in the levels of AICD after the addition of the dimerization compound. This was not expected because both Aβ and AICD are derived by γ-secretase activity (9–11), and it has been reported that the generation of Aβ and AICD are equimolar, at least under basal conditions (46). Aβ generation appears to initially start at the ϵ-cleavage near the cytoplasmic face that first releases AICD from the membrane tether, before ζ-cleavage, and finally, γ-secretase cleavages occur (47, 48). In this model these processive cleavages can be perturbed while keeping ϵ-cleavage relatively intact. In fact, a recent publication showed that mutations within the G*XXX*G motif in the APP transmembrane domain led to a reduction in Aβ40 and Aβ42 without altering AICD levels (23). In this latter case, however, the drop in Aβ40 and Aβ42 levels was accompanied by an increase in Aβ34 species (21), indicating that mutations at the G*XXX*G motif were specific for the generation of Aβ peptides, presumably due to alterations to γ-secretase cleavage. For this reason we specifically examined the profile of Aβ peptides in the APP-FKBP chimera by both Western blotting and MALDI-TOF (Fig. 7), and we did

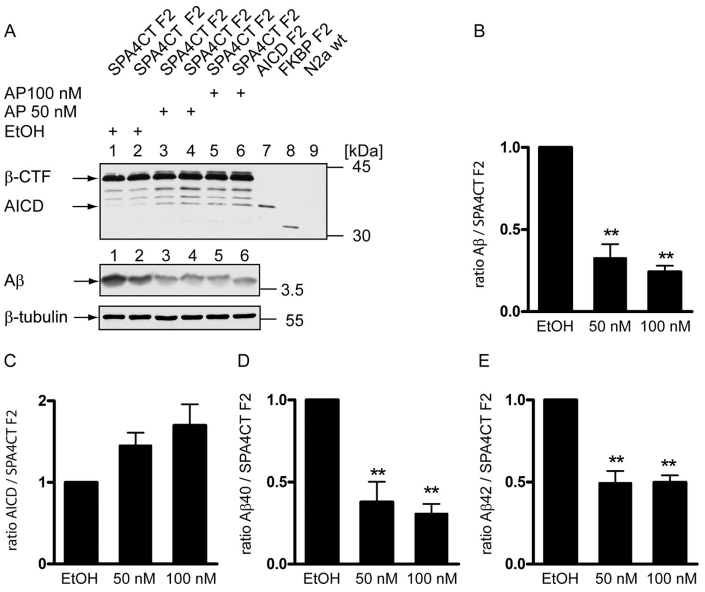


FIGURE 8. **Processing of SPA4CT F2 after induced dimerization.** *A*, N2a cells were transiently transfected with SPA4CT F2, and dimerization was induced with 50 and 100 nM AP20187 overnight. The *upper panel* shows immunoblotting of C99 and AICD fragments by an anti-HA antibody. The *middle panel* shows immunoprecipitation/Western blotting of Aβ from the treated cells. In the *lower panel* β-tubulin of cell lysates was immunoblotted with antibody E7 as a loading control. *B* and *C*, quantification of Aβ and AICD from the blots shown in *panel A* from three independent experiments ±S.D. *D* and *E*, conditioned media were also analyzed by an Aβ40 (*D*) or Aβ42 (*E*) ELISA from three different experiments ±S.D. (one-way analysis of variance followed by Tukey's post hoc analyses. *, $p < 0.05$; **, $p < 0.01$; ***, $p < 0.001$).

not detect any alterations in the profile of Aβ peptides generated from the APP-FKBP chimeric molecules before or after dimerization. Another possibility is that the stability of AICD fusion peptides is different from untagged molecules. Normally, AICD is rapidly turned over, but it is likely that the stability of AICD-FKBP fusion peptides is enhanced, a characteristic shown by other APP C-terminal fusion tags (9, 35, 38). Given this, it is possible that dimerized AICD-FKBP species are even more stable than monomeric AICD-FKBP peptides. Finally, there are other examples wherein Aβ and AICD production are not linked. For example, a number of mutations within the APP transmembrane region were shown to have distinct effects on the two cleavage events (23, 49, 50). And, TMP21, a member of the p24 cargo protein family, appeared to selectively inhibit APP processing at the γ-site without affecting ε-cleavage (51).

Our results are consistent with the report by Ren *et al.* (35) showing that the SPA4CT-GVP mutant K28S showed a 90% reduction of total Aβ production, whereas AICD levels were basically unaffected. Because both the K28A and K28C mutations also led to a marked reduction in Aβ secretion (Fig. 1), our results are in agreement with the observations that these mutations likely perturbed γ-secretase cleavage. In particular, although the K28C resulted in high levels of APP dimers, this itself was insufficient to augment Aβ generation and release. On the other hand, the Aβ reduction we saw in induced dimerization of APP-FKBP chimeras may be supra-physiologic, as the degree of APP dimerization that takes place normally in cultured cells appears to be far less than what was achieved by AP20187-induced dimerization. Furthermore, dimerization at the APP C terminus may not be equivalent to dimerization within other APP domains. However, it remains to be determined what percentage of APP is dimerized *in vivo*, as this has not been examined in detail. It has also been suggested that APP dimerization increases the susceptibility of cells to a variety of injury, including Aβ (24). Therefore, it is possible that even though APP dimerization may not directly impact Aβ production, this process may still play an important role in synaptic loss or neuronal death in Alzheimer disease. Last, these observations are all in accord with recent publications showing that γ-secretase is likely a monomeric rather than a dimeric complex, as was originally proposed (37, 52–54). Given these findings, γ-secretase is likely to function in the monomeric state and cleaves one rather than two substrate APP molecules within the complex.

*Acknowledgments—We thank Prof. Dr. Todd Golde for Ab9, 13.1.1, and 2.1.3, Dr. Maria Kounnas for B436, and Prof. Dr. Konrad Beyreuther for WO2 antibodies, Dr. Stefan Lichtenthaler for SPA4CT DA pCEP4 and Dr. Peter Soba for APP695 pUAST and APP695 NT HA pCDNA3.1+ plasmids, ARIAD Pharmaceuticals for providing the homodimerization kit, and the University of California San Diego Mass Spectrometry facility (Drs. E. Komives and J. Torpey) for assistance.*

## REFERENCES

1. Glenner, G. G., and Wong, C. W. (1984) *Biochem. Biophys. Res. Commun.* **120,** 885–890
2. Masters, C. L., Simms, G., Weinman, N. A., Multhaup, G., McDonald, B. L., and Beyreuther, K. (1985) *Proc. Natl. Acad. Sci. U.S.A.* **82,** 4245–4249
3. Kang, J., Lemaire, H. G., Unterbeck, A., Salbaum, J. M., Masters, C. L., Grzeschik, K. H., Multhaup, G., Beyreuther, K., and Müller-Hill, B. (1987) *Nature* **325,** 733–736
4. Vassar, R., Bennett, B. D., Babu-Khan, S., Kahn, S., Mendiaz, E. A., Denis, P., Teplow, D. B., Ross, S., Amarante, P., Loeloff, R., Luo, Y., Fisher, S., Fuller, J., Edenson, S., Lile, J., Jarosinski, M. A., Biere, A. L., Curran, E., Burgess, T., Louis, J. C., Collins, F., Treanor, J., Rogers, G., and Citron, M. (1999) *Science* **286,** 735–741
5. Sinha, S., Anderson, J. P., Barbour, R., Basi, G. S., Caccavello, R., Davis, D., Doan, M., Dovey, H. F., Frigon, N., Hong, J., Jacobson-Croak, K., Jewett,

N., Keim, P., Knops, J., Lieberburg, I., Power, M., Tan, H., Tatsuno, G., Tung, J., Schenk, D., Seubert, P., Suomensaari, S. M., Wang, S., Walker, D., Zhao, J., McConlogue, L., and John, V. (1999) *Nature* **402,** 537–540
6. Yan, R., Bienkowski, M. J., Shuck, M. E., Miao, H., Tory, M. C., Pauley, A. M., Brashier, J. R., Stratman, N. C., Mathews, W. R., Buhl, A. E., Carter, D. B., Tomasselli, A. G., Parodi, L. A., Heinrikson, R. L., and Gurney, M. E. (1999) *Nature* **402,** 533–537
7. De Strooper, B. (2003) *Neuron* **38,** 9–12
8. Koo, E. H., and Kopan, R. (2004) *Nat Med.* **10,** (suppl.) 26–33
9. Weidemann, A., Eggert, S., Reinhard, F. B., Vogel, M., Paliga, K., Baier, G., Masters, C. L., Beyreuther, K., and Evin, G. (2002) *Biochemistry* **41,** 2825–2835
10. Sastre, M., Steiner, H., Fuchs, K., Capell, A., Multhaup, G., Condron, M. M., Teplow, D. B., and Haass, C. (2001) *EMBO Rep.* **2,** 835–841
11. Gu, Y., Misonou, H., Sato, T., Dohmae, N., Takio, K., and Ihara, Y. (2001) *J. Biol. Chem.* **276,** 35235–35238
12. Edbauer, D., Winkler, E., Regula, J. T., Pesold, B., Steiner, H., and Haass, C. (2003) *Nat. Cell Biol.* **5,** 486–488
13. Wolfe, M. S., Xia, W., Ostaszewski, B. L., Diehl, T. S., Kimberly, W. T., and Selkoe, D. J. (1999) *Nature* **398,** 513–517
14. Esch, F. S., Keim, P. S., Beattie, E. C., Blacher, R. W., Culwell, A. R., Oltersdorf, T., McClure, D., and Ward, P. J. (1990) *Science* **248,** 1122–1124
15. Wang, R., Meschia, J. F., Cotter, R. J., and Sisodia, S. S. (1991) *J. Biol. Chem.* **266,** 16960–16964
16. Dyrks, T., Weidemann, A., Multhaup, G., Salbaum, J. M., Lemaire, H. G., Kang, J., Müller-Hill, B., Masters, C. L., and Beyreuther, K. (1988) *EMBO J.* **7,** 949–957
17. Soba, P., Eggert, S., Wagner, K., Zentgraf, H., Siehl, K., Kreger, S., Löwer, A., Langer, A., Merdes, G., Paro, R., Masters, C. L., Müller, U., Kins, S., and Beyreuther, K. (2005) *EMBO J.* **24,** 3624–3634
18. Bai, Y., Markham, K., Chen, F., Weerasekera, R., Watts, J., Horne, P., Wakutani, Y., Bagshaw, R., Mathews, P. M., Fraser, P. E., Westaway, D., St George-Hyslop, P., and Schmitt-Ulms, G. (2008) *Mol. Cell Proteomics* **7,** 15–34
19. Wang, Y., and Ha, Y. (2004) *Mol. Cell* **15,** 343–353
20. Shaked, G. M., Kummer, M. P., Lu, D. C., Galvan, V., Bredesen, D. E., and Koo, E. H. (2006) *FASEB J.* **20,** 1254–1256
21. Munter, L. M., Voigt, P., Harmeier, A., Kaden, D., Gottschalk, K. E., Weise, C., Pipkorn, R., Schaefer, M., Langosch, D., and Multhaup, G. (2007) *EMBO J.* **26,** 1702–1712
22. Vooijs, M., Schroeter, E. H., Pan, Y., Blandford, M., and Kopan, R. (2004) *J. Biol. Chem.* **279,** 50864–50873
23. Kienlen-Campard, P., Tasiaux, B., Van Hees, J., Li, M., Huysseune, S., Sato, T., Fei, J. Z., Aimoto, S., Courtoy, P. J., Smith, S. O., Constantinescu, S. N., and Octave, J. N. (2008) *J. Biol. Chem.* **283,** 7733–7744
24. Lu, D. C., Shaked, G. M., Masliah, E., Bredesen, D. E., and Koo, E. H. (2003) *Ann. Neurol.* **54,** 781–789
25. Scheuermann, S., Hambsch, B., Hesse, L., Stumm, J., Schmidt, C., Beher, D., Bayer, T. A., Beyreuther, K., and Multhaup, G. (2001) *J. Biol. Chem.* **276,** 33923–33929
26. Walsh, D. M., Tseng, B. P., Rydel, R. E., Podlisny, M. B., and Selkoe, D. J. (2000) *Biochemistry* **39,** 10831–10839
27. Struhl, G., and Adachi, A. (2000) *Mol. Cell* **6,** 625–636
28. Lichtenthaler, S. F., Multhaup, G., Masters, C. L., and Beyreuther, K. (1999) *FEBS Lett.* **453,** 288–292
29. Vetrivel, K. S., Gong, P., Bowen, J. W., Cheng, H., Chen, Y., Carter, M., Nguyen, P. D., Placanica, L., Wieland, F. T., Li, Y. M., Kounnas, M. Z., and Thinakaran, G. (2007) *Mol. Neurodegener.* **2,** 4
30. Ida, N., Hartmann, T., Pantel, J., Schröder, J., Zerfass, R., Förstl, H., Sandbrink, R., Masters, C. L., and Beyreuther, K. (1996) *J. Biol. Chem.* **271,** 22908–22914
31. Levites, Y., Das, P., Price, R. W., Rochette, M. J., Kostura, L. A., McGowan, E. M., Murphy, M. P., and Golde, T. E. (2006) *J. Clin. Invest.* **116,** 193–201
32. Schägger, H., and von Jagow, G. (1987) *Anal. Biochem.* **166,** 368–379
33. Schägger, H., Cramer, W. A., and von Jagow, G. (1994) *Anal. Biochem.* **217,** 220–230
34. Kukar, T. L., Ladd, T. B., Bann, M. A., Fraering, P. C., Narlawar, R., Maharvi, G. M., Healy, B., Chapman, R., Welzel, A. T., Price, R. W., Moore, B., Rangachari, V., Cusack, B., Eriksen, J., Jansen-West, K., Verbeeck, C., Yager, D., Eckman, C., Ye, W., Sagi, S., Cottrell, B. A., Torpey, J., Rosenberry, T. L., Fauq, A., Wolfe, M. S., Schmidt, B., Walsh, D. M., Koo, E. H., and Golde, T. E. (2008) *Nature* **453,** 925–929
35. Ren, Z., Schenk, D., Basi, G. S., and Shapiro, I. P. (2007) *J. Biol. Chem.* **282,** 35350–35360
36. Clackson, T. (2006) *Chem. Biol. Drug Design* **67,** 440–442
37. Sato, T., Diehl, T. S., Narayanan, S., Funamoto, S., Ihara, Y., De Strooper, B., Steiner, H., Haass, C., and Wolfe, M. S. (2007) *J. Biol. Chem.* **282,** 33985–33993
38. Kaether, C., Schmitt, S., Willem, M., and Haass, C. (2006) *Traffic* **7,** 408–415
39. Yamasaki, A., Eimer, S., Okochi, M., Smialowska, A., Kaether, C., Baumeister, R., Haass, C., and Steiner, H. (2006) *J. Neurosci.* **26,** 3821–3828
40. Eggert, S., Paliga, K., Soba, P., Evin, G., Masters, C. L., Weidemann, A., and Beyreuther, K. (2004) *J. Biol. Chem.* **279,** 18146–18156
41. Kaether, C., Skehel, P., and Dotti, C. G. (2000) *Mol. Biol. Cell* **11,** 1213–1224
42. Rebelo, S., Vieira, S. I., Esselmann, H., Wiltfang, J., da Cruz e Silva, E. F., and da Cruz e Silva, O. A. (2007) *J. Mol. Neurosci.* **32,** 1–8
43. Chan, S. L., Kim, W. S., Kwok, J. B., Hill, A. F., Cappai, R., Rye, K. A., and Garner, B. (2008) *J. Neurochem.* **106,** 793–804
44. Florean, C., Zampese, E., Zanese, M., Brunello, L., Ichas, F., De Giorgi, F., and Pizzo, P. (2008) *Biochim. Biophys. Acta* **1783,** 1551–1560
45. Goldsbury, C., Thies, E., Konzack, S., and Mandelkow, E. M. (2007) *J. Neurosci.* **27,** 3357–3363
46. Kakuda, N., Funamoto, S., Yagishita, S., Takami, M., Osawa, S., Dohmae, N., and Ihara, Y. (2006) *J. Biol. Chem.* **281,** 14776–14786
47. Zhao, G., Cui, M. Z., Mao, G., Dong, Y., Tan, J., Sun, L., and Xu, X. (2005) *J. Biol. Chem.* **280,** 37689–37697
48. Qi-Takahara, Y., Morishima-Kawashima, M., Tanimura, Y., Dolios, G., Hirotani, N., Horikoshi, Y., Kametani, F., Maeda, M., Saido, T. C., Wang, R., and Ihara, Y. (2005) *J. Neurosci.* **25,** 436–445
49. Hecimovic, S., Wang, J., Dolios, G., Martinez, M., Wang, R., and Goate, A. M. (2004) *Neurobiol. Dis.* **17,** 205–218
50. Tesco, G., Ginestroni, A., Hiltunen, M., Kim, M., Dolios, G., Hyman, B. T., Wang, R., Berezovska, O., and Tanzi, R. E. (2005) *J. Neurochem.* **95,** 446–456
51. Chen, F., Hasegawa, H., Schmitt-Ulms, G., Kawarai, T., Bohm, C., Katayama, T., Gu, Y., Sanjo, N., Glista, M., Rogaeva, E., Wakutani, Y., Pardossi-Piquard, R., Ruan, X., Tandon, A., Checler, F., Marambaud, P., Hansen, K., Westaway, D., St George-Hyslop, P., and Fraser, P. (2006) *Nature* **440,** 1208–1212
52. Steiner, H., Winkler, E., and Haass, C. (2008) *J. Biol. Chem.* **283,** 34677–34686
53. Evin, G., Canterford, L. D., Hoke, D. E., Sharples, R. A., Culvenor, J. G., and Masters, C. L. (2005) *Biochemistry* **44,** 4332–4341
54. Schroeter, E. H., Ilagan, M. X., Brunkan, A. L., Hecimovic, S., Li, Y. M., Xu, M., Lewis, H. D., Saxena, M. T., De Strooper, B., Coonrod, A., Tomita, T., Iwatsubo, T., Moore, C. L., Goate, A., Wolfe, M. S., Shearman, M., and Kopan, R. (2003) *Proc. Natl. Acad. Sci. U.S.A.* **100,** 13075–13080

# IV.F. Supplementary Figures

Supplementary Figure 1

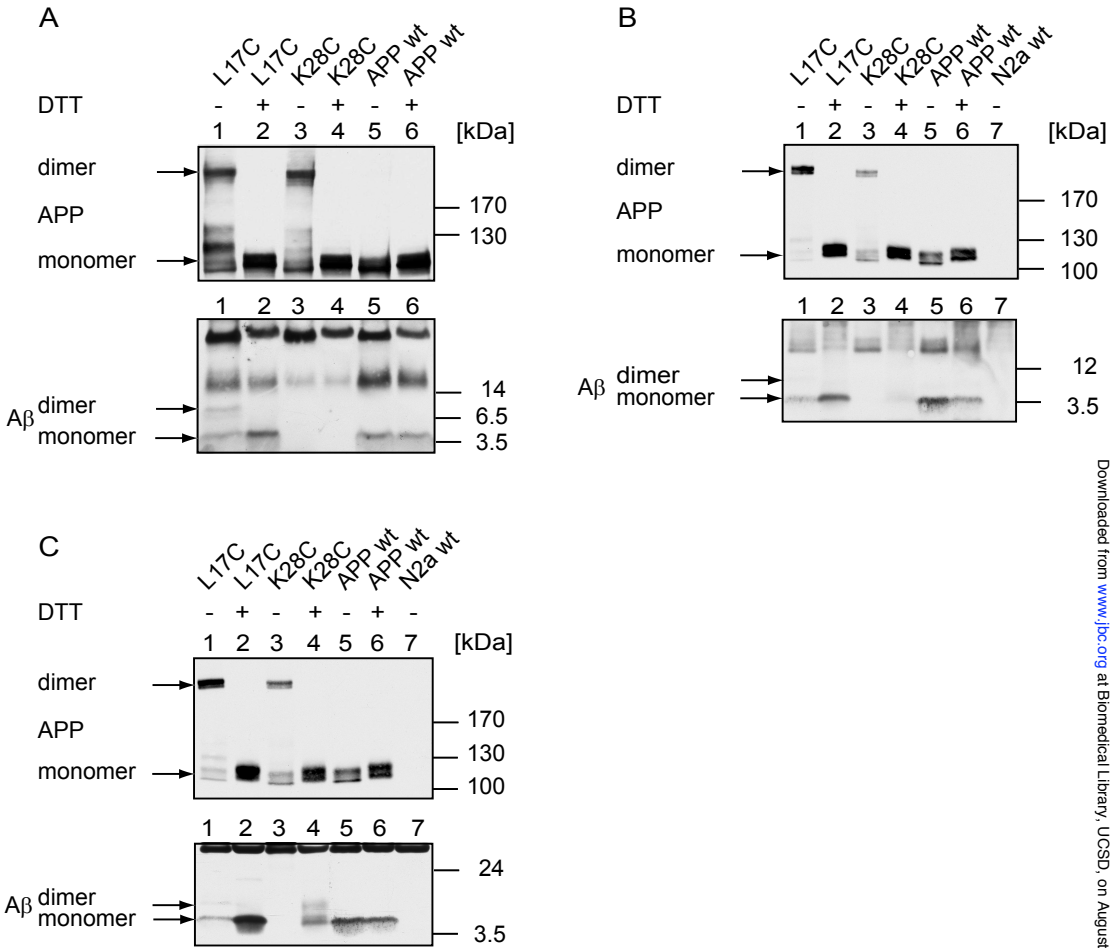




Suppl. Fig. 1. **Different Aβ antibodies show similar results from APP cysteine mutants.** For all Blots shown in suppl. Fig. 1, N2a cells were transiently transfected in with L17C, K28C or APP695 CT HA wt constructs. Samples 1, 3 and 5 were incubated in sample buffer without DTT, while samples 2, 4 and 6 were treated with sample buffer including DTT. APP dimers can be detected from L17C or K28C mutant samples without DTT. Full length APP in all panels was immunoblotted with an anti-HA antibody. Aβ was detected from medium by immunoprecipitations/western blotting with Ab9/Ab9 **(A)** WO2/WO2 (B) or B436/82E1 **(C)** All three antibody combinations gave essentially the same result in that there was a substantial decrease in Aβ levels in the K28C mutant.

Supplementary Figure 2

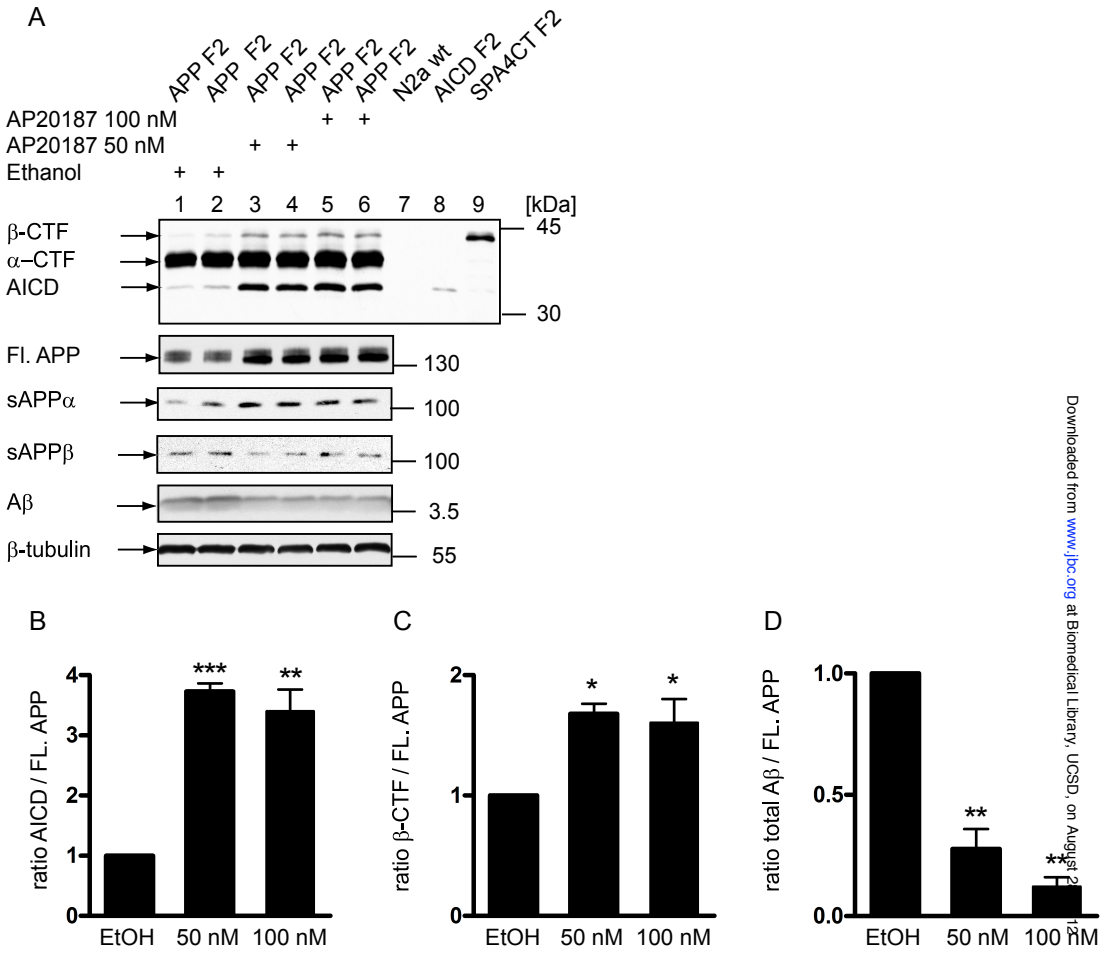




Suppl. Fig. 2. **Processing of APP695 F2 after induced dimerization**. N2a cells were transiently transfected with APP695 F2 and dimerization was induced with 50 nM and 100 nM AP20187 over night. **A** Cell lysates from N2a cells transiently transfected with APP695 F2 and treated overnight with AP20187 (50 nM or 100 nM) were analyzed by immunoblotting for full length APP, CTFs, and AICD with anti-HA antibody. Conditioned media were immunoblotted by antibody 6E10 for sAPPα and an sAPPβ specific antibody for sAPPβ. Immunoprecipitation and western blotting of total Aβ was carried out as before. Quantification of **B** AICD, **C** β-CTF, **D** Aβ from the blots shown in panel A from three independent experiments ± S.D. (One-way ANOVA followed by Tukey's post hoc analyses .*, $p < 0.05$, **, $p < 0.01$, ***, $p < 0.001$).

Supplementary Figure 3

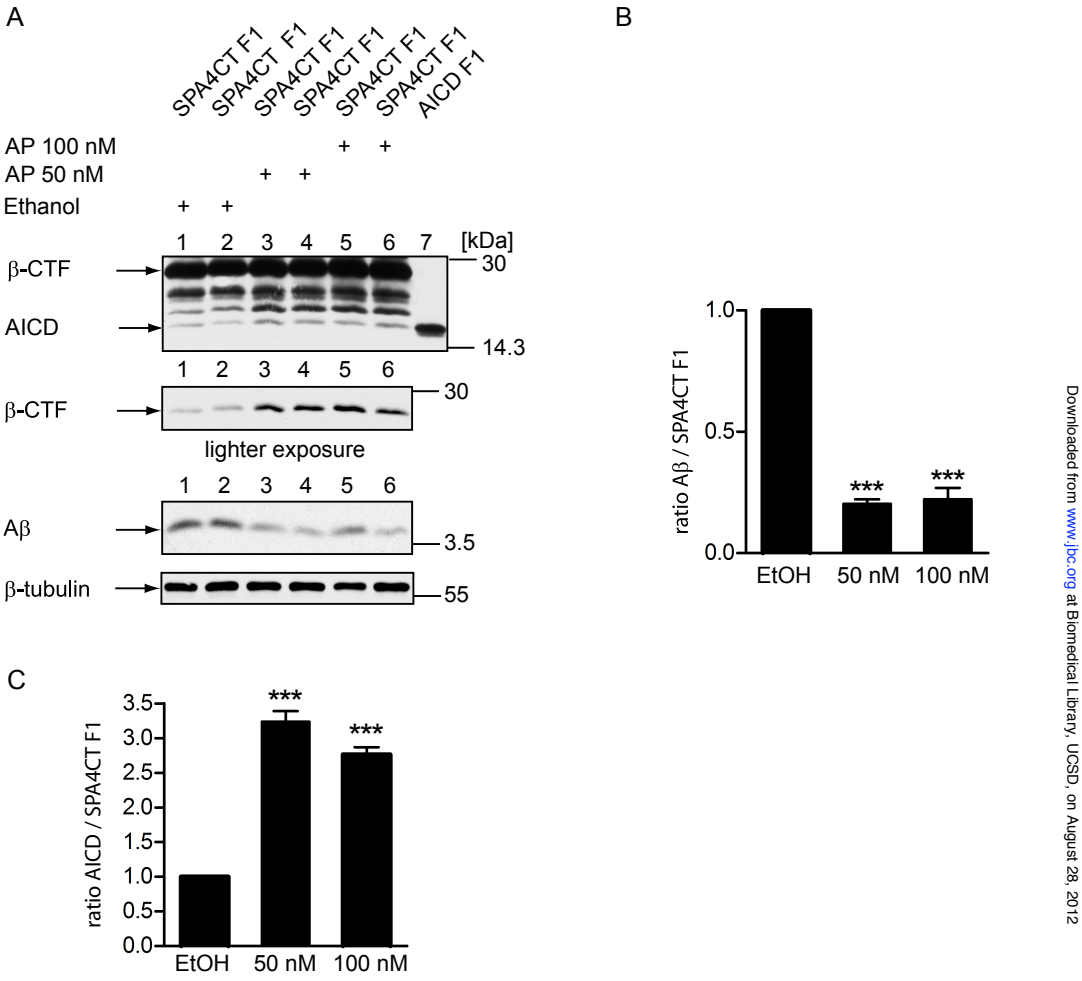


Suppl. Fig. 3. **Processing of SPA4CT F1 after induced dimerization.** **A** N2a cells were transiently transfected with SPA4CT F1 and dimerization was induced with 50 nM and 100 nM AP20187 over night. Upper panel shows immunoblotting of C99 and AICD fragments by an anti-HA antibody. Middle panel shows immunoprecipitation/western blotting of Aβ from the treated cells. B, Ç Quantification of Aβ and AICD from the blots shown in panel A from three independent experiments ± S.D.

Supplementary figure 4

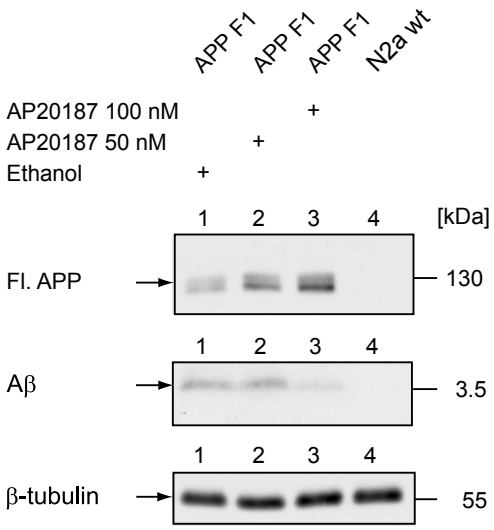




Suppl. Fig. 4. **APP695 F1 induced dimerization does not lead to increased intracellular Aβ levels.** N2a cells were transiently transfected with APP695 F1 and dimerization was induced with 50 nM and 100 nM AP20187 over night. Cell lysates were analyzed by immunoblotting for full length APP with anti-HA antibody and for β-tubulin with antibody E7. Immunoprecipitation of total Aβ in the cell lysates was carried out with Aβ antibody B436 and immunoblotted with antibody 82E1.

Chapter IV, in full, is a reprint of the material as it appears in Journal of Biological Chemistry, 2009. Eggert, Simone; Midthune, Brea; Cottrell, Barbara; Koo Edward H. "Induced dimerization of the amyloid precursor protein leads to decreased amyloid-beta protein production", Journal of Biological Chemistry, 2009 Oct 16;284(42):28943-52. The dissertation author was the second author of this paper and contributed to the experiments working with SPA4CT (C99), figures 8 and S3.

# Chapter V: Final Words

For this dissertation project, I looked into various molecular mechanisms involved in Aβ-induced synaptic dysfunction. While several lines of evidence indicate that synapses are the initial site of Aβ toxicity, emerging evidence indicates that caspase activation contributes to early synaptic dysfunction in AD.

Here, I brought together these two observations to directly test whether caspase cleavage of APP was relevant in Aβ-driven synaptic dysfunction. First, we utilized a whole-cell patch clamp method to allow us to directly compare the post-synaptic effects of Aβ toxicity from neurons overexpressing APP relative to neighboring 'wild-type' neurons. This approach is unique in that it allows for localized, acute APP expression and a more physiological distribution of Aβ production and dissemination as compared to traditional exogenous methods of Aβ treatment. Through a combination of pharmacological and genetic manipulation of this system, we first showed that caspases are involved in Aβ-driven synaptic depression and that this is mediated by effector caspase, caspase-3. Next, we showed that absence of the APP caspase cleavage site ameliorated Aβ-induced synaptic depression. All together, the results indicate a role for caspases and caspase cleavage of APP in Aβ-driven synaptic depression.

Additionally, I showed that this caspase cleavage-mediated toxicity was specific to APP and tested this by asking whether APP homologue, APLP2 could also contribute to Aβ-mediated synaptic dysfunction. To do this, I first characterized the neuronal structure and function of APLP2 $^{-/-}$ mice and demonstrated that although APP and APLP2

contain a high degree of functional redundancy, APP and APLP2 appear to diverge in this context. While APP $^{-/-}$ animals contain abnormal dendritic arbors, contain fewer dendritic spines, and display deficits in synaptic function, the neuronal structure and function of APLP2 $^{-/-}$ animals appear to be completely normal. To test the relevance of APLP2 in Aβ-driven synaptic dysfunction, we utilized the knock out animals and tested LTP after incubation with Aβ. While we previously showed that APP $^{-/-}$ mice displayed normal levels of LTP after incubation with Aβ, we saw no difference in APLP2$^{-/-}$ as compared to wt animals, indicating that APLP2, although highly homologous with APP, is not necessary for Aβ toxicity, thus lending to the idea that this effect is specific to APP.

Additionally, with work that was spearheaded by Simone Eggert, Ph.D., I looked at the effect of dimerization of APP derivative, C99 (or SPA4CT). We were interested in this effect because our model of APP-driven Aβ toxicity involves the dimerization of APP upon binding of Aβ. Utilizing a chemical based system, we were able to convincingly show that dimerization and oligomerization of APP and C99 leads to decreased Aβ production. While it isn't surprising that dimerization affects cleavage and production of Aβ, this could act as a negative feedback system, whereby Aβ regulates its own production, thus regulating toxicity. Studies have previously suggested a negative feedback system involving synaptic activity and Aβ and perhaps the Aβ /APP interaction is acting in a similar manner.

Altogether, this project covered various aspects of APP-mediated Aβ synaptotoxicity and demonstrated that this toxicity involves caspase activity. While the

work just described is very straightforward, it is interesting to surmise how it fits into the big picture. The fact that caspase activation is garnering much attention due to its physiological role in synaptic plasticity is very intriguing, particularly in the context of AD. While it seems rational to infer that pathological caspase activity in AD may just be the result of a slight perturbation of a delicate balance of normal caspase activation, I would argue that the results in this dissertation and the resemblance of APP to a 'death ligand' suggests a more regulated or specific event. Alternatively, both of these scenarios may be contributing to the progression of AD independently. Age could play a major factor in rendering the neurons more susceptible to increased and uncontrolled caspase activation and may lead to unwanted cleavage of caspase substrates, such as APP.

At first glance, targeting caspases in neurodegenerative diseases seem promising, however, previous caspase inhibitors have led to toxicity with questionable efficacy. While new generations of caspase inhibitors are being created, the emerging results that indicate a role for caspase-3 in normal neuronal function weakens the argument that caspase inhibition may be useful in treating neurodegenerative diseases, though it is too soon to rule them out altogether. That being said, it seems evident that other therapeutic avenues will have to be pursued for optimal efficacy and while the mode of toxicity exerted by the caspase cleavage of APP is currently unknown, perhaps the pursuit for this answer will lead us toward the creation of a more efficacious treatment for AD.

.